The Thesis Committee for Austin David Weidner
Certifies that this is the approved version of the following thesis:

Balancing Ammonia and Alkalinity for Nitrification at Walnut Creek Wastewater Treatment Plant

APPROVED BY
SUPERVISING COMMITTEE:

Supervisor:

Desmond F. Lawler

Mary Jo Kirisits

Balancing Ammonia and Alkalinity for Nitrification at Walnut Creek Wastewater Treatment Plant

by

Austin David Weidner, B.S.

Thesis

Presented to the Faculty of the Graduate School of

The University of Texas at Austin

in Partial Fulfillment

of the Requirements

for the Degree of

Master of Science in Engineering

The University of Texas at Austin

May 2014

Dedication

This thesis is dedicated to my family.

Acknowledgements

I would first like to thank my advisor, Dr. Desmond F. Lawler, for providing me the opportunity to work on this project and guidance and encouragement throughout my entire time at UT. His knowledge of water treatment, dedication to research and teaching, and patience were all both enormously helpful and inspirational to me.

I would like to acknowledge Dr. Mary Jo Kirisits for her guidance and suggestions while preparing this thesis and throughout the project. Also, I would like to thank Dr. Lynn Katz for sharing her knowledge of water chemistry and offering suggestions when needed.

I would like to thank the Austin Water Utility for their support of this research. I especially want to thank Judy Musgrove, Henry Dress, Dana White, Paul George, Tammy West, all the operators and staff at Walnut Creek and South Austin Regional Wastewater Treatment Plants. Throughout the course of the project, they were always extremely helpful whenever I needed to collect water samples, obtain data, or have questions. It was a pleasure to work with them all.

I would be remiss if I did not also acknowledge my friends and colleagues in the EWRE Department for helping me growth both academically and personally. The sense of community amongst this group certainly made my time at UT very enjoyable.

Lastly, I would like to thank my family for continuously providing me with love and support through all my personal endeavors.

Abstract

Balancing Ammonia and Alkalinity for Nitrification at Walnut Creek Wastewater Treatment Plant

Austin David Weidner, M.S.E.

The University of Texas at Austin, 2014

Supervisor: Desmond F. Lawler

The Walnut Creek Wastewater Treatment Plant in Austin, Texas, has recently experienced increasing influent ammonia concentrations. Nitrification, the biological process used to treat ammonia, consumes alkalinity, which makes it difficult to properly treat ammonia while still maintaining the pH above the required discharge level of pH 6. Operators have looked to the addition of chemicals to supplement alkalinity; one creative alkalinity source was $CaCO_3$ solids, which are generated by the lime-softening process at Davis Water Treatment Plant. In 2011, the utility began transferring solids to Walnut Creek and immediately noticed improvements in both the nitrification efficiency and the effluent pH. However, undissolved solids accumulated at Walnut Creek and had a detrimental effect on the biosolids treatment efficiency at Hornsby Bend Biosolids Management Plant. Ultimately the costs of the poor biosolids treatment forced the utility to examine an alternative alkalinity source.

The objective of this thesis is to help Walnut Creek optimize the use of various alkalinity sources to find a long-term solution that will improve the alkalinity and ammonia balance for adequate nitrification. Analysis of the plant's influent characteristics suggested that industrial users, especially the semiconductor industry, are major contributors of ammonia and sulfate to the wastewater. A theoretical modeling based on chemical equilibrium predicted that using the $CaCO_3$ solids would provide a maximum alkalinity benefit of 47 mg/L as $CaCO_3$. Experimental dissolution jar tests were conducted to verify the model predictions and estimate the kinetics of dissolution. Results from these tests showed no significant dissolution of $CaCO_3$, and that the solids remained unchanged throughout the test. These results indicate that $CaCO_3$ solids are not recommended to provide alkalinity at Walnut Creek. Finally, the use of $Mg(OH)_2$ for alkalinity was employed at Walnut Creek and allowed operators to reduce the blowers that provide aeration. To quantify this observation, bubbling column tests were conducted to measure differences in the oxygen transfer rate at various $Mg(OH)_2$ concentrations. However experimental results did not match the expectations, so future work is required.

Table of Contents

List of Tables

List of Figures

Chapter 1: Introduction

1.1 MOTIVATION

The purpose of municipal wastewater treatment is to remove organic content, biological nutrients, and inorganic and organic contaminants from wastewater to protect the health of the receiving surface waters. Nitrogen, which enters the wastewater treatment plant primarily in the form of ammonia (NH_3), is an important biological nutrient. According to Metcalf and Eddy (2003), the influent ammonia concentration to a typical wastewater treatment plant in the United States is 25 mg/L NH_4^+-N. Treatment of ammonia is necessary because it is toxic to many aquatic organisms, causes eutrophication in surface water, and depletes dissolved oxygen concentrations necessary for aquatic life. The most common treatment technique is nitrification, a biological process, which utilizes microorganisms to first oxidize ammonia to nitrite (NO_2^-) and then oxidize nitrite to nitrate (NO_3^-).

A side effect of nitrification is that the process consumes alkalinity. Alkalinity is a measure of the capacity of an aqueous solution to resist a change in pH. As the alkalinity decreases in a nitrification system, maintaining the pH within a suitable range to support effective microbial activity and above regulatory discharge requirements becomes difficult. Wastewater treatment plants that struggle to maintain the balance between ammonia and alkalinity can use denitrification, a biological process that reduces nitrate to nitrogen gas (N_2) while generating alkalinity, or chemical additions to add alkalinity to improve their treatment efficiency.

The Walnut Creek Wastewater Treatment Plant in Austin, Texas, is one such plant that has recently struggled with the nitrification of increasing influent

concentrations of ammonia. Unfortunately, the treatment plant was not designed with a designated denitrification system, so in the short term, the staff at Walnut Creek have been investigating creative ways to improve the nitrification capacity. In 2011, the Austin Water Utility (AWU), which operates Walnut Creek, began releasing lime-softening waste solids, which were generated at one of the utility's drinking water treatment plants, into the wastewater collection system. The solids, primarily composed of calcium carbonate ($CaCO_3$), dissolved in the collection network and thereby increase the alkalinity of the wastewater. Immediately, the nitrification efficiency improved notably and the pH of the effluent safely met the discharge requirements.

Despite the benefit of the lime-softening solids addition to Walnut Creek, indirect problems arose. Large quantities of undissolved solids accumulated in the sedimentation basins at Walnut Creek. These solids, along with the expected biosolids from the wastewater itself, are treated at Hornsby Bend Biosolids Management Plant. In addition to the added cost of treating the extra volume of solids, the efficiency of the operations at Hornsby Bend deteriorated due to the high percentage of lime-softening solids. Ultimately, the costs outweighed the benefits, and so AWU stopped addition of the lime-softening solids in 2013 and began investigating alternative solutions for providing adequate alkalinity to balance nitrification.

1.2 Plant Overview

Walnut Creek Wastewater Treatment Plant uses a conventional activated sludge process. The plant has an overall capacity of 75 million gallons per day (MGD) with an average treatment flow of 55 MGD. There is no designated infrastructure specifically for denitrification. However, in 2007, the city stopped aeration at the head of the aeration

basins to establish pseudo-denitrification zones. These zones denitrify approximately 20-25% of the influent nitrogen concentration.

1.3 OBJECTIVES

The purpose of this research was to aid AWU in developing a long-term solution to providing sufficient alkalinity to effectively nitrify the observed influent ammonia concentrations. First, it was important to completely understand the problem and its cause so that possible solutions could be developed. Since the lime-softening solids from the drinking water treatment plant provided beneficial alkalinity at no cost to Walnut Creek, it was investigated as an ideal supplemental alkalinity source. Optimizing the use of these solids is critical, so that Hornsby Bend is not detrimentally impacted. Finally, side effects of other alkalinity sources used at Walnut Creek were assessed to provide quantitative information to optimize treatment.

1.4 APPROACH

To achieve these objectives, this research used data analysis, theoretical modeling, and experimental tests. The overall approach consists of four steps:

1.) Analyze operational and water quality data from Walnut Creek to provide context and fully understand the situation.
2.) Build theoretical models to predict expected results.
3.) Conduct laboratory-scale experiments to simulate the conditions of the full-scale system under different scenarios.
4.) Compare model and experimental results to evaluate the overall impact the solution might have on Walnut Creek.

Of the four steps used in this research, experimental testing played the biggest role in understanding the effectiveness of the proposed solutions. Although necessary, theoretical modeling was limited for this study because wastewater is a very complex medium and thus difficult to model.

1.5 THESIS STRUCTURE

This thesis strays from the conventional structure of presenting methods, then results, and finally analyzing the findings. Since each step in the above approach is somewhat independent and contains its own literature review, set of methods, results, and discussion, this research is instead presented so that each chapter contains one step of the above approach. That is to say, although connections between chapters do exist, each chapter was written such that it can stand alone as its own study.

In total, this thesis has six chapters. Chapter 2 aims to understand the causes that lead to difficulties with nitrification treatment at Walnut Creek. It contains background information about nitrification and analysis of historic water quality and operational data from Walnut Creek from 2002 to the present. In addition, industrial waste data are analyzed to identify possible sources of high ammonia loadings to the wastewater. Chapter 3 describes the mathematical modeling that was done to estimate various parameters of using lime-softening solids as a potential alkalinity source. Specifically, the quantity of solids transferring to Walnut Creek, the maximum amount of alkalinity the solids provide based on chemical equilibrium, and the observed alkalinity deficit required to completely nitrify the influent ammonia were quantified. Chapter 4 focuses on $CaCO_3$ dissolution laboratory experiments used to verify the model predictions calculated in Chapter 3. Chapter 5 is somewhat removed from the overall approach so it was added at the end. It contains an investigation into the effects that $Mg(OH)_2$, one of the

supplemental alkalinity sources used at Walnut Creek, has on the aeration efficiency at the plant. Finally, Chapter 6 summarizes all the findings in the entire thesis, including a comparison of the theoretical and experimental results. In addition, it presents recommendations to AWU.

Chapter 2: Influent Characteristics

2.1 INTRODUCTION

Plant operators and engineers from the AWU have struggled to maintain the required effluent discharge levels for ammonia and pH at Walnut Creek (WC) Wastewater Treatment Plant. The genesis of this research was that city personnel believed that increasing ammonia concentrations in the influent wastewater were adding excessive treatment loads on the plant. Leading to this hypothesis is the fact that ammonia is removed from the wastewater using a biological process, nitrification, which consumes alkalinity at the treatment plant. Therefore the treatment of higher levels of ammonia would consume larger quantities of alkalinity, thus making it difficult to maintain an adequate pH. To understand this problem, it is first important to fully understand the influent characteristics of the wastewater at Walnut Creek. In addition, it is important to identify the cause of the higher ammonia concentrations.

The purpose of this chapter is to analyze the wastewater characteristics and identify the cause of higher ammonia concentrations observed at WC. Section 2.2 provides an introduction to the chemistry and biology of nitrification processes. Analysis of influent wastewater data of the two wastewater treatment plants operated by the AWU, Walnut Creek and South Austin Regional (SAR), is presented in Section 2.3. The analysis of the historical wastewater data led to the investigation of industrial waste data to determine a possible cause. The methods used to analyze the industrial waste data are discussed in Section 2.4, and the results of the investigation are shown in Section 2.5. Finally, Section 2.6 summarizes these findings and provides recommendations to AWU.

2.2 LITERATURE REVIEW

Ammonia is a highly soluble, odorous gas. In water, ammonia forms a monoprotic weak acid-base system with the conjugate weak acid, ammonium ion (NH_4^+). The acid-base reaction for ammonia and ammonium ion is shown in Equation 2.1 and has an equilibrium constant, K_a, of $10^{-9.24}$ (Morel and Hering 1993). Given its low K_a value, ammonia is primarily found in natural waters as ammonium ion. However, the term "ammonia" is generally used to describe the combination of both compounds in water.

$$NH_4^+ \leftrightarrow NH_3 + H^+$$

(Equation 2.1)

Ammonia is commonly found throughout nature and has an important role within the nitrogen cycle. In wastewater, ammonia is prevalent because it is excreted by humans via urine. Removal of ammonia at wastewater treatment plants is necessary because it is toxic to many aquatic species, will lower the dissolved oxygen (DO) concentration of the receiving body, and is a nutrient that could lead to eutrophication (Metcalf and Eddy 2003). By far the most common method to remove ammonia is through the biological processes, nitrification and denitrification. Nitrification is a two-step process in which ammonia is oxidized to nitrite (NO_2^-) and then further oxidized from nitrite to nitrate (NO_3^-). In contrast, the denitrification process reduces nitrate into a series of nitrogen-based gases, including nitric oxide (NO) and nitrous oxide (N_2O), until ultimately reducing it into pure nitrogen gas (N_2) (Metcalf and Eddy 2003).

Nitrification is typically described by the overall reaction shown in Equation 2.2.

$$NH_4^+ + 2O_2 \rightarrow NO_3^- + 2H^+ + H_2O$$

(Equation 2.2)

Equation 2.2 combines the oxidation half reactions of ammonia and nitrite with the reduction half reaction of oxygen into water. Since oxygen is the terminal electron

acceptor, nitrification systems require aerobic conditions, and so nitrification commonly takes place in the aeration basins at a wastewater treatment plant. To completely oxidize ammonia to nitrate, two moles of oxygen are required per mole of ammonia. Converted into units of mass, 4.57 g O_2 per g N are required. Similarly, nitrification creates two equivalents of hydrogen ion per equivalent of ammonia, so 7.14 g of alkalinity as $CaCO_3$ are consumed per g N. When uptake of nitrogen by microorganisms for cell synthesis is accounted for, the ratio of grams of alkalinity consumed per gram of nitrogen becomes 7.07 g alkalinity as $CaCO_3$ per g N (Metcalf and Eddy 2003). Diminished alkalinity reduces the wastewater's capacity to buffer acids; thus it becomes more difficult to maintain the pH between 7 and 8. It is important to maintain this pH range because below the range, the nitrification rate decreases to the point where excess ammonia is discharged. A secondary concern is that the pH must be kept above 6 to meet the regulatory discharge requirements.

Autotrophic microorganisms largely are responsible for nitrification and can be classified into two groups: ammonia-oxidizing bacteria (AOB) and nitrite-oxidizing bacteria (NOB). The two primary AOB genera are *Nitrosomonas* and *Nitrosospira,* while *Nitrobacter* and *Nitrospira* are the two main NOB genera (Dytczak et al. 2008; Metcalf and Eddy 2003). The presence of varying nitrifying microbial communities and the nitrification rates are impacted by chemical and physical parameters of the wastewater including pH, alkalinity, salinity, temperature, carbon-to-nitrogen ratio, DO concentration, and the concentration of available substrates ammonium and nitrite (Dytczak et al. 2008). Since nitrogen removal via nitrification is an important process in wastewater treatment, carefully monitoring and maintaining suitable environmental conditions for nitrifying bacteria is critical.

Denitrification, on the other hand, is shown by the reaction in Equation 2.3.

$$5CH_3OH + 6NO_3^- \rightarrow 3N_2 + 5CO_2 + 7H_2O + 6OH^-$$

(Equation 2.3)

Denitrification requires an electron donor, which in Equation 2.3 is represented by methanol, but in many wastewater treatment plant applications, is provided by carboneous BOD remaining in the water. Regardless of the electron donor, denitrification produces one equivalent of alkalinity per equivalent of nitrate reduced. That is, 3.57 mg/L of alkalinity as $CaCO_3$ is produced per mg/L of nitrate as nitrogen (Metcalf and Eddy 2003). A variety of facultative heterotrophic and autotrophic bacteria have been found to be capable of denitrification. It is important to note that, even though facultative bacteria could use both oxygen and nitrate as the electron acceptor, anoxic conditions are required to accomplish denitrification.

2.3 Historic Influent Data at Walnut Creek WWTP

Water quality data are collected and recorded for numerous water quality parameters and locations throughout the wastewater treatment plant for operational and regulatory purposes. The data from both SAR and WC wastewater treatment plants were collected dating back to 2002 and compared in order to understand the differences in trends between a plant functioning well (SAR) and one experiencing problems meeting the treatment standards (WC). The five main water quality parameters that were compared were alkalinity, biochemical oxygen demand (BOD), total suspended solids (TSS), ammonia, and sulfate concentrations.

The record of the influent alkalinity concentrations at WC and SAR is shown in Figure 2.1. The SAR alkalinity values remained roughly constant at approximately 250 mg/L, whereas the WC concentrations were roughly 30 mg/L lower than SAR from January 2007 until July 2011. After July 2011, the WC alkalinity concentrations increase and vary considerably, which can be explained by the addition of lime sludge into the wastewater collection network from the Davis Water Treatment Plant. Before this time, only a portion of the lime sludge leaked into the system, showing little impact on alkalinity concentrations. However, in the summer of 2011, as part of an effort to combat the low alkalinity problems at WC, utility officials decided that allowing all of the lime sludge into the plant would artificially raise the alkalinity to successfully treat ammonia. Although this approach seemed to solve some of the problems at WC, the increase in sludge caused problems for Hornsby Bend, Austin Water Utility's biosolids treatment facility. By June 2013, the Utility decided to cease the dumping of the lime sludge and instead provide supplemental alkalinity via $Mg(OH)_2$ addition. This procedural change can be seen in the data as the influent alkalinity data returns to approximately 220 – 250 mg/L after June 2013.

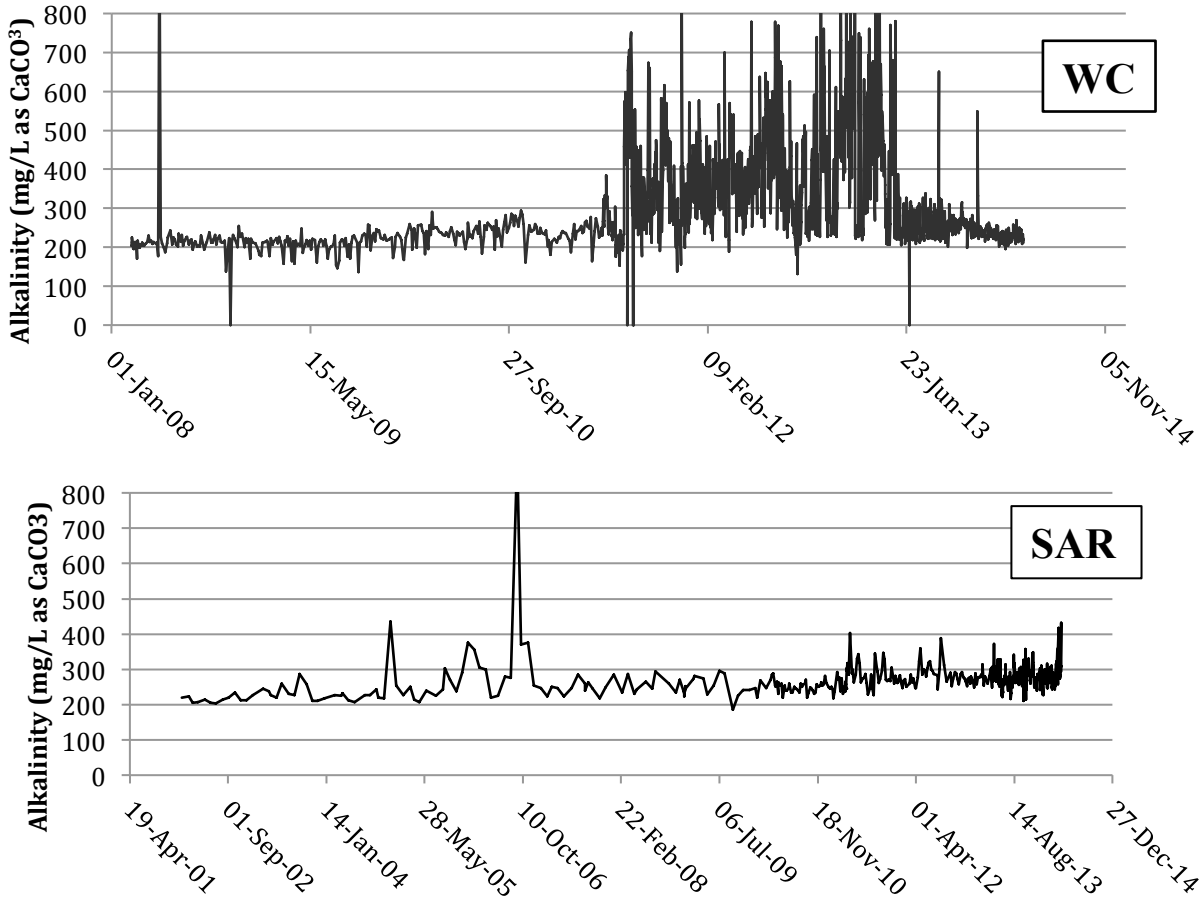

Figure 2.1: Daily alkalinity measurements from the influent at WC and SAR WWTP.

Figure 2.2 shows the influent BOD concentrations from WC and SAR over the past 10 years. BOD is a commonly used parameter in wastewater treatment to describe the amount of degradable organic matter in the wastewater. These data show no discernible trends over time, but do indicate that SAR's influent wastewater varies more over time and is stronger, i.e., more concentrated, than that of WC. The average BOD concentration at WC is approximately 160 mg/L whereas the SAR average is 37% higher at 220 mg/L. Compared to the typical medium strength BOD value of 190 mg/L (Metcalf and Eddy, 2003), it is clear that WC received a weaker strength wastewater. It is unlikely

that the difference in wastewater strength can be attributed to differences in residential use in the two parts of the city. Two possible explanations are that one or more industrial users are diluting the WC wastewater by contributing wastewater with very low BOD, or industrial users are wasting highly concentrated BOD waste into the SAR drainage basin. In addition, it is possible that the difference is caused by greater groundwater inflow into the WC collection system than the SAR system.

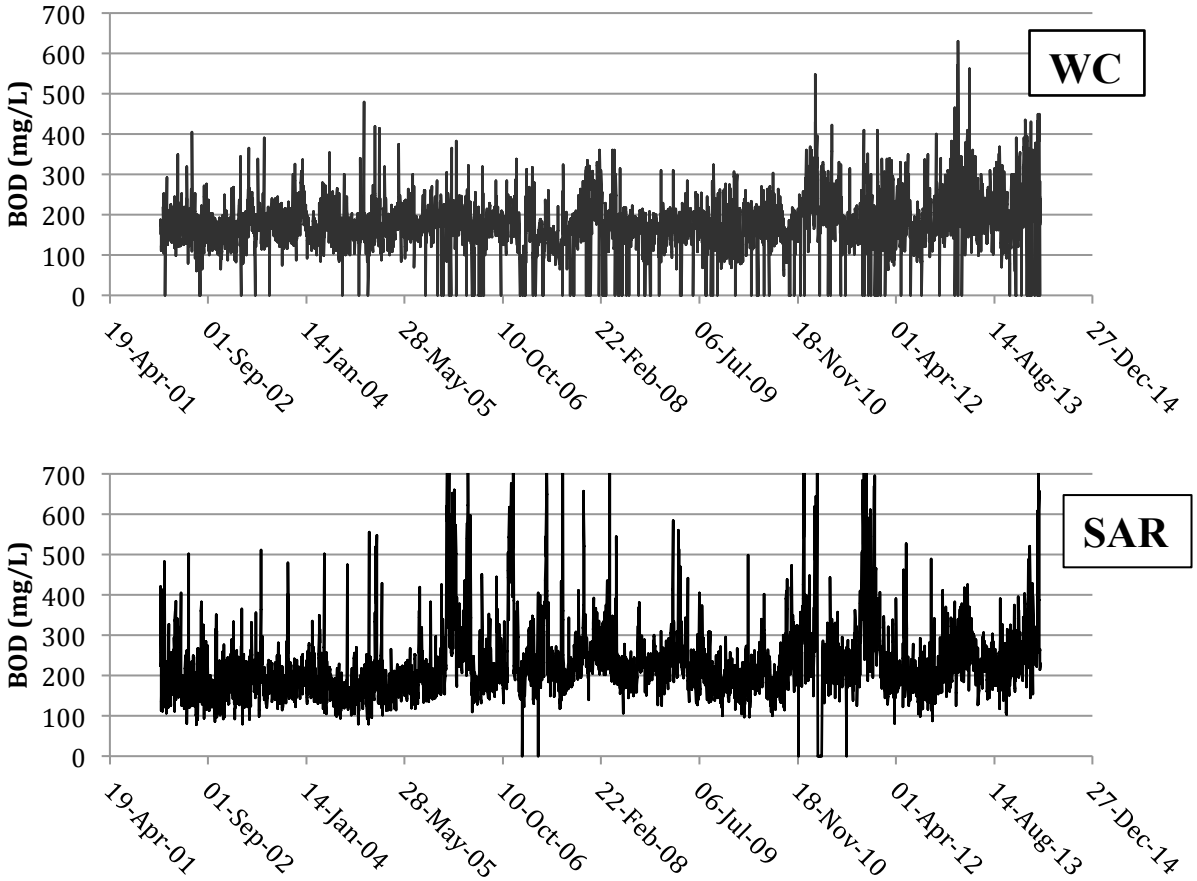

Figure 2.2: Daily Biochemical Oxygen Demand (BOD) measurements from the influent at WC and SAR WWTP.

Although TSS concentrations (Figure 2.3) are not drastically different between the two plants, SAR's influent exhibits much more frequent and higher peaks, which indicates more concentrated wastewater. Again, these data indicate no dramatic change over time, though both plants experienced a slow rise throughout the time period, perhaps a reflection of the Utility's efforts in water conservation and in sealing the wastewater collection system from infiltration. The median concentrations seen at both plants (226 mg/L for WC and 240 mg/L for SAR) are similar to the average medium strength TSS concentration of 210 mg/L (Metcalf and Eddy 2003). It is important to note that influent TSS data at WC between mid-2011 and mid-2013 are approximately 100 mg/L higher on average compared to the previous concentrations. As noted earlier, this time range matches the dates during which lime-softening solids from Davis WTP were being wasted, so it is believed that the higher TSS concentrations are attributed to these solids.

As seen in Figure 2.4, the ammonia data over the entire time period show a nearly matching increasing trend at both WWTPs. This increasing trend is likely strongly influenced by the increasing use of low-flow toilets, and perhaps also influenced by improvements to the wastewater collection network. One might expect to see a similar increasing trend in the BOD and TSS data if the low-flow toilets were a major cause of the rise, but such a rise was not seen in those data. However, for residential and commercial customers, urine is nearly the sole source of ammonia nitrogen whereas food and other organic wastes from sources other than toilets provide much of the BOD and TSS in their wastewater. Hence, the lack of matching trends in the three parameters does not refute the thought that low-flow toilets are part of the cause of the time trend in the ammonia data. Looking more closely, one can see the data rise and fall over three

several-month-periods throughout the ten-year span. Until the beginning of 2009, these extended peaks are almost identical between the two WWTPs.

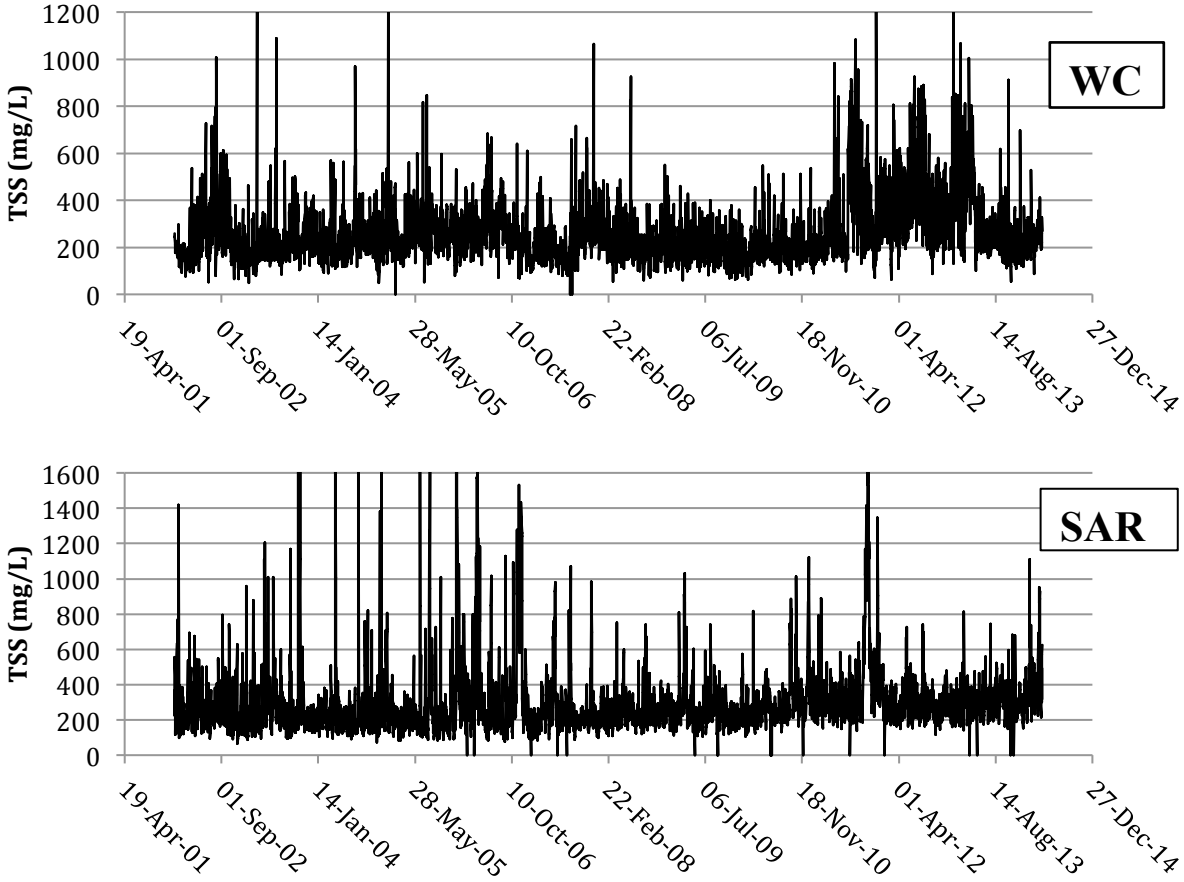

Figure 2.3: Daily Total Suspended Solids (TSS) measurements from the influent WC and SAR WWTP.

The data show that since 2010, the ammonia concentration at Walnut Creek has risen quite significantly, and the rise has been much more dramatic at WC than at SAR. For example, prior to 2010, only a few outlier values were above 30 mg/L as N, but since that time, the influent concentration has often exceeded this value. According to Metcalf and Eddy (2003), medium strength wastewater typically has ammonia concentrations of

approximately 25 mg/L as N. Historically, Walnut Creek has fallen below that value, but since 2011, it has been consistently above, adding a higher demand to be treated.

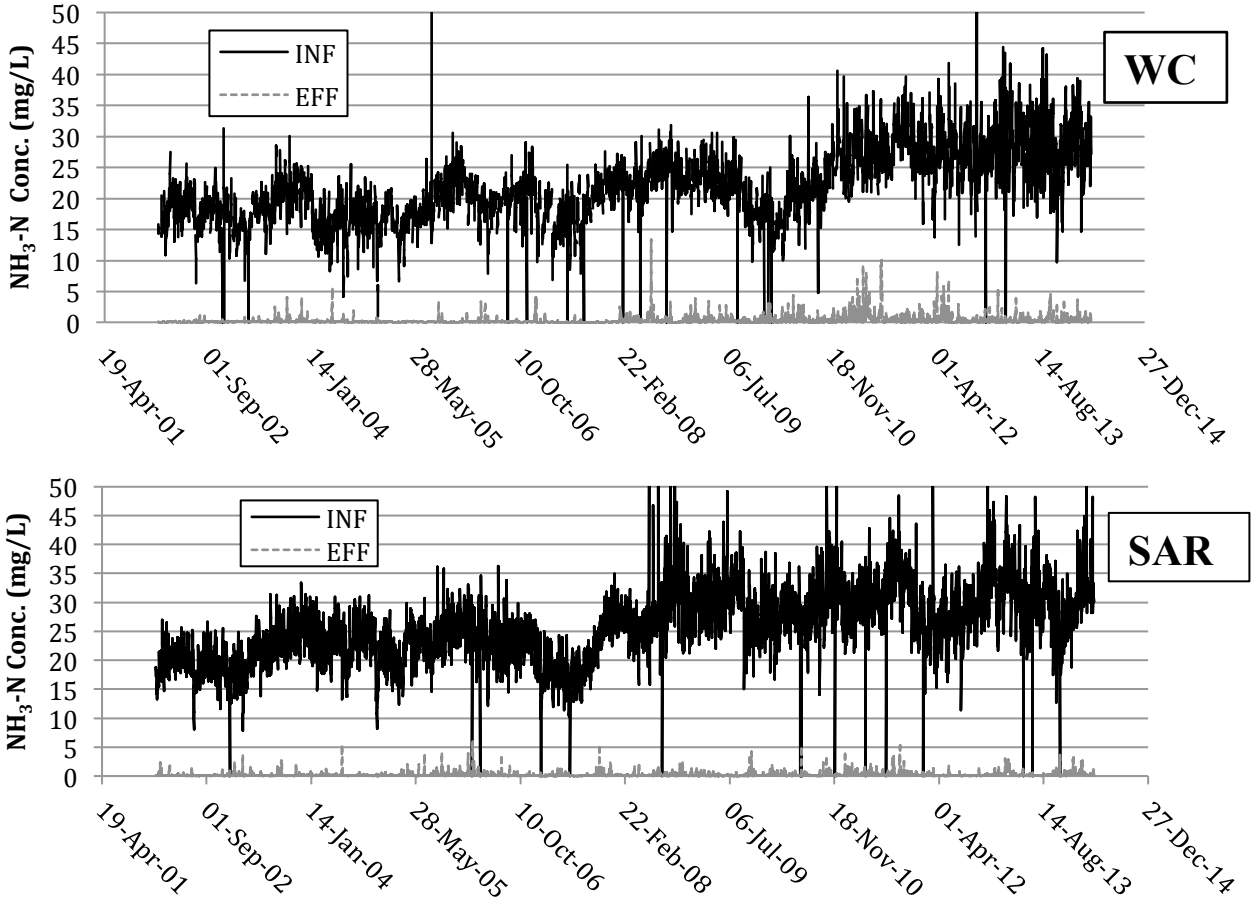

Figure 2.4: Daily Ammonia (NH_3-N) measurements of the influent and effluent at WC and SAR WWTP.

It is also important to note the effluent ammonia concentrations at both plants, shown in Figure 2.4. Except for a few outliers, SAR has very little problem meeting the effluent ammonia limit of 2 mg/L as N. The data for WC, on the other hand, show higher effluent concentrations especially after the influent ammonia concentrations began to rise in 2010, which reflects the struggle that Walnut Creek is facing in treating ammonia.

The last important constituent that was analyzed was the sulfate concentration shown in Figure 2.5. Sulfate measurements are only made monthly, so the data set is much more sparse than those reported above for the other parameters that are measured daily. Influent sulfate concentrations primarily fluctuated between 50 and 100 mg/L; SAR had rather constant sulfate concentrations near 60 mg/L and WC had sulfate concentrations increase from 50 to 100 mg/L until 2010. Most noticeable is the significant peak in sulfate of approximately 300 mg/L at WC since 2010. Sulfate does not get removed in biological wastewater treatment systems, as indicated by the almost identical effluent concentration data, nor does it have any direct negative effect on the system. However, as a strong acid anion, sulfate reduces the alkalinity, which indirectly reduces the plant's ammonia treating capacity via nitrification.

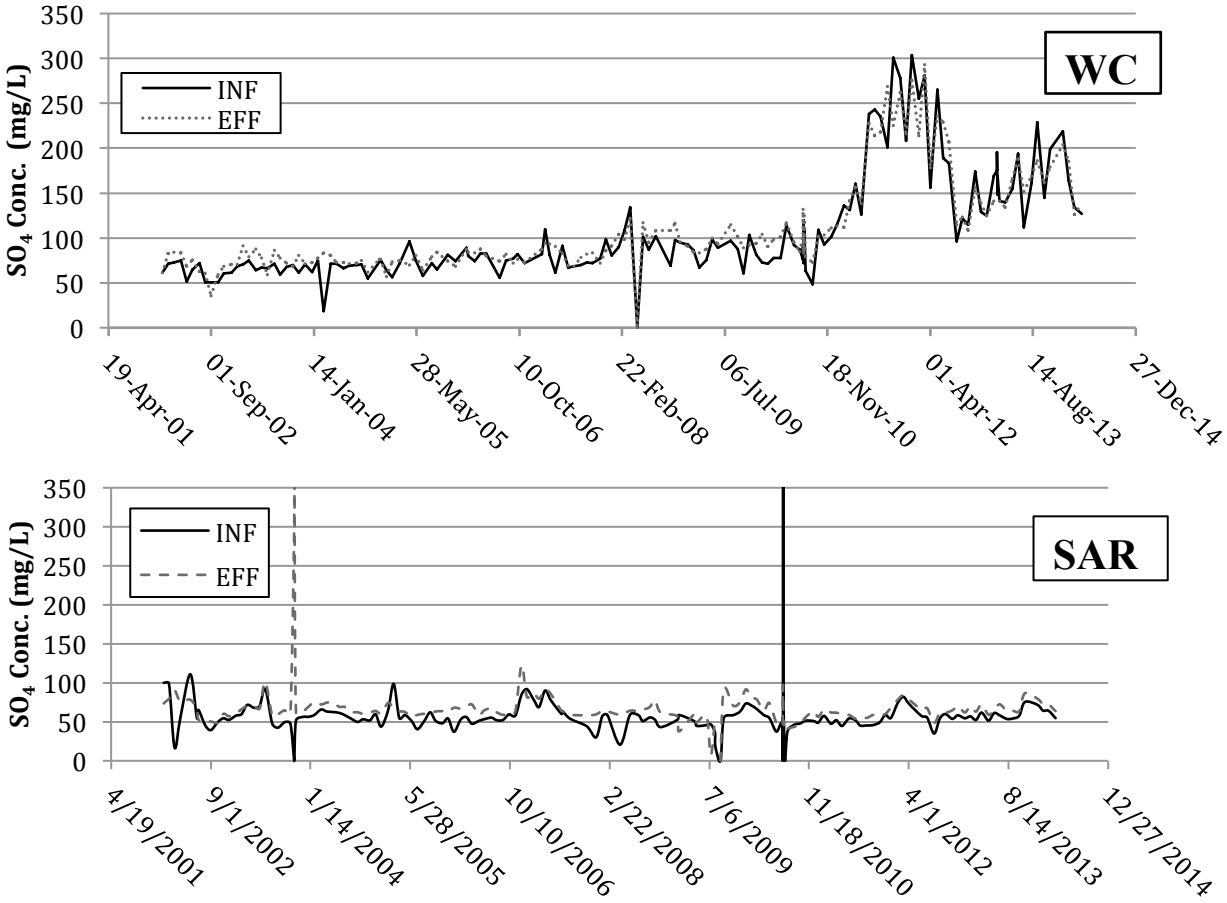

Figure 2.5: Monthly Sulfate (SO_4) measurements of the influent and effluent at Walnut Creek WWTP

With sulfate levels above the medium strength concentration of 60 mg/L (Metcalf and Eddy 2003) for much of the past decade including the large spike, it is safe to assume that the sulfate plays a key role in the problems at WC. We can further conclude that the dramatic rise in sulfate in the last few years (and perhaps the more gradual rise in the previous several years) can be attributed to industrial users because sulfates are not commonly added to water from typical residential and commercial uses.

2.4 Methods for Analysis of Industrial Waste Contributions to Austin's Wastewater

The data used in the analysis came from two sources within the Austin Water Utility. The influent and effluent data for both treatment plants (shown above) came from Dana White and reflect the values that are measured at the treatment plants. These data sets generally included a daily measurement of the constituent at multiple locations throughout the plant from 2002 to the present. In addition, the Utility's industrial waste division provided flow, sulfate, and ammonia data for each industrial user. These data were obtained during required annual sampling directly from the outfall of each site. Compared to the wastewater treatment plant data, the industrial waste data set was very small. In general, the data included only four sampling dates for each industrial plant—one for each year since 2009. These data were analyzed as indicated in the following paragraphs.

The analysis was conducted so that the contribution of flow, sulfate, and ammonia from each industrial user to the wastewater treatment plant could be compared. First, for each industrial user and for each specific sampling day, the sulfate and ammonia mass loadings were calculated by multiplying the industrial user's flow with the constituent concentration and necessary unit conversions. A similar calculation was done for the mass loading of sulfate and ammonia in the wastewater treatment plant influent. The wastewater influent concentration data were selected to match the date of the sampling for the industrial users. However, for sulfate, only monthly influent measurements were available for the two treatment plants. Thus, for sulfate, the monthly measurement date closest to the industrial sampling date was used.

Once sulfate and ammonia mass loadings were calculated for each industrial customer, they were divided by the value obtained for the appropriate City's wastewater

plant (i.e., the one to which that industry's wastewater goes) to obtain a percent contribution to the wastewater treatment plant. Lastly, the percentages for all the data points of a particular user were averaged, for two reasons. First, one date is too small of a sample to adequately judge an industrial user. For example, an industrial user might use a batch process, which dumps highly concentrated waste for a short time. If the city collected its sample at one of these times, then the mass loading would be uncharacteristically high. Second, to compare individual dates, the city must have collected data from each industrial user on the same day, which was not the case. By averaging the data, we obtain one set of values that has minimized fluctuations and can be compared. A summary of the averaged values for each industrial user can be found in Appendix A.

It is important to note that the results, although as accurate as possible given the available data, are just estimates based on a sparse data set. Therefore, the results should not be interpreted as exact numbers, but rather as a reasonable estimate that builds a clear, overall picture of the situation.

2.5 RESULTS

The analysis was conducted separately for the industries in the WC drainage basin and the SAR drainage basin. Figure 2.6 shows the percent flows, and percent mass loadings of sulfate and ammonia for every major industry in the Walnut Creek basin. The main component of the flow is attributed to all other residential and commercial water users, as indicated by the horizontal line hatching. Only 11% of the flow comes from industrial users. Semiconductor A, the black spotted hatching, is the largest industrial water user, responsible for 5.7% of the flow.

Despite contributing only 5.7% of the flow, Semiconductor A contributes approximately 60% of the mass loading of sulfate and 32% of the ammonia, according to the available data. The other significant contributor to sulfate and ammonia is Semiconductor B, represented by the bold diagonal lines. They contribute 1.43% of the flow and approximately 4% and 2% of sulfate and ammonia, respectively. All other industrial users do not contribute a sufficient amount of flow, sulfate, or ammonia to be of concern.

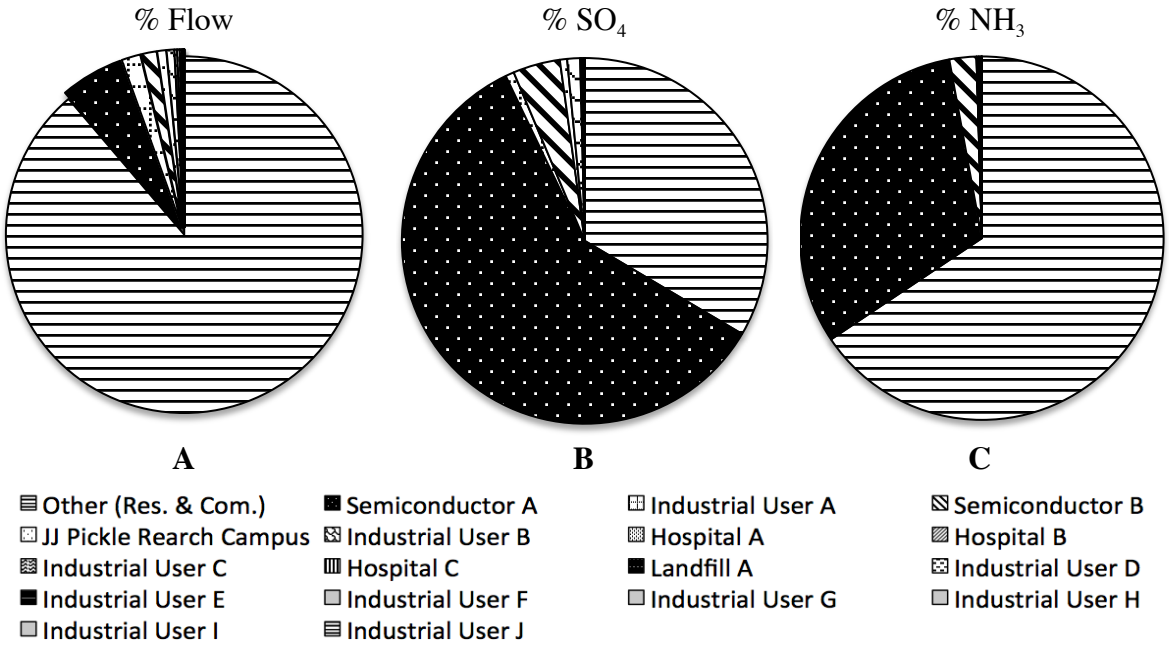

Figure 2.6: Contributions of industrial users to Walnut Creek WWTP: A) Percent flows, B) Percent sulfate, and C) Percent ammonia.

The results for the SAR WWTP, seen in Figure 2.7, show that industries only make up approximately 7% of the flow. The largest flow contributors are The University of Texas (square hatching), Semiconductor C (black spotted hatching), and

Semiconductor B (diagonal line hatching). Semiconductor B has two sites in the city, which explains why it appears on both the WC and SAR industry lists.

Those same industrial water users also contribute the most sulfate and ammonia, although the University of Texas (UT) contributes much less compared to Semiconductor C and Semiconductor B. The ammonia loading from UT is proportionally similar to that of a typical residential neighborhood and so is not considered an issue. Sulfate from UT makes up 3% of the sulfate in SAR's influent and it is believed to be from the many science laboratories. The sulfate and ammonia released from Semiconductor C make up 17% and 8% of SAR's influent while Semiconductor B is responsible for 7.5% and 1.5%, respectively.

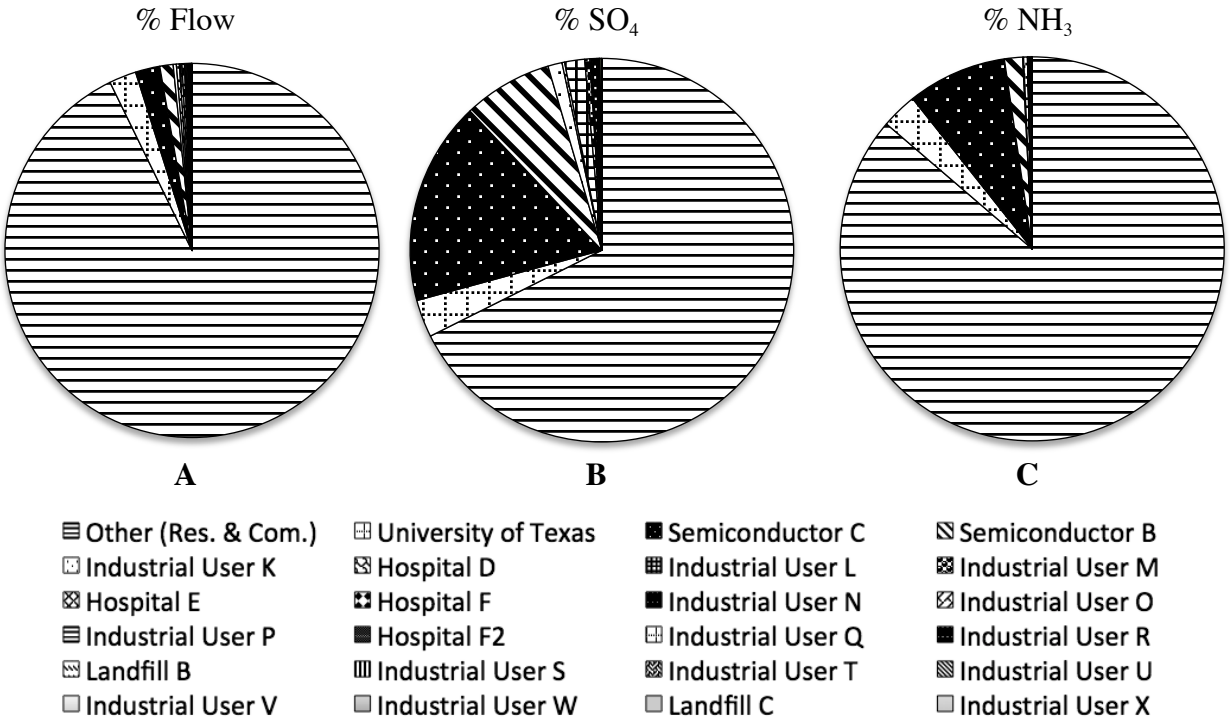

Figure 2.7: Contributions of Industrial users to South Austin Regional WWTP: A) Percent flows, B) Percent sulfate, and C) Percent ammonia.

An interesting connection can be drawn between each of the major contributors to the wastewater plant's influent sulfate and ammonia and their main product. Semiconductor A, Semiconductor B, and Semiconductor C all manufacture semiconductors that are used in computer chips. A summary of the contributions from these industries is shown in Table 2.1. Sulfuric acid and ammonia compounds are used in various cleaning steps during the manufacturing process, leading to the high concentrations in their effluents.

Calculations in the last two columns of Table 2.1 show the ratios between sulfate and flow and between ammonia and flow, respectively, in terms of their percent contribution to the influent. In essence, this ratio is a measure of how much higher their effluent concentration is in these two constituents than the average value in the overall wastewater flow arriving at each treatment plant. It is interesting to note that Semiconductor A and Semiconductor C contribute much more sulfate and ammonia per percent flow compared to Semiconductor B. This might indicate that Semiconductor B's process uses much less ammonia and sulfate, or that they pretreat their waste stream more effectively than the other two semiconductor industries.

Table 2.1: Data Comparison of Semiconductor Manufacturing Industries

Industrial User	WWTP	% Flows	% SO_4	% NH_3	%SO_4 : %Flow	%NH_3 : %Flow
Semiconductor B	SAR	1.15%	7.54%	1.53%	6.54	1.33
Semiconductor B	WC	1.43%	4.17%	2.40%	2.91	1.68
Semiconductor A	WC	5.73%	59.39%	31.53%	10.36	5.50
Semiconductor C	SAR	2.11%	17.15%	8.37%	8.11	3.96

2.6 CONCLUSIONS

The operational problems with respect to pH control and nitrogen removal at the Walnut Creek Wastewater Treatment Plant can be directly explained using the results of this analysis. From the analysis of the influent data at the two wastewater treatment plants, it is clear that the WC influent is relatively weak in terms of BOD concentrations (relative both to SAR and to average values in the US). For many years, it was also weak in its influent ammonia concentration, but in the past four years or so, the WC influent ammonia concentration has risen dramatically. Both of Austin's WWTPs have experienced a rise in the influent ammonia concentration over the past ten years, but the rise at WC is greater than at SAR.

High concentrations of sulfate and ammonia in the treatment plants' influent, especially at WC, were found to be directly attributed to the semiconductor manufacturers within the city. This combination of influent characteristics as a result of the semiconductor manufacturing industries reduces the overall alkalinity, which decreases the ability for the plant to remove standard ammonia concentrations, let alone the increased concentrations from the semiconductor manufacturers. Due to its large water consumption and high concentrations (relative to residential wastewater and even relative to other semi-conductor manufacturers), Semiconductor A appears to be especially responsible, contributing (according to the sparse data available) 60% of the sulfate mass loading and 30% of the ammonia mass loading at WC.

The difficulties faced at the Walnut Creek WWTP to remain within the permitted ammonia and pH effluent limits are likely to get worse as the semiconductor manufacturing industries plan to expand. Therefore, a long-term solution is required. Enacting policies that require industrial water users to meet a new, more stringent local

limit for sulfate and ammonia in their effluent appears to be the best solution. While not within the Utility's control, it is also possible that Semiconductor A and Semiconductor C could be encouraged to find ways to reduce their waste sulfate and ammonia concentrations; the savings in chemical use could be substantial enough to make it worth their effort. The fact that the contributions of these constituents from Semiconductor B are not as great in comparison to their flow suggests that waste reduction might be possible.

Implementing a new policy to limit the effluent concentrations is a slow process that would take several years. Therefore, it is recommended that a short-term fix be investigated until the local limit changes take effect. Possible short-term solutions would focus on operational adjustments at the WWTP such as employing a more effective denitrification process, which would generate alkalinity through the further degradation of nitrate into nitrogen gas. Promising new technologies for nitrification and denitrification that reduce the oxygen requirements and reduce the destruction of alkalinity have been investigated elsewhere, primarily on digester supernatant streams that have high ammonia concentrations. Whether they could be applied at full-scale to the Austin wastewater is perhaps worth investigating.

In the process of performing this analysis, we learned that the wastewater from the University of Texas and much of downtown Austin goes to SAR rather than to WC, even though SAR generally serves the area south of the Colorado River and WC serves the area north. If the piping is available, the Utility could consider diverting some or all of the wastewater from UT and the downtown district to WC. This may correct the relative imbalance of BOD, ammonia, and sulfate (compared to average values in the US)

between the two WWTPs. An experimental investigation of the value of this possible change would have to be performed first.

The Utility has tried to combat the problem of low alkalinity at WC by diverting sludge (primarily $CaCO_3$) from the Davis Water Treatment Plant to the sewer. These sludge solids only provide alkalinity to the extent that they are dissolved in the sewer or at the plant prior to the need for alkalinity in the nitrification process. Undissolved sludge that remains in solid form would be removed in the primary sedimentation tanks, and thus would not provide any benefit of increased alkalinity to the nitrification process. It is possible that the flow of solids could be controlled such that only the volume needed to meet the alkalinity deficit would be added and therefore not harm the sludge handling processes at Hornsby Bend. Further investigation into this idea is explained in greater detail in subsequent chapters of this thesis.

Chapter 3: Dissolution Modeling

3.1 INTRODUCTION

The previous chapter identified that an imbalance between ammonia and alkalinity in the influent wastewater at WC leads to inefficient nitrogen removal and difficulty maintaining the pH above 6 as required by the discharge permit. The AWU can solve these problems in three general ways: enact a local limit or regulation on the amount of ammonia that Austin wastewater customers can discharge, use denitrification, or add a supplementary alkalinity source. Denitrification would be the ideal solution. As a complementary biological process to nitrification, denitrification reduces nitrate to nitrogen gas while generating approximately half of the alkalinity consumed during nitrification. However, this solution is not practical, at least in the short term, for AWU since WC was not designed with the designated anoxic zones that are needed for denitrification. The other two solutions are currently being investigated by AWU. The focus of the work explained in this chapter was to determine the efficient use of a supplemental alkalinity source to solve treatment problems at WC.

The Austin Water Utility began supplementing alkalinity to WC after realizing that accidental leaking of lime-softening solids from the Davis Drinking Water Treatment Plant (WTP) was significantly increasing alkalinity concentrations of WC's influent wastewater. The solids, primarily a calcium carbonate ($CaCO_3$) precipitate, dissolve to some extent in the wastewater collection system, providing alkalinity. Upon fixing the leak, the treatment conditions at WC quickly degraded, and it became clear that a supplemental source of alkalinity must be used at WC. From December 2012 to mid-May 2013, the utility authorized releasing all of the $CaCO_3$ solids from Davis WTP into the wastewater collection system. However, a majority of the solids did not dissolve before

reaching WC and were removed in the plant's primary sedimentation basins; since only dissolved solids provide alkalinity, the excess solids were unnecessary and created additional problems. The excess solids along with the rest of the WWTP biosolids are treated at Hornsby Bend Biosolids Management Plant. The increased quantity and higher inorganic content of the solids due to the $CaCO_3$ solids significantly decreased the efficiency of the anaerobic digesters at Hornsby Bend. Although the $CaCO_3$ solids were a cost-free option for providing alkalinity, the resulting problems at Hornsby Bend outweighed the benefits of that additional alkalinity.

In response, AWU began purchasing magnesium hydroxide ($Mg(OH)_2$) in June 2013 to replace the $CaCO_3$ solids as the supplemental alkalinity source. Although utilizing magnesium hydroxide balances the necessary ammonia/alkalinity ratio and does not harm the anaerobic reactors, these benefits come at a relatively high cost to the Utility.

The focus of this portion of the research was to answer a number of questions pertaining to the effectiveness of using the calcium carbonate sludge. Specifically:

- What is the composition of the $CaCO_3$ waste solids?
- What is the daily mass loading of $CaCO_3$ solids that can be sent to WC?
- How much of the solids dissolve before reaching WC's aeration basins?
- What is the alkalinity deficit that must be met by the addition of $CaCO_3$ solids?

3.2 METHODS

3.2.1 Solids Characterization

To understand the composition of the solids produced at the Davis WTP, a solids analysis was conducted on the two waste streams that contribute solids to Walnut Creek WWTP. These two waste streams are the centrate and the equalization tank overflow, as shown in Figure 3.1. Samples of both the centrate and overflow were taken on June 6, 2013. Since the overflow waste stream could not be sampled directly, a sample of the recycled solids line was analyzed to represent the overflow since both flows should have the identical concentration and composition, assuming mixing of the equalization tank is sufficient. The solids analysis was conducted in accordance with Standard Methods (APHA et al. 2005). Duplicates were run and the results averaged for each sample. In addition, data detailing the cation composition of the waste solids were provided by AWU and analyzed.

3.2.2 Solids Mass Loading to Walnut Creek

The analysis to determine the daily mass loading of solids that were being sent to Walnut Creek WWTP from Davis WTP was conducted based on actual data provided by the Utility for both plants. The wastewater treatment plant data include daily averages of flow and standard water quality parameters sampled at multiple places throughout the treatment train from January 2002 to April 2013. The data from Davis WTP contain daily readings of total plant flow, flow of settled solids, and flow to the centrifuges, all in million gallons per day (MGD), from November 2012 to June 2013.

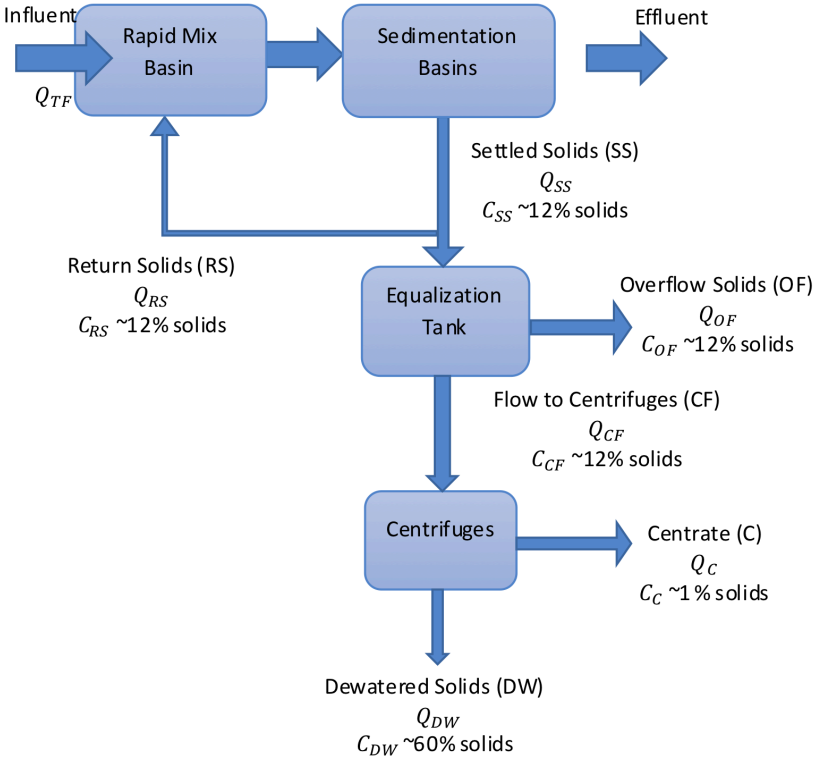

Figure 3.1: Schematic of Solids Flow at Davis Water Treatment Plant

A flow schematic of the solids through Davis WTP is shown in Figure 3.1. The solids are removed from the sedimentation basins and sent to an Equalization (EQ) Tank. A portion of the solids are returned to the head of the plant to provide seed crystals for the lime softening process. Typically, the solids travel to the centrifuges for dewatering from the EQ tank. The centrate from the centrifuges is wasted to the sanitary sewer and travels to WC. During overflow periods, the flow of solids to the centrifuges was cut off and the EQ tank overflowed into the sanitary sewer to WC. The percent of solids by weight for all flow lines is also shown in Figure 3.1.

Only three of these flow lines, influent, settled solids, and flow to centrifuges, are metered. The other flows can be estimated using assumptions and mass balance

calculations. First, the flow of returned solids was estimated by Brian Haws, Davis WTP Process Engineer, as 1% of the total plant flow. Scattered grab samples indicate the actual range is between 0.6 and 1.2%. The second assumption was that the overflow and centrifuge flow are mutually exclusive. That is, when the equalization tank overflows, no flow goes to the centrifuges and vice versa. The latter is justified by the fact that the capacity of the centrifuges is sufficient to process all of the solids flow. The metered flow data to the centrifuges indicates whether the plant was in the centrifuge mode or the equalization overflow mode.

A mass balance around the EQ tank can now be calculated to determine the amount of overflow. It is important to note that the flow to the centrifuges is not included in this calculation because this flow is assumed to be zero during overflow periods. Since all flows have equal solids concentrations, the mass balance simplifies to a flow balance.

Flow In = Flow Out

$$Q_{SS} = Q_{RS} + Q_{OF} = 0.01 Q_{TF} + Q_{OF} \quad \text{(Equation 3.1)}$$

where:

Q_{SS} = flow of settled solids from sedimentation basins
Q_{RS} = flow of returned solids to head of plant
Q_{OF} = flow of solids overflowed from EQ tank
Q_{TF} = total plant flow

Equation 3.1 is then solved for Q_{OF}.

$$Q_{OF} = Q_{SS} - 0.01\, Q_{TF} \quad \text{(Equation 3.2)}$$

To determine the flow of centrate, another mass balance must be conducted on the centrifuges. This time, because the concentrations of solids in the various streams are different, they must be incorporated into the mass balance. Because the concentration of

the solids in the centrate and overflow waste streams vary with time and are not routinely measured, assumed values of 1% and 12% solids for the centrate and overflow, respectively, were used, as suggested by Brian Haws. However, the assumed concentrations are in terms of percent solids, and thus must first be converted to concentration in terms of mass per volume by multiplying by the suspension density. In dilute solutions, the conversion is easily computed by assuming that the density of the suspension is equal to the density of water (1.00 kg/L), but since the percent solids concentrations in this mass balance are both quite large, the actual densities must be used in the conversion. The densities of each solids stream are calculated using Equation 3.3 (Engineering Toolbox 2013). The calculated densities and concentrations in terms of gram per liter are shown in Table 3.1. It should be noted that the composition of the solids was assumed to be 100% $CaCO_3$ for the purpose of this analysis, even though it is known that the solids do contain other inorganic salts and organic matter.

$$\rho_m = \frac{100}{\frac{c_w}{\rho_s} + \frac{100 - c_w}{\rho_l}} \qquad \text{(Equation 3.3)}$$

where:

ρ_m = density of suspension (kg/m^3)
c_w = concentration of solids by weight in suspension (%)
ρ_s = density of the solids (kg/m^3)
ρ_l = density of water (kg/m^3)
Density of Calcite: 2710 (kg/m^3)
Density of Water: 1000 (kg/m^3)

Table 3.1: Summary of Suspension Density and Solids Concentration

% wt. –	ρ_m (kg/m^3)	Conc. (g/L)
1.0	1006	10.1
12	1082	130
60	1609	965

With the concentrations known, the mass balance around the centrifuges was calculated as follows:

$$Q_{CF}\, C_{CF} = (Q_{CF} - Q_C) C_{DW} + Q_C C_C$$

(Equation 3.4)

where:

Q_{CF} = flow to the centrifuges
C_{CF} = concentration of solids in flow to centrifuges
Q_C = centrate flow
C_C = concentration of solids in centrate
C_{DW} = concentration of solids in the dewatered solids stream

Finally, Q_C was solved by plugging in the known concentrations calculated in Table 3.1.

$$Q_C = Q_{CF} \left(\frac{C_{CF} - C_{DW}}{C_C - C_{DW}}\right)$$

$$= Q_{CF} \left(\frac{130\, {}^{g}/_{L} - 965\, {}^{g}/_{L}}{10.1\, {}^{g}/_{L} - 965\, {}^{g}/_{L}}\right)$$

$$Q_C = 0.875\, Q_{CF}$$

(Equation 3.5)

Once the daily flows were estimated for all the data points, they were converted into daily solids loadings that were wasted using Equation 3.6. The concentration in g/L depended on whether Davis WTP was wasting overflow or centrate. If centrate was wasted for the particular day, then 10.1 g/L (1% solids) was used. Conversely, during overflow days, 130 g/L (12% solids) was used.

$$\frac{MG}{day} \times \frac{1{,}000{,}000\ gal}{1\ MG} \times \frac{3.785 L}{gal} \times Conc. \frac{g}{L} \times \frac{1\ lb}{454\ g} = \frac{lb}{day}$$

(Equation 3.6)

3.2.3: Equilibrium Model

Calculating the daily loading of lime sludge solids sent to Walnut Creek is only the first step to determine the alkalinity these solids could provide. In reality, the solids only contribute to the alkalinity of WC once they dissolve. Because the units of alkalinity are commonly expressed as mg/L as $CaCO_3$, the amount of dissolved solids exactly equals the amount of alkalinity provided. Finding the amount of dissolution is not only important to determine how much alkalinity the Davis DWTP solids are expected to provide, but also to determine the mass of solids that were being sent to Hornsby Bend.

Theoretically, the amount of solids that will dissolve is limited by equilibrium, regardless of how much excess is present in the system. If the solids concentration is less than this equilibrium point, then complete dissociation could occur. The dissolution reaction for calcium carbonate is shown in Equation 3.7 and the mass law that governs the dissolution is shown in Equation 3.8 (Morel and Hering 1993). The goal is to calculate the maximum amount of dissolution, which can be done using an equilibrium model.

$$CaCO_{3_{(s)}} \leftrightarrow Ca^{2+} + {CO_3}^{2-}$$

(Equation 3.7)

$$K_{sp} = 10^{-8.35} = [Ca^{2+}]\left[{CO_3}^{2-}\right]$$

(Equation 3.8)

Stumm and Morgan (1996) present models for $CaCO_3$ dissolution in pure water systems both open and closed to the atmosphere, i.e., allowing or not allowing equilibrium with the CO_2 in the atmosphere. Their model used the electroneutrality equation, as seen in Equation 3.9 and its simplified form in Equation 3.10, to solve for the equilibrium conditions in a water with no other ions present.

$$2[Ca^{2+}] + [H^+] = [HCO_3^-] + 2\left[CO_3^{2-}\right] + [OH^-]$$

(Equation 3.9)

$$2[Ca^{2+}] + [H^+] = C_T(\alpha_1 + 2\alpha_2) + \frac{K_w}{[H^+]}$$

(Equation 3.10)

where:

C_T = total carbonate concentration (M)
α_1 = ionization fraction for bicarbonate ion $(-)$
α_2 = ionization fraction for carbonate ion $(-)$
K_w = ionic product constant for water, $(-)$

Using Stumm and Morgan's model as a basis, a model for $CaCO_3$ dissolution in wastewater was developed for this research. The main difference between pure water and wastewater is that there are numerous other dissolved chemicals and particulate matter present in wastewater that affect the dissolution equilibrium. The biggest influence on the equilibrium is caused by acids and bases that shift the pH. To account for these constituents, generic terms that represent the concentration of strong acids and bases, C_A and $C_{B,}$ respectively, were added to the electroneutrality equation. We also assumed that no other weak acid/base systems besides the carbonate system are present in significant concentrations. This assumption is clearly not completely correct because, for example, some phosphate is in all municipal wastewaters. Also, the portion of the total ammonia that is present as NH_3 would be titrated to NH_4^+ in the alkalinity titration and contribute to the total alkalinity. However, these and other acid/base systems are generally in sufficiently small concentration ratios to make the assumption reasonable. With these assumptions, the complete equation is shown in Equation 3.11.

$$2[Ca^{2+}] + C_A - C_B = C_T(\alpha_1 + 2\alpha_2) - [H^+] + \frac{K_w}{[H^+]}$$

(Equation 3.11)

The major assumption of this developed model was that the system was closed to the atmosphere. The atmospheric considerations are important because CO_2 gas exchange will impact the amount of dissolved carbonate and significantly alter the equilibrium. Although the solids dissolve within the wastewater collection system and primary sedimentation tank, both of which are in contact with air, it was assumed that the surface area to water volume ratio was small enough to limit the rate of gas transfer, so that a closed system model is more realistic than an open system model. Also, in the sewer system, one could expect a heightened concentration of CO_2 in the air space due to biological activity, so that CO_2 would not significantly diffuse out of the water as it could in a normal atmosphere.

By definition, both sides of Equation 3.11 are equal to the alkalinity. Therefore, we can substitute one side or the other for the alkalinity of the water. Since we do not know C_A or C_B it is best to set the left side equal to alkalinity as shown in Equation 3.12.

$$Alk = C_T(\alpha_1 + 2\alpha_2) - [H^+] + \frac{K_w}{[H^+]}$$

(Equation 3.12)

In a closed atmosphere condition, the total concentration of carbonate in the system, C_T, will not change due to any external factors. Thus we assume that any change in C_T is directly due to the $CaCO_3$ solids, where an increase in C_T is caused by dissolution and a decrease is caused by precipitation. To find the amount of dissolution, we must find two C_T values, C_T with solids present and C_T without any solids present. Since Equation 3.12 can be solved for C_T by defining the alkalinity and the pH of the wastewater, we simply set the pH and alkalinity terms to the average influent values calculated from the data before and after the solids were added and solve for each unique C_T. The solids from Davis WTP began providing alkalinity to WC in mid-2011 and

continued until mid-2013; however, the exact start date is unknown because the solids were unknowingly and inadvertently transferred due to a leak in the system. Therefore, the average pH and alkalinity with solids present were calculated from the WC WWTP influent data between 2012 and mid-2013, while the same parameters without solids were calculated from 2002-2011, assuming all other characteristics of the wastewater remained relatively similar. The difference between the two average C_T values in molar units is interpreted as the maximum dissolution of $CaCO_3$ solids at equilibrium in wastewater.

The WC influent alkalinity data during solids overflow was not used for these calculations because it is misrepresentative of the true alkalinity. When alkalinity measurements are made using the titration method, the addition of acid would cause $CaCO_3$ to dissolve during the titration, resulting in a higher alkalinity value than under the original pH conditions. Instead, alkalinity data from the primary sedimentation tanks at Walnut Creek was used for this analysis because the sedimentation would remove a majority of the solids that would affect the alkalinity measurement.

3.2.4: Comparison to Walnut Creek

Once the maximum dissolution value was calculated, the daily flows of solids from Davis WTP to WC WWTP could be converted to daily alkalinity loadings. First, the maximum dissolution value was set as a threshold for dissolution. That is, for any solids loading above the threshold, the maximum amount of solids that dissolved was capped at the threshold value, and solids loadings below the threshold were assumed to completely dissolve. Since alkalinity is usually expressed in terms of $CaCO_3$, one gram of dissolved solids provides one gram of alkalinity, and therefore, the alkalinity loading is equivalent to the dissolved solids loading.

The next step was to compare the daily alkalinity loading provided by the Davis WTP solids to the total influent alkalinity at WC to see what the maximum benefit of the solids might have been. Daily average alkalinity concentrations at WC were converted to mass loadings in lb/day using Equation 3.6. The final step was to divide the alkalinity loading from the Davis WTP solids by the total alkalinity loading of the WC WWTP influent to get the percent alkalinity contributed by the solids.

3.3 RESULTS

3.3.1: Solids Characterization

The results of the solids analysis on the centrate and overflow are shown in Table 3.2. Table 3.2 contains both the concentrations of the various solid types in mg/L as well as each solid type as a percentage of total solids, which makes analyzing the data easier. The centrate was found to be 8 g/L or 0.8% solids while the overflow was approximately 130 g/L or 12% solids. It is important to note that the operating conditions at the Davis WTP vary daily, so these results only represent what was occurring on the specific sampling day, June 6th, 2013.

Table 3.2: Solids Analysis Results in mg/L

AVERAGE	TS	TDS	TSS	TFS	TVS	VSS	FSS	VDS	FDS
Centrate	7945	613	8183	6695	1250	1815	6368	437	177
Overflow	130973	210	131480	125538	5435	5463	126018	72	138
% of TS									
Centrate	100%	8%	103%	84%	16%	23%	80%	5%	2%
Overflow	100%	0%	100%	96%	4%	4%	96%	0%	0%

TS = total solids; TDS = total dissolved solids; TSS = total suspended solids; TFS = total fixed solids; TVS = total volatile solids; VSS = volatile suspended solids; FSS = fixed suspended solids; VDS = volatile dissolved solids; and FDS = fixed dissolved solids

By looking at the data for the various solids types, we can get a sense of the solids composition. The dissolved solids concentration (TDS) is quite small compared to the amount of suspended solids (TSS) in both of these streams. Further, the TSS is primarily composed of fixed solids (FSS), which make up 80% and 96% of the total solids concentration for the centrate and overflow, respectively. Fixed solids generally imply an inorganic composition. The data reinforces the understanding that the solids are primarily $CaCO_3$. Both streams show measureable volatile solids (TVS), which are characteristic of organic components. The results, however, do not necessarily mean that the solids samples were high in volatile organic compounds. Instead, the high TVS concentrations can be attributed to the degradation of inorganic salts, especially magnesium carbonate ($MgCO_3$), that are present in the solids samples. Measuring volatile solids requires heating the sample to a temperature of 550ºC to volatize most organic compounds. At this temperature, $MgCO_3$ degrades as shown in Equation 3.13, releasing more CO_2. The release of CO_2 reduces the measurable mass of the sample, resulting in a higher measured volatile solids concentration than is actually present (Sawyer et al. 2002).

$$MgCO_3 \xrightarrow[350^oC]{} MgO + CO_2 \uparrow$$

(Equation 3.13)

In addition to the solids analysis performed in our laboratory, the Utility provided data of a chemical analysis of the Davis WTP solids. The analytical results (Table 3.3) show that 91.8% of all cation mass is calcium while 6.6% is magnesium. Again, this reinforces our initial solid composition assumption, since both calcium and magnesium (but primarily calcium) are targeted for removal in a lime-softening plant. The other significant cation is iron (Fe) at 1.2%, which is due to an iron-based coagulant that is added to treat the drinking water. All other heavy metals have very low concentrations,

which is important because high concentrations of heavy metals can be detrimental to microbial communities that are needed at the wastewater treatment plant. In other words, these data show that the addition of the Davis WTP solids should not negatively affect WC's treatment processes in other ways.

Table 3.3: Solid Cation Assay

Cation	% of Total Cation Mass
Na	0.1%
Mg	6.6%
Ca	91.8%
Al	0.2%
As	0.0%
Cd	0.0%
Cr	0.0%
Cu	0.0%
Fe	1.2%
Hg	0.0%
Mo	0.0%
Ni	0.0%
Pb	0.0%
Se	0.0%
Zn	0.0%

3.3.2: Solids Mass Loading to WC

The first aspect of analyzing the data is to understand the operating conditions at Davis WTP. Over the nine-month period depicted in Figure 3.2, the Davis WTP treated an average of 65.3 MGD. Figure 3.2 also indicates the relationship between the plant's treatment flow to the amount of solids produced. As expected, these two conditions generally show similar trends—the more water that is treated, the more solids that are produced as a result.

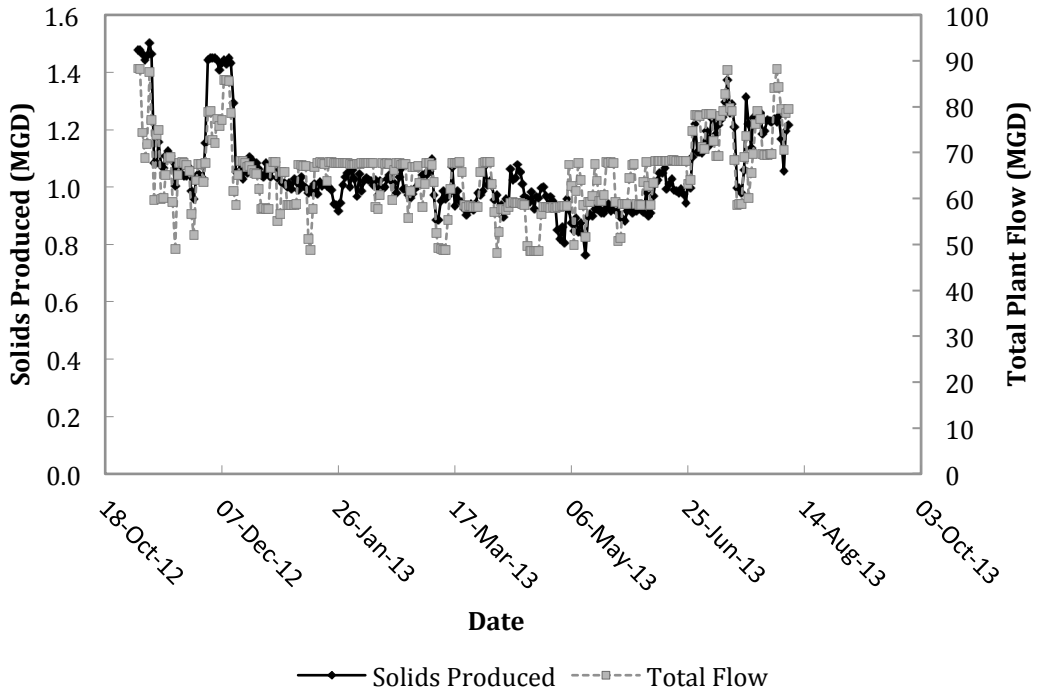

Figure 3.2: Davis WTP Operating Conditions

The daily mass of solids that were wasted from the Davis WTP to WC is shown in Figure 3.3. From January 1, 2013 until April 28, 2013 and briefly from November 17 through 30, 2013, the Davis WTP was sending overflowed solids to WC, while only centrate was wasted during the rest of the days in the available data. It is clear in Figure 3.3 that the solids loading from the overflow is significantly larger than the centrate loading. Table 3.4 shows a summary of the average flows and solids loadings for each condition. The overflow average loading is 395,000 lb/day of suspended solids while only 8,700 lb/day for the centrate, an approximately 45-fold increase. The overflow loading is larger because it is approximately 12 times as concentrated and because it has a higher flow. The average overflow flow rate was found to be 253 gal/min compared to only 72 gal/min for the centrate.

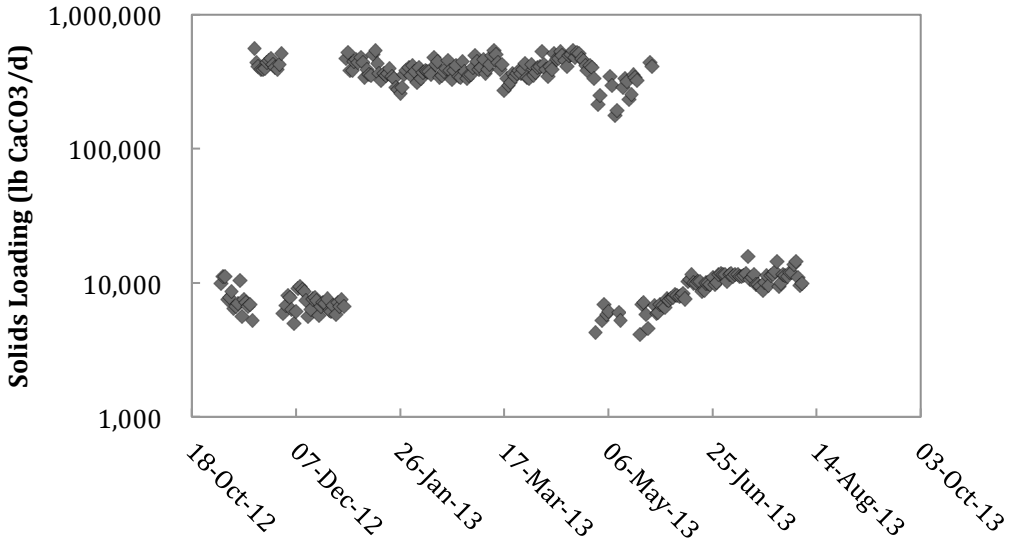

Figure 3.3: Solids Loading to Walnut Creek WWTP

Table 3.4: Summary of Flow and Solids Loading

	Overflow		**Centrate**	
	Average	St. Dev.	Average	St. Dev.
Flow (gpm)	253	47	72	20
Solids Loading (lb/day)	395,000	73,000	8,700	2,400

Two major assumptions lead to possible error in calculating the solids loading. The first was to assume Davis WTP's internal recycled solids flow to be 1% of the total plant operating flow. The error in this estimation was carried through the mass balance to the overflow calculation. With daily variations between 0.6 to 1.2% of the total flow, this assumption could have a large effect on the amount of waste discharged as overflow. The second assumption was to use estimated concentrations of 1% and 12% solids for the

centrate and overflow waste streams, respectively. Even though daily variations in concentration are common, such data were not available. Since the concentrations were a major part of determining the solids loading, this assumption is possibly a significant source of error.

3.3.3: Equilibrium Model

Table 3.5 summarizes the pH and alkalinity values that were used as inputs for the equilibrium model and the C_T values that were calculated as a result. The average influent wastewater data shows that the alkalinity could have increased 50.0 mg/L as $CaCO_3$ as a result of the additional solids present in the system. The pH also increased from 7.44 to 7.61 as a result of the dissolution of added solids. This pH rise is expected because dissolution of $CaCO_3$ results in increased CO_3^{2-} concentrations, a weak base.

Table 3.5: Summary of Walnut Creek Input Parameters For Model

Condition	Time Period	Average Parameters		C_T
		pH	Alkalinity (mg/L as $CaCO_3$)	(M)
w/o Solids	1/02-1/11	7.44	212.6	0.00227
w/ Solids	1/12-6/13	7.61	262.6	0.00275

As explained above, the difference between the C_T with solids and the C_T without solids equals the molar amount of $CaCO_3$ that dissolved in the sewer. This value equals 0.00047 M and, converted to mg/L as $CaCO_3$, is 47 mg/L. This value is significant because it can be used as a threshold to determine whether the solids concentration from Davis WTP, when diluted into the entire wastewater flow, would completely dissolve.

Solids concentrations below 47 mg/L are expected to completely dissolve. Conversely, if the concentration is greater than 47 mg/L, then, at equilibrium only 47 mg/L of solids would be expected to dissolve. Excess solids would accumulate in the sedimentation basins at WC and could negatively impact the operations at Hornsby Bend.

Although this model already represents an improvement over the pure water model described in Stumm and Morgan, it is still not completely representative of all the complexities in wastewater. The model described in this work only accounts for acid and base effects that would alter the equilibrium, but it does not account for ionic strength effects or complexation and precipitation of Ca^{+2} with other ligands. Wastewater has a high TDS concentration, and consequently a high ionic strength, which would reduce the reaction activity of the solution. A higher activity makes it more difficult for ions to interact, and that would decrease the amount of predicted dissolution. Complexation or precipitation of Ca^{+2} with other ligands such as OH^-, SO_4^{-2}, and PO_4^{-3} would consume free Ca^{+2}, driving more $CaCO_3$ dissolution to reach equilibrium. This level of complexity is difficult to model and, given the level of uncertainty in the data and assumptions, is not warranted at this time.

3.3.4: Comparison to Walnut Creek

To understand the contribution of alkalinity to Walnut Creek, the flow and alkalinity loading leaving Davis were compared to the daily average values measured in the influent at WC. The summary of this comparison is shown in Table 3.6. During the overflow periods, the percent flow was calculated to be 0.69% of the WC influent wastewater, while the centrate was only 0.17%. The difference in the percent flow contribution between the overflow and the centrate waste stream is a result of the

overflow having a solids concentration 12 times that of the centrate. Such a significant increase in the solids concentration means there is a significant difference in the volume of the suspension that is wasted to WC WWTP.

Table 3.6: Summary of the Average Flow and Potential Alkalinity Contribution to Walnut Creek WWTP From Davis WTP

Condition	WC Influent		Solids from Davis		% Flow	% ALK Loading
	MGD	ALK (lb/d)	MGD	ALK (lb/d)		
During Overflow	53.18	121,000	0.37	20,800	0.69%	17.6%
Centrate Only	49.88	103,000	0.09	7,250	0.17%	7.2%

The average potential alkalinity that could be provided during overflow is 20,800 lb/day, which makes up 17.6% of the total alkalinity loading of WC's influent. Clearly, the solids impact the alkalinity as the predicted alkalinity of WC's influent was observed to increase from 103,000 lb/day to 121,000 lb/day. Compared to the overflow, the percent contribution of the centrate is calculated to be on average only 7.2% of the total WC alkalinity loading. This result is expected because, as shown in the solids flow analysis, the centrate provides only 1/45 (approximately 2%) of the mass loading of solids as the overflow.

Figure 3.4 shows the daily values of the percent of the flow and alkalinity entering WC that can be attributed to the Davis WTP solids. The days when the centrifuges were running and centrate was being sent to WC are easily seen at two separate intervals between Nov. 2012 and Jan. 2013, since the percent alkalinity and flow are both very low. The rest of the dates were during overflow periods. It is important to

note that the variability seen in the overflow dates is much greater than the variability of the centrate. The variability could be due to the fact that the slight variations in the amount of water treated at Davis WTP, which affect the flow of both waste streams, are more noticeable with the overflow because the variations are compounded by the higher concentrations. In addition, the natural variations in WC's influent alkalinity concentrations, due to external effects, play some role in the variability of the percent alkalinity and flow data that differs from dividing the average flow and alkalinity values directly.

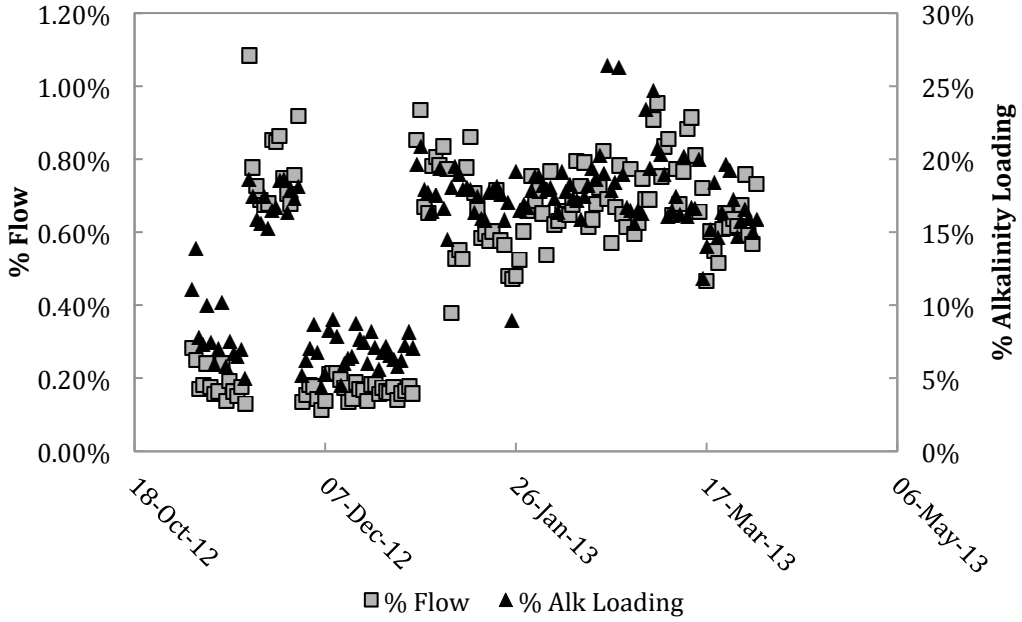

Figure 3.4: Percent Flow and Predicted Alkalinity Contributions from Davis WTP to WC

This analysis also allows us to estimate how much of the solids did not dissolve and thus accumulated in the sedimentation basin at WC. Figure 3.5 shows the daily solids accumulation at WC. The dates when only the centrate was being wasted result in no

accumulated solids. That is, all the centrate solids were predicted to dissolve. The average accumulation of solids during the overflow times is 374,000 lb/day. On average, only 5.4% of all the solids wasted as overflow to WC could have dissolved and provided alkalinity. This means that the Utility was adding 20 times as much solids as could dissolve; or said another way, the Utility could reap the same alkalinity benefit by adding only 1/20 as much solids. This result is significant because it indicates that, if the Davis WTP could control the amount of solids it sends to WC, then the Utility could maximize the benefits of using free $CaCO_3$ solids from Davis WTP as an alkalinity source while eliminating the excess solids that negatively impact the sludge processing at Hornsby Bend.

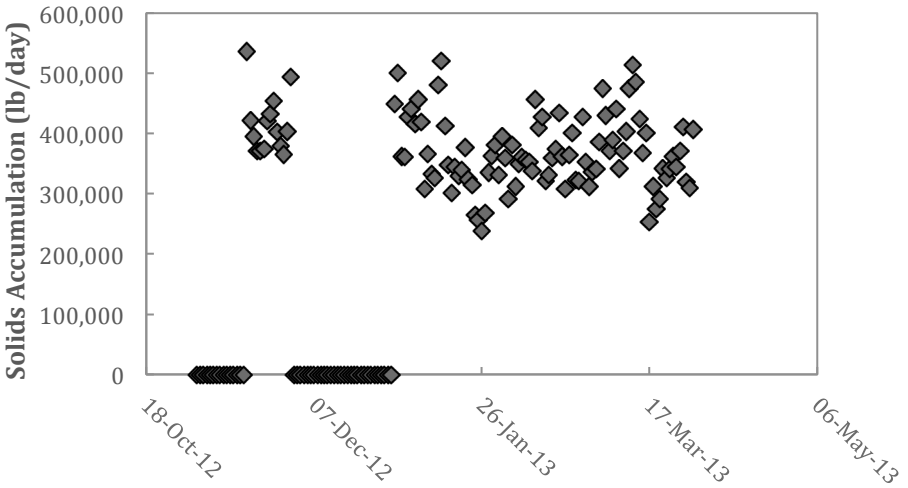

Figure 3.5: Daily Amount of Undissolved Solids that Accumulated at WC

3.3.5: Alkalinity Deficit at Walnut Creek

The final question that was answered was how much alkalinity is required to meet the deficit observed at WC and effectively treat the influent ammonia concentrations. It is important to determine the deficiency for two reasons. First, it is possible that WC requires more alkalinity than the 47 mg/L as $CaCO_3$ that is the maximum equilibrium value that can be provided by the Davis solids. Conversely, the alkalinity deficit might be less than the equilibrium value, so providing 47 mg/L as $CaCO_3$ would be excessive and might lead to other indirect problems.

A spreadsheet developed by Henry Dress, the process engineer at Walnut Creek, was used to estimate the alkalinity deficiency. The methodology of the spreadsheet was based on an alkalinity mass balance, which is expressed in words in Equation 3.14. Median influent concentrations from Walnut Creek data from 2011-2013 were used as inputs into the spreadsheet and are shown in Table 3.7. In addition, standard deviations were calculated to account for both seasonal and daily variations.

$$\begin{bmatrix}\text{Deficit or}\\ \text{Surplus}\\ \text{Alkalinitiy}\end{bmatrix} = \begin{bmatrix}\text{Alkalinity}\\ \text{provided by}\\ \text{Influent}\end{bmatrix} + \begin{bmatrix}\text{Alkalinity}\\ \text{generated by}\\ \text{Denitrification}\end{bmatrix} - \begin{bmatrix}\text{Alkalinity}\\ \text{destroyed by}\\ \text{Nitrification}\end{bmatrix} - \begin{bmatrix}\text{Alkalinity}\\ \text{required in}\\ \text{Effluent}\end{bmatrix} \quad \text{(Equation 3.14)}$$

Table 3.7: Summary of median and standard deviation values for influent and effluent characteristics at Walnut Creek WW from 2011-2013

Parameter	Units	Influent		Effluent	
		Median	Stnd. Dev.	Median	Stnd. Dev.
Flow	MGD	53.0	7.3	49.0	7.5
Alkalinity	mg/L as $CaCO_3$	245	30.2	75*	—
TKN †	mg/L –N	46.7	7.9	—	—
NH_3	mg/L –N	27.4	4.8	0.3	1.1
NO_3^-	mg/L –N	—	—	27.2	11.1
NO_2^-	mg/L –N	<0.05	—	<0.05	—

* Effluent alkalinity is not from data, but rather estimated as required alkalinity to maintain adequate pH conditions.

† TKN = Total Kjeldahl Nitrogen, which is the sum of organic and ammonia nitrogen

Alkalinity destroyed by nitrification and created by denitrification was assumed to be equal to the theoretical values, 7.07 and 3.57 mg as $CaCO_3$ per mg of ammonia, respectively. Since the Walnut Creek WWTP was not designed to denitrify, only a fraction of nitrate is converted to N_2 gas in the pseudo anoxic zones at Walnut Creek. The denitrification efficiency is an important parameter in calculating the alkalinity created by denitrification, but it is difficult to estimate accurately. A nitrogen mass balance, shown in Equation 3.15, was employed to determine the amount of nitrogen that escapes the wastewater treatment plant as N_2 gas.

$$\begin{bmatrix}\text{Influent}\\ \text{TKN}\end{bmatrix}+\begin{bmatrix}\text{Influent}\\ NO_3^-\end{bmatrix}=\begin{bmatrix}\text{Effluent}\\ NH_3\end{bmatrix}+\begin{bmatrix}\text{Effluent}\\ NO_3^-\end{bmatrix}+\begin{bmatrix}\text{Nitrogen}\\ \text{assimilation}\\ \text{by biomass}\end{bmatrix}+\begin{bmatrix}N_2\text{ released}\\ \text{by}\\ \text{denitrification}\end{bmatrix} \quad \text{(Equation 3.15)}$$

For the influent and effluent concentration terms in Equation 3.15, median concentrations as shown in Table 3.7 above were used. The biomass consumption term

was calculated from an estimate of bacterial growth yield using Equation 3.16 (Metcalf and Eddy 2003). Approximations for the constants were taken from Metcalf and Eddy (2003) while substrate data were based on actual influent and effluent BOD concentrations at WC WWTP.

$$P_{x,bio} = 1.6\, Y_{obs}(S_o - S) = 1.6\frac{mg\ bCOD}{mg\ BOD}\left(0.21\ \frac{mg\ biomass}{mg\ bCOD}\right)\left(188\frac{mg}{L} - 2.6\frac{mg}{L}\right)$$

$$P_{x,bio} = 62.2\ \frac{mg\ biomass}{L}$$

(Equation 3.16)

Where:

$P_{x,bio}$ = net biomass growth (mg biomass/L)
Y_{obs} = observed yield (g biomass / g biological COD), 0.21
S_o = influent substrate concentration (mg BOD/L), 188
S = effluent substrate concentration (mg BOD/L), 2.6
1.6 = conversion from BOD to bCOD (biodegradable fraction of the Chemical Oxygen Demand)

If we further assume that the chemical formula for biomass is $C_5H_7O_2N$, which is commonly accepted for wastewater, then 12% of the biomass by weight is nitrogen. Therefore, the amount of nitrogen assimilated by biomass is 7.5 mg-N/L via Equation 3.17.

$$\begin{bmatrix}\text{Nitrogen}\\ \text{consumed by}\\ \text{biomass}\end{bmatrix} = 0.12\, P_{x,bio} = 0.12 \times 62.2\frac{mg\ biomass}{L} = 7.5\frac{mg\ N}{L}$$

(Equation 3.17)

Combining all the terms in the nitrogen mass balance (Equation 3.15) results in 11.5 mg-N/L that is denitrified.

$$[46.7\ mg/L] + [0\ mg/L] = [0.3\ mg/L] + [27.4\ mg/L] + [7.5\ mg/L] + \begin{bmatrix}N_2\ \text{released}\\ \text{by}\\ \text{denitrification}\end{bmatrix}$$

$$\begin{bmatrix}N_2\ \text{released}\\ \text{by}\\ \text{denitrification}\end{bmatrix} = 11.5\ mg/L$$

(Equation 3.18)

Therefore, the denitrification efficiency is 24.6% by dividing the concentration of nitrogen released by denitrification by the total influent nitrogen concentration.

Given the denitrification efficiency calculated above, the original alkalinity balance can now be completed to find the alkalinity deficit. Incorporating all of the aforementioned terms into the alkalinity balance from Equation 3.14 yields an average alkalinity deficiency of -6.3 mg/L as $CaCO_3$. A negative result means that there is no deficit but rather a slight alkalinity surplus when considering the median influent conditions into Walnut Creek over the past two years. This result is surprising because we know that alkalinity is in fact deficient; however, several assumptions were made in determining this value, and so it is possible that there is substantial error associated with the calculation. As an engineering system, it is also important to be conservative, and therefore, for the purposes of finding the deficiency, it is best to consider the deficiency that would occur under a possible scenario where the influent alkalinity concentration is below average and ammonia is above average. The standard deviation was used to adjust the concentrations in order to achieve this conservative scenario; the median alkalinity concentration was reduced by one standard deviation and the median ammonia concentration was raised by one standard deviation. Thus, the alkalinity deficit under this scenario was calculated to be 53.6 mg/L as $CaCO_3$.

To understand the significance of this value, it is compared to the maximum alkalinity that could be provided by the Davis WTP solids, which was estimated above to be 47 mg/L as $CaCO_3$. If the solids are used as the sole alkalinity source, they would not entirely meet the required alkalinity demand under the above conditions, so an additional alkalinity source would be required. It is important to remember that the above deficit value only represents one specific influent condition, so this comparison is not true when

alkalinity and ammonia are in closer balanced. However, since one standard deviation still represents 68% of the representative dates, the frequency at which the deficit would exceed the maximum alkalinity provided by the solids is not insignificant.

2.6 CONCLUSIONS

The Walnut Creek Wastewater Treatment Plant requires a supplemental alkalinity source to maintain a suitable pH level to nitrify increasing ammonia concentrations. The main focus of this report was to better understand how waste lime-softening solids generated at the Davis Water Treatment Plant can play a role in providing a portion of the required alkalinity at zero cost, while ensuring that the Hornsby Bend biosolids operations remain effective and efficient. This objective was accomplished by first analyzing historical data from the time periods the Utility authorized the wasting of the solids, and then developing an equilibrium model to determine the theoretical maximum amount of solids' dissolution.

The solids can be transferred from Davis WTP by two streams: equalization tank overflow which had a concentration of approximately 12% solids and centrate at approximately 1% solids. The overflow was calculated to contribute an average of 395,000 lb/day of solids, of which only 5.4% could dissolve to provide 17.6% of the total alkalinity at WC WWTP. The centrate waste stream was predicted to have a smaller impact, contributing an average of 7,250 lb/day of solids. Even though it was found that all the centrate solids dissolved, this alkalinity benefit was only 7.2% of the total WC alkalinity. Using the developed equilibrium model, the maximum concentration of $CaCO_3$ solids that could dissolve at equilibrium is 47 mg/L as $CaCO_3$.

Since this portion of the research was based on theoretical calculations (with several assumptions and simplifications), it is important to verify the results of the model using experimental methods. In addition, it is necessary to understand the kinetics of the $CaCO_3$ dissolution reaction for this situation. The theoretical model only explains equilibrium conditions, but with no sense of how fast the dissolution occurs, it is unclear whether equilibrium will ever be reached during the time it takes for the solids to travel from Davis DWTP to WC. The following chapter details the experimental study used to test these two concerns.

Chapter 4: Calcium Carbonate Dissolution Experiments

4.1 INTRODUCTION

Between 2011 and 2013, the City of Austin Water Utility had utilized lime-softening solids generated at the Davis Drinking Water Treatment Plant (DWTP) to provide supplemental alkalinity to the influent wastewater at Walnut Creek Wastewater Treatment Plant (WC). The use of these solids greatly benefited the treatment operations at WC especially in terms of nitrifying an increased influent concentration of ammonia. However, undissolved solids accumulated and decreased the efficiency of the anaerobic digestors Hornsby Bend Biosolids Management Facility. It is believed that the flow of solids can be optimally managed so that they can still be used to provide a cost effective alkalinity source while not harming the biosolids treatment operations.

As discussed in Chapter 3, the maximum quantity of calcium carbonate ($CaCO_3$) solids that can dissolve at equilibrium in wastewater was calculated as 47 mg/L. Analysis of operational data from Davis DWTP and WC WWTP, shown in Chapter 3, made it clear that indeed, the amount of solids that were being added to WC was in great excess compared to the amount required to meet the alkalinity deficit. To verify the results of the theoretical modeling in Chapter 3 and to better understand the dissolution kinetics, experimental laboratory studies were proposed. The bench-scale experiments would mimic the conditions of the wastewater at WC and test the amount of calcium carbonate that could dissolve.

This chapter describes the methods and results of these experimental dissolution tests. In general, the jar tests mixed $CaCO_3$ from Davis DWTP with wastewater samples at varying initial concentrations and under various wastewater conditions. Observed dissolution was measured over time. Section 4.2 contains a literature review, which

provides background information about dissolution kinetics and modeling of $CaCO_3$. Section 4.3 outlines the methodology and procedures of the jar tests while Section 4.4 discusses the experimental results. Finally, the conclusions and recommendations can be found in Section 4.5.

4.2 LITERATURE REVIEW

4.2.1 Basics of Dissolution Kinetics

Precipitation and dissolution of calcium carbonate ($CaCO_3$) have been well studied because $CaCO_3$ plays an important role in sedimentology, oceanography, and limnology fields as well as in water treatment and energy generation applications (Hamza and Hamdona 1992). The precipitation or dissolution reaction for $CaCO_3$ is described by (Equation 4.1) and is governed by the equilibrium expression shown in (Equation 4.2):

$$CaCO_{3_{(s)}} \leftrightarrow Ca^{2+} + {CO_3}^{2-}$$

(Equation 4.1)

$$K_{sp} = (a_{Ca^{2+}})(a_{{CO_3}^{2-}})$$

(Equation 4.2)

where K_{sp} is the solubility product equilibrium constant and a_i is the activity of the respective ions within the solution. The K_{sp} for $CaCO_3$ is $10^{-8.35}$ (Morel and Hering 1993). In dilute solutions, it is commonly assumed that the activity of the ions is equal to the molar concentrations of the ions in solution as in Equation 4.3.

$$K_{sp} = [Ca^{2+}][{CO_3}^{2-}]$$

(Equation 4.3)

The product of the ion concentrations in a given solution, Q, can be compared to the K_{sp} to determine the degree of disequilibrium and whether dissolution or precipitation

will occur. If Q equals K_{sp}, then the solution is at equilibrium and no net change in the solution will occur. When Q is less than K_{sp}, the system is undersaturated and solid $CaCO_3$ (if any is present) will dissolve until equilibrium conditions are met. Similarly, when Q is greater than K_{sp}, the system is oversaturated and precipitation will occur.

The kinetics of dissolution or precipitation reactions are generally expressed by the degree of disequilibrium; that is, the rate decreases as the reaction moves closer to equilibrium. The standard rate expression is:

$$r_d = k_d\left(K_{sp} - Q\right)^n$$

(Equation 4.4)

where r_d is the rate of dissolution, k_d is the dissolution rate coefficient, and n is the reaction order. The logarithmic form of Equation 4.4, shown as (Equation 4.5, is in the form of a linear equation.

$$\log r_d = n \log\left(K_{sp} - Q\right) + \log k_d$$

(Equation 4.5)

The rate coefficient and reaction order can then be determined empirically by plotting $\log\left(r_d\right)$ versus $\log\left(K_{sp} - Q\right)$. The resulting slope is the reaction order, n, and the y-intercept is equal to $\log\left(k_d\right)$ (Morse 1983).

Although the empirical method of determining dissolution kinetics discussed above is simple, it does not provide further understanding of the specific mechanism or the effects that external factors have on the dissolution kinetics. For more in-depth analysis, a dissolution model can be developed. The goal of such a model is to determine what aspect of the dissolution is the rate-limiting step and therefore controls the overall reaction rate under different physical and chemical conditions. Given that $CaCO_3$ is subject to carbonate acid-base chemistry, determining the rate-limiting pathway given the

environmental conditions is quite complex (Morse 1983). Plummer et al. (1978) found three main dissolution mechanisms and the regions at which each dominates the rate based on the pH and partial pressure of CO_2 (pCO_2) of the system. These mechanisms are explained by the following three reactions:

$$H_2O + CaCO_{3(s)} \rightarrow Ca^{2+} + {CO_3}^{2-}$$

(Equation 4.6)

$$H^+ + CaCO_{3(s)} \rightarrow Ca^{2+} + {HCO_3}^-$$

(Equation 4.7)

$$H_2CO_3 + CaCO_{3(s)} \rightarrow Ca^{2+} + 2{HCO_3}^-$$

(Equation 4.8)

In addition to the chemical equilibrium kinetics, physical factors, such as temperature and diffusion, also can impact dissolution and precipitation rates. Most importantly is the rate of transport (primarily by diffusion) of solutes back and forth between the bulk solution and the crystal surface through an interfacial boundary layer. When dissolution is near equilibrium, the surface reactions slow down and limit the overall reaction rate. However, far from equilibrium the surface reactions are quite fast, and the diffusion-controlled rate limits the overall reaction. Mixing the bulk solution increases transport and lowers the impact that diffusion-controlled rates have on the overall kinetics (Morse 1983).

4.2.2 Inhibitory Factors

The description given above only focuses on dissolution of $CaCO_3$ in simple solutions, but since the goal of this research is to understand $CaCO_3$ dissolution in wastewater, it is important to also consider dissolution in complex solutions. The most

important difference between simple and complex solutions is the presence of additional constituents in the water that inhibit dissolution, and thus decrease the rate of dissolution. Foreign ions can inhibit dissolution in two main ways: by adsorbing to the crystal surface and blocking reaction sites, or by influencing the solution chemistry and therefore changing the activity coefficients of the reaction ions. The most intensively studied inhibitors for $CaCO_3$ include dissolved magnesium (Mg^{+2}), phosphate (PO_4^{-3}), sulfate (SO_4^{-2}), and in some cases, organic matter (Morse 1983).

To understand how foreign ions inhibit crystal growth and dissolution, it is first important to understand how a crystal grows and dissolves. For $CaCO_3$, crystal growth can be modeled using the Burton, Cabrera, and Frank (BCF) conceptual model of the crystal surface (Morse 1983). The BCF model, shown in Figure 4.1, assumes the crystal is portioned into blocks. Visualizing the crystal as blocks allows us to easily define steps and kinks, where a step is an edge along the crystal surface, and a kink is an empty space within the step face. Kinks and steps provide heterogeneous active energy sites at which the crystal can grow or dissolve. For example, in precipitation, the crystal grows by building off the kink, to form a new step, which subsequently forms a new crystal layer. In contrast, dissolution occurs when blocks adjacent to the kink are removed into the bulk fluid. As the crystal dissolves, the steps recede revealing new kinks in crystal layers to continue the dissolution process. However, inhibitors can sorb to the active kink sites, and immobilize the progression of step formation. Inhibitor ions are shown as black spheres in Figure 4.1 (Burton et al. 1951).

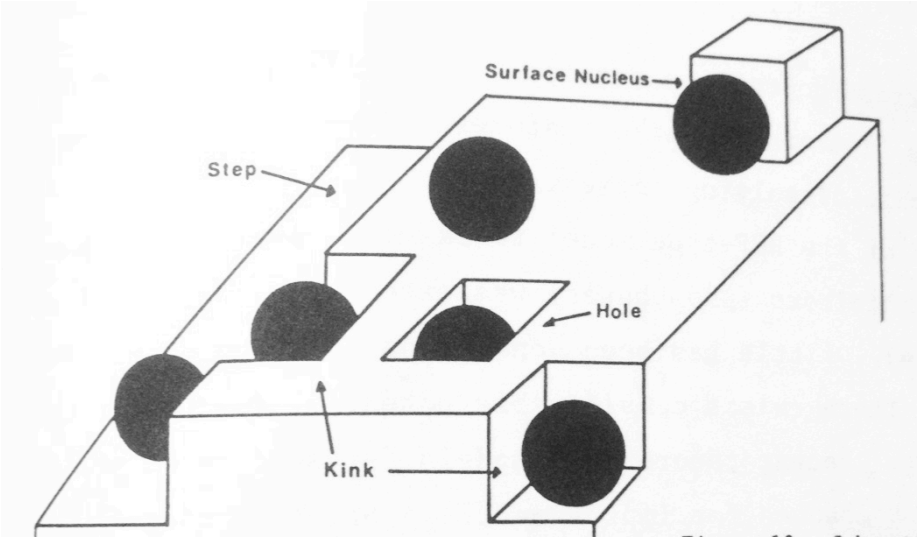

Figure 4.1: BCF Conceptual Diagram of a Crystal Structure [from (Morse 1983)**]**

Each inhibitor might impact the dissolution or precipitation rate in different ways. The most commonly studied inhibitor is Mg^{+2}. Of the many theories on how Mg^{+2} inhibits growth, the most favorable is crystal growth due to poisoning of the crystal surface by Mg^{+2} adsorption (Folk 1974; Reddy and Wang 1980). Sjörberg (1978) found that the sorption of Mg^{+2} onto the surface of $CaCO_3$ can be described by the Langmuir isotherm. Since Mg^{+2} has a smaller atomic radius, Folk (1974) found that, when it sorbs to the edge of a $CaCO_3$ crystal, the upper and lower carbonate sheets must crunch up at the edges, which limits growth in the latitudinal direction. Therefore, when magnesium is present, $CaCO_3$ crystal growth is restricted in all directions except up and down, resulting in a needle-like crystal structure. In contrast, rapid precipitation rates and a low Mg:Ca ratio allow for fast sideward growth that results in the formation of hexagonal step crystals that are approximately 10 μm in diameter (Folk 1974). Figure 4.2 illustrates these changes in $CaCO_3$ crystalline structure in the presence and absence of magnesium.

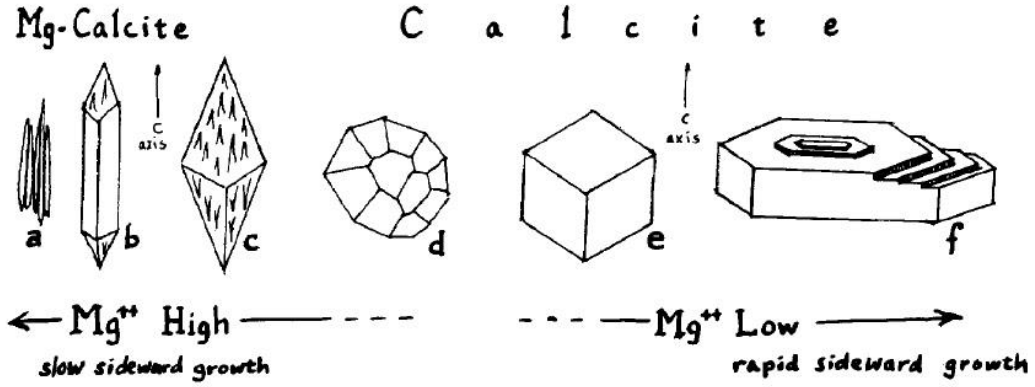

Figure 4.2: Diagram of structure properties depending on Mg [from (Folk 1974)]

4.3 EXPERIMENTAL METHODS

To determine the possible amount of $CaCO_3$ that would dissolve in the wastewater collection system, bench-scale jar test experiments were conducted. The experimental conditions of each jar test were varied to mimic the variations of the wastewater in the collection system. Specifically, initial solid $CaCO_3$ concentration, atmospheric conditions, and wastewater characteristics of the sample were varied throughout the tests. A summary of the individual tests and the analyses performed during each test is in Table 4.1. Throughout the jar tests, chemical parameters such as alkalinity, pH, and calcium ion concentration were measured at specific time intervals. As a deeper understanding was obtained from previous tests, the procedure was altered to test specific hypotheses. For example, in Jar Test 5, sulfide concentrations were measured and Scanning Electron Microscopy (SEM) with Energy Dispersive X-ray Spectrometry (EDX) was used to further understand the solid composition. To account for the different procedures for each set of jar tests, an overview of the general jar test procedure is provided followed by the analytic methods used to measure certain parameters. Specific variations between tests are noted.

Table 4.1: Summary of Calcium Carbonate Dissolution Tests and Analytical Procedures

Jar Test	Date	Water Source	$CaCO_3$ Solids Source	Analyses Conducted				
				pH	Ca^{+2}	Alkalinity	SEM/ EDX	Sulfide
1	10/23/13	DI water	Lab grade	✓	✓			
2	11/13/13	DI water	Davis Solids	✓	✓			
3	11/25/13	SAR Raw Influent, C	Davis Solids	✓	✓			
4	12/18/13	WC Raw Influent	Davis Solids	✓	✓	✓		
5	2/12/14	WC Raw Influent	Davis Solids	✓	✓	✓	✓	✓
6	3/26/14	WC Raw Influent	Davis Solids	✓	✓	✓		

4.3.1 Dissolution Test

The dissolution experiments were conducted using Plexiglas reactors of dimensions, 4.5in x 4.5in x 4.5in. The reactors had matching floating lids that sealed the contents of the reactor from atmospheric influences. A jar test mixer with paddles was used to continuously mix the reactors, keeping the solid particles in suspension. The jar tester was set to a speed of approximately 70 rpm, and was monitored throughout the experiments to maintain a constant speed. The typical jar test setup is shown in Figure 4.3.

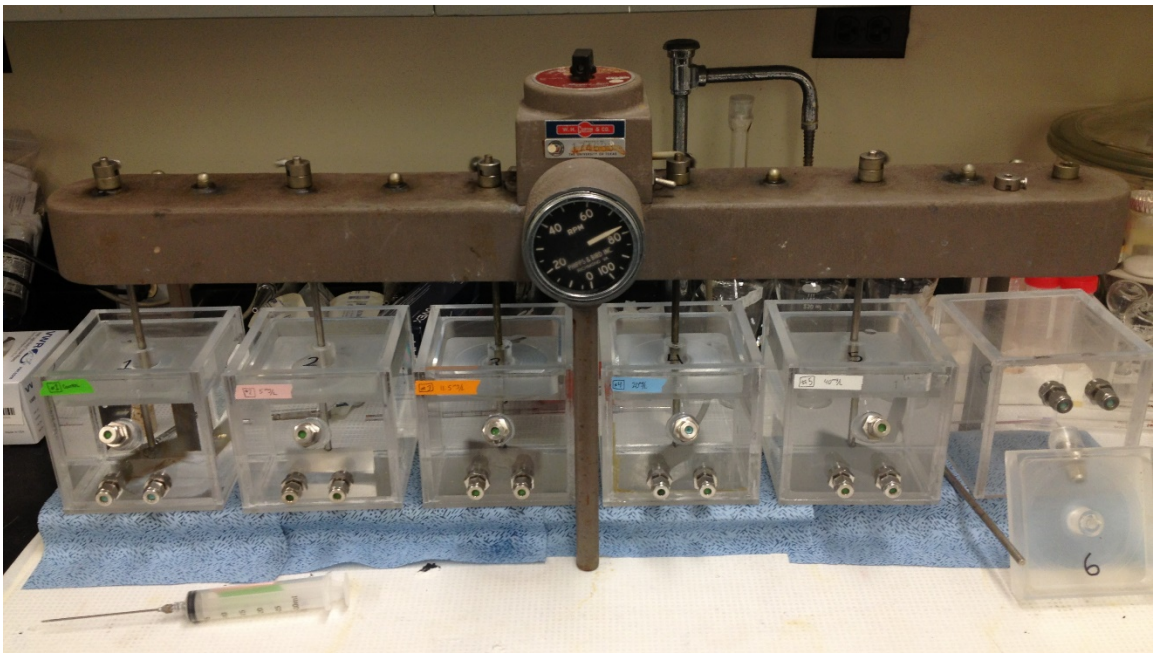

Figure 4.3: Jar Test Apparatus

A total of 1250 mL of liquid was added to each reactor and quickly sealed from the environment in the case of non-aerated reactors at the zero hour point. In Jar Test 1 and 2, Millipore water was used to verify the theoretical model described in Chapter 3. Raw influent wastewater from South Austin Regional (SAR) WWTP was used in Jar Test 3 and wastewater from Walnut Creek (WC) WWTP in Jar Tests 4 through 6. For jar tests 3 and 4, wastewater samples were collected approximately 24 hours before the start of the experiment and stored at 4ºC to limit biological activity. After realizing that, despite refrigeration, the wastewater characteristics changed during the 24 hours between sampling and the experiment, wastewater for Jar Tests 5 and 6 was collected only 1 to 2 hours prior to the start of the experiment.

Each reactor contained a desired concentration of $CaCO_3$ that was added to the reactor and wastewater at the same initial time. Jar Test 1 was conducted with laboratory

grade $CaCO_3$ (Sigma-Aldrich 99%) as a point of comparison. All other Jar Tests used lime-softening solids collected from the sedimentation basins at the Davis Water Treatment Plant. As shown in Chapter 3, the solids concentration on the day sampled from Davis WTP was measured to be 131,000 mg/L and consists primarily of $CaCO_3$. The dilution equation (Equation 4.9) was used to determine the volume of solids' slurry needed to achieve the desired $CaCO_3$ concentration of the reactor. Given the high solids concentration of the original sample, the necessary volume ranged from 0.17 mL to 1.91 mL for desired reactor concentrations of 17.5 mg/L to 200 mg/L. To insure that the slurry was homogenous, it was continuously mixed with a magnetic stir plate as the desired aliquot was drawn. Such small volumes could be a potential source of error, but the success of the test hinges on the relative change in dissolved solids and not the absolute concentrations themselves, so this error should not critically impact the results.

$$Vol_{solids} = \frac{Vol_{wastewater} \times Desired\ Conc.}{Solids' Conc.} = \frac{1250\ mL \times Desired\ Conc.}{131{,}000 mg/L} \quad \text{(Equation 4.9)}$$

The concentrations of solids that were initially added to each reactor were selected based on the theoretical equilibrium model predictions and analysis of the influent wastewater to determine the required need or alkalinity deficit, which was described in Chapter 3. In all jar tests, a control reactor was included in which no solids were added to the reactor solution as a base comparison. From Chapter 3, the equilibrium model predicted that 11.5 mg/L and 47 mg/L of solids would dissolve in a closed environment for Millipore water and influent wastewater, respectively. These equilibrium values were included in the test as initial solids concentrations. In addition to the equilibrium values, initial solids concentrations well above the equilibrium concentration

were included. It would be expected that regardless of the initial solids concentration, the solids of any reactors above would only show dissolution up to the equilibrium concentration. Therefore, including these higher concentrations was an additional method to verify the model predictions.

The alkalinity deficit was a critical concentration to test. In Chapter 3, the alkalinity deficit at WC under the conservative assumptions that alkalinity is one standard deviation less than the median while the ammonia concentration is one standard deviation above the median was found to be 53.6 mg/L as $CaCO_3$. To account for possible error in the deficit estimation, the deficit concentration was rounded down to 40 mg/L as $CaCO_3$ so that it more closely represented the median conditions. Since the 40 mg/L deficit was very close to the 47 mg/L equilibrium value, only the 40 mg/L was tested because it was more relevant to the objectives. In jar tests using wastewater, an additional reactor solids concentration of 17.5 mg/L was included, which was calculated to be the minimum concentration of solids provided continuously by Davis DWTP via the centrate waste stream. Lastly, in order to fill any gaps in initial concentrations, additional reactors were added to the testing plan. Table 4.2 shows a summary of the initial solids concentrations added for each reactor using both Millipore water and raw influent wastewater.

Table 4.2: Davis Solids' Concentrations Initially Added Depending on Water Type

Reactor	Millipore water (mg/L)	Wastewater (mg/L)
1	0	0
2	5	17.5
3	11.5	40
4	20	100
5	40	200

Once the initial $CaCO_3$ solids concentrations were added to the reactor, the mixer was started and the experiments began. To monitor changes in the solution characteristics, samples of solution were taken from the reactor for analysis at 0, 0.5, 1, 2, 4, 6, 10 hours. For jar tests 5 and 6, a 24-hour sample time was added. Since the idea was trying to mimic the conditions of dissolution as the solids travel from Davis WTP to Walnut Creek WWTP, the sampling intervals were determined based on the estimated detention time of the wastewater collection system of approximately 6 hours. More samples were taken in the early stage to monitor rapid changes in solution composition. Finally, the start times of the parallel reactors were offset by five minutes to stagger the sampling times and allow enough time to analyze all the samples directly after collection.

Samples were taken from the reactor using a syringe and needle. This technique allowed sample collection through septum ports built into the reactor as shown in Figure 4.3, so as to limit the amount of atmospheric interaction with the solution that could occur if the reactor lids were removed. Once collected, the pH of the sample was measured using an Orion pH probe and meter. Samples were then filtered through a 0.45 μm nylon filter to remove particles. Concentrated nitric acid was added as well as Millipore water to dilute and preserve the sample before analyzing it for Ca^{+2} ion using a Varian 710-ES Inductively Coupled Plasma (ICP) Optical Emission Spectrometer. For select jar tests, additional analysis of samples for alkalinity, sulfide, and solids' properties was conducted. Alkalinity was measured in accordance with Standard Methods and is detailed in section 4.3.3. General methods for the Sulfide Analysis and SEM/EDX can be found in greater detail in Appendix B.

4.3.2 ICP Analysis

Inductively Coupled Plasma Spectrometry (ICP) is an analytical technique to measure metals in water samples. An ICP excites metal ions using a high-temperature plasma. The excited ions release a specific wavelength of light, which is absorbed by the instrument. Using Beer's Law, the amount of light absorbed is directly related to the concentration of the metal in the solution by a linear relationship. The benefits of using ICP for metal analyses instead of Atomic Adsorption techniques is the ability to analyze multiple metals at multiple wavelengths simultaneously and a lower detection limit.

To obtain accurate results from the ICP, samples must be prepared in particular ways to protect the instrument and preserve the sample. Filtering the sample removes particles that could clog or damage the ICP. Adding acid ensures that metals in the sample are stable ions in solution and do not form precipitates in between filtration and analysis. Concentrated (69-70%) ACS Grade Nitric Acid was added to each sample for this purpose. Generally, lowering the pH of the sample below pH 1 is enough to ensure preservation. This procedure was used in jar tests with Millipore water (Tests 1 and 2), where only 0.1 mL of acid was added. However, in more complex solutions like wastewater, more acid must be added so that the solution is also stable from a thermodynamic perspective. Therefore, in all other jar tests using wastewater, acid was added to achieve a 3% by volume concentration in the sample, which is the maximum acid concentration that the ICP can tolerate.

In addition to acid, Millipore water was added to dilute each sample. The purpose of dilution is to ensure that the Ca^{+2} concentrations are lowered to the point where they fall within the linear range of the ICP's standard curve for calcium. No dilution was necessary in jar test samples using Millipore water (Test 1 and 2), but, due to the high

background concentration of Ca^{+2} in the wastewater, a dilution of 1 to 20 was used for all other jar test samples. If the sample is diluted 1:20 directly after sampling and before the addition of the acid, then there is a possibility that the true sample Ca^{+2} concentration is misrepresented since some Ca^{+2} might still be bound in a precipitate. Therefore, the 1:20 dilution was completed in two steps: a 1:2 dilution followed by a 1:10 dilution. The determined volumetric acid and Millipore water additions are shown in Table 4.3 for wastewater jar tests. Two and a half milliliters of filtered sample were mixed with 1.5 mL of acid and 1 mL of DI to produce the first dilution at 1:2. The first dilution allowed all calcium species to dissolve and stabilize thermodynamically in the presence of excess acid. After sitting overnight at 4°C, the sample was assumed to be more homogenous and thus could be diluted 1:10 using Millipore water without concern for additional error.

Table 4.3: Volumetric Acid and Millipore Water (mL) added to each sample in two-step dilution process for ICP analysis.

	1st Dilution	2nd Dilution
Sample	2.5	
Acid	1.5	
Millipore	1	9
1:2 Dilution	0	1
Dilution Factor	2	10

Calcium ion standards were created at concentrations of 0, 1, 2, 3, 4, and 6 mg/L from a 1000 mg/L Ca^{+2} reference solution to create a standard curve. A typical standard curve is shown in Figure 4.4. According to Standard Methods, the ideal wavelength to measure Ca^{+2} using ICP is 317.93 nm (APHA et al. 2005). In addition, wavelengths 393.37 nm 396.85 nm, and 422.67 nm were selected since they showed the highest

absorbance. A standard curve for each wavelength was constructed and used to determine the Ca^{+2} concentration of each sample. All standard calibration curves had an R^2 value above 0.99, indicating very accurate results. Ca^{+2} concentrations for all wavelengths were averaged to reduce wavelength bias. Finally, for wastewater samples that were diluted 1:20, the outputted concentration was multiplied by 20 to achieve the actual concentration in the reactor.

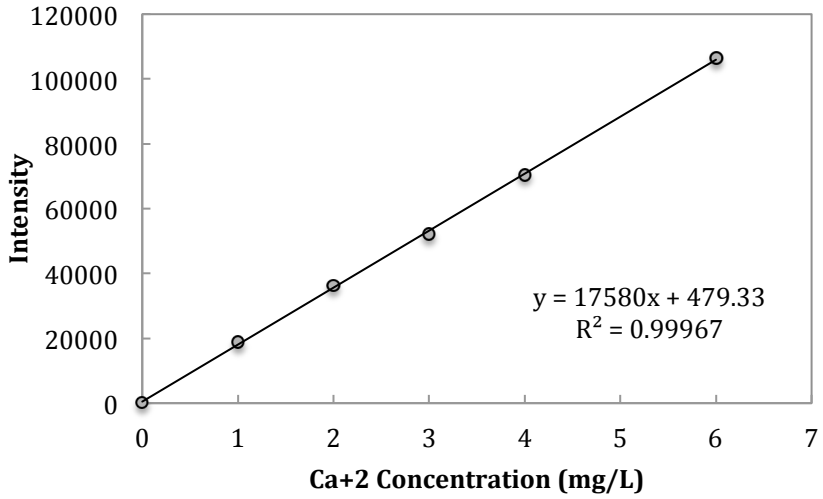

Figure 4.4: Typical Standard Curve at wavelength of 317.93 nm

4.3.3 Alkalinity

Alkalinity was only measured in jar tests 4, 5, and 6 and was accomplished with the titration method described in Standard Methods 2320 (APHA et al. 2005). For Test 4, the alkalinity of each reactor was only taken at the beginning and conclusion of the experiment, while for jar tests 5 and 6, it was measured throughout the test at time intervals 0, 0.5, 1, 2, 6, and 24 hours for each reactor. The volume of sample titrated was 10 mL for Tests 4 and 5 and 20 mL for Test 6. The titrating acid was 0.01 N hydrochloric acid and was standardized using 0.05 N Na_2CO_3 as per Standard Methods. Lastly, to

remove solids that might dissolve and lead to misrepresentative alkalinity values, Jar Test 6 samples were centrifuged for two minutes at 1500 rpm, and the supernatant was used for alkalinity measurements.

4.4 Results and Discussion

The results of all six jar tests are discussed in the following section and are organized not necessarily in order but by their intended purpose and findings. First, results from Jar Test 1 and 2 show how dissolution of $CaCO_3$ solids in Millipore water closely matched the predicted model equilibrium. After that, jar tests measuring dissolution in Walnut Creek wastewater are shown, including comparisons between varying aeration conditions. Finally, the results of the solids' analysis using SEM and EDX are discussed to gain a deeper understanding of the composition of the solids and the chemistry occurring in the reactors.

Initial conditions of the water in all six jar tests are shown in Table 4.4. All wastewater samples showed considerable variation in initial conditions, which is expected given the variable nature of wastewater. On any given day, depending on how users interact with the system, these conditions can dramatically change. It is important to note the changes in dissolved calcium and alkalinity because these concentrations directly impact the possible dissolution of $CaCO_3$ solids following Equation 4.3; namely, higher concentrations of either compound could lead to less dissolution. According to Metcalf and Eddy, it is common in most wastewater systems to see Ca^{+2} concentrations in influent wastewater to increase by 6-16 mg/L above the average concentration in drinking water. In the third quarter of 2013, the City of Austin Water Utility reported an average Ca^{+2} concentration of 10 mg/L in the drinking water, so it was expected that the maximum influent wastewater calcium concentration would be near 26 mg/L.

Table 4.4: Summary of Initial Water Conditions for each Jar Tests

Jar Test	Date	Water Source	$CaCO_3$ Solids Source	Initial Water Characteristics			
				Alkalinity (mg/L as $CaCO_3$)	BOD (mg/L)	TSS (mg/L)	Ca^{+2} (mg/L)
1	10/23/13	Millipore water	Lab grade	0	0	0	0
2	11/13/13	Millipore water	Davis Solids	0	0	0	0
3	11/25/13	SAR Raw Influent, C	Davis Solids	290	--	204	40.4
4	12/18/13	WC Raw Influent	Davis Solids	229	312	160	52.8
5	2/12/14	WC Raw Influent	Davis Solids	250	--	--	49.9
6	3/26/14	WC Raw Influent	Davis Solids	270	--	--	38.3

As shown in Table 4.4, Ca^{+2} of the wastewater tested was approximately 1.5 times the expected concentration. The difference could be attributed to the limestone bedrock underlying Austin, which would lead to highly alkaline and Ca^{+2} concentrated groundwater to infiltrate into the wastewater collection system. Weather is an important factor that contributes to the variation in calcium and alkalinity concentrations seen in the wastewater. After rain events, the ground water level rise would cause an increase in infiltration into the wastewater collection system. Jar Test 4 showed the highest Ca^{+2} concentration and was hypothesized by city engineers to be attributed to high groundwater infiltration.

4.4.1: $CaCO_3$ Dissolution in Millipore Water

The purpose of measuring the dissolution in Millipore water was to ensure the effectiveness of the experimental procedure by comparing experimental results to the expected model predictions as calculated in Chapter 3. We expect that the model results should be quite close to experimental results since the solution matrix using Millipore water is much simpler compared to wastewater, so modeling it is much less difficult. pH

measurements and Ca^{+2} concentration results from Jar Test 2 are shown in Figure 4.5 A and B, respectively.

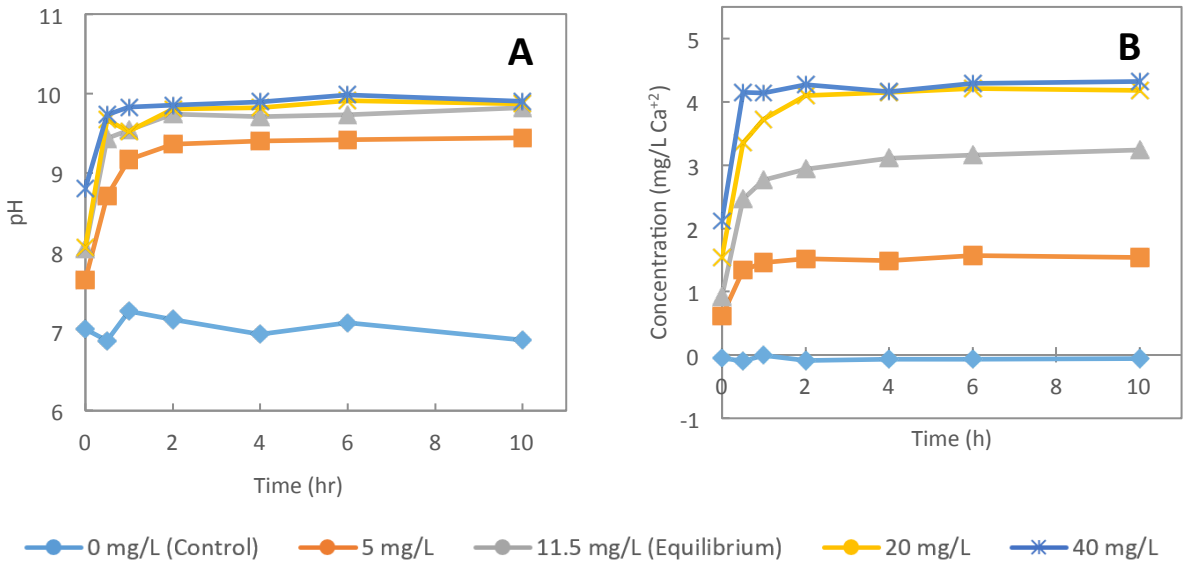

Figure 4.5: pH (A) and Ca^{+2} Concentration (B) from Jar Test 2 (Millipore Water and Davis Solids) for varying $CaCO_3$ concentrations.

The pH and the Ca^{+2} concentration of the control reactor remained unchanged at pH 7.0 and 0 mg/L, which is expected as the control, and shows that neither the reactors nor the experimental procedure have influence on the solution chemistry. All reactors containing added $CaCO_3$ solids show a dramatic increase in pH and some increase in Ca^{+2} concentration, which indicates that dissolution of the solids was occurring. Further, we can clearly see that the equilibrium pH and concentration, the values at which the data plateau, are a function of the initial solids addition. Larger amounts of added solids result in more dissolution and thus a higher pH and a higher Ca^{+2} concentration. All reactors reached their steady-state concentration within the first 2 hours, which is promising

because it suggests that the solids could completely dissolve within the detention time of the wastewater collection system and thus provide the maximum alkalinity possible.

According to the model, the equilibrium pH and dissolution of initial solids were predicted to be 9.91 and 11.5 mg/L. The 20 and 40 mg/L reactors are both oversaturated with respect to equilibrium and thus only 11.5 mg/L of solids are expected to dissolve in both reactors. As seen in Figure 4.5 B, the observed Ca^{+2} concentrations at equilibrium are the same in both the 20 and 40 mg/L reactor confirming the expectations. Moreover, the 40 mg/L reaches the equilibrium concentration within 0.5 hours, while the 20 mg/L reaches equilibrium in 2 hours. It is unclear why the rate is faster since the kinetic expression is not dependent on the amount of solids, so it could just be error.

To compare model results to the experimental results accurately, the observed experimental Ca^{+2} concentrations were plotted as a percentage of expected dissolution. Using the predicted model equilibrium of 11.5 mg/L solids, reactors with 5 and 11.5 mg/L solids were expected to completely dissolve, while reactors with 20 and 40 mg/L were only expected to dissolve up to the equilibrium value. Dividing the observed concentration by the expected concentration yields the results shown in Figure 4.6. Since no dissolution was expected to occur in the control sample, these data are not included in Figure 4.6. If the model predicted the experimental results without any error, all reactors would reach 100% of the expected dissolution by 10 hours. Unfortunately none of the reactors reach 100% dissolution; however, all reactors achieved at least 80% of the expected dissolution, and all except the 5 mg/L initial solids reactor achieved at least 90%. These results confirm that dissolution is occurring in the reactors and matches the predicted equilibrium closely.

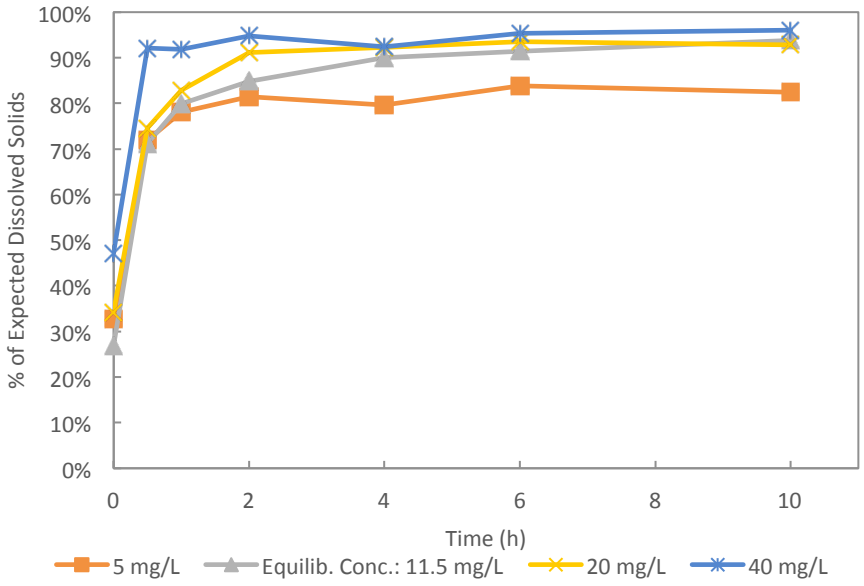

Figure 4.6: Jar Test 2 results shown as a percent of expected dissolution.

4.4.2: Jar Test Dissolution in Walnut Creek Wastewater

Jar Tests 4, 5, and 6 were conducted using WC wastewater as the reactor solution. Jar Test 3 is not shown since it was a test condition to make sure the procedure was accurate and used SAR wastewater, which cannot be compared to the rest of the jar test results using WC wastewater. Not only do these tests help determine whether dissolution of $CaCO_3$ solids from Davis WTP are dissolving as expected, but also we can gain an understanding of how quickly the dissolution occurs and whether this time falls within the detention time of the wastewater collection system. Results from Jar Test 4 and 5 are presented together since they are very similar and provide a clear description of how the solids interact with wastewater in an environment closed to atmospheric effects. In comparison, results from Jar Test 6, which was slightly aerated, are shown to demonstrate the influence of an open environment on dissolution.

Measurements of pH are shown in Figure 4.7 A and B for Jar Test 4 and 5, respectively. In general, the pH decreases throughout the duration of the test for all reactors. The decrease in pH is also observed in the control reactor in both tests, which indicates that the decrease is attributed to a change in the wastewater characteristics and not necessarily the addition of the solids. In fact, as the concentration of added $CaCO_3$ solids increases, the effects of the pH decrease are offset. We can see that the pH values at the final time point fall in order of initial solids concentration—the highest final pH is seen in the reactor with 200 mg/L of solids while the lowest final pH is seen in the control reactor. Slight exceptions are present and could explained by laboratory error. It is believed that some dissolution is occurring to offset the decrease in pH.

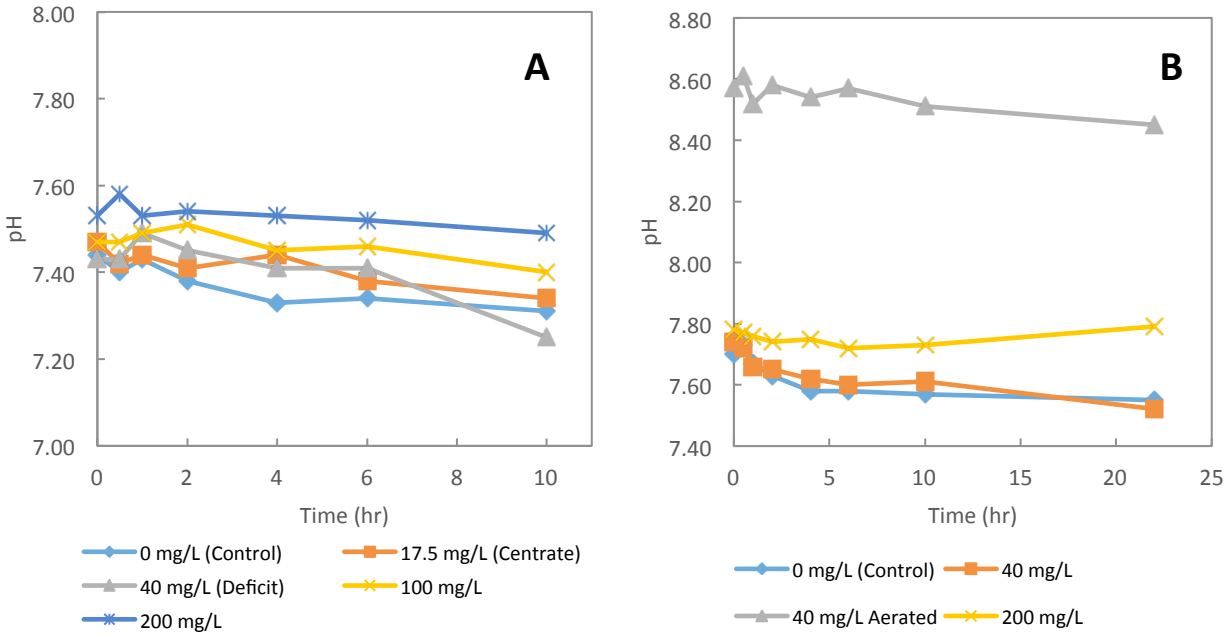

Figure 4.7: pH results for Jar Test 4 (A) and 5 (B) (WC Wastewater and Davis Solids) for varying initial $CaCO_3$ concentrations.

One possible explanation for the decrease in pH could be a build-up in CO_2, which is produced by microorganisms present in the wastewater. When open to the atmosphere, dissolved CO_2 gas would reach equilibrium with the concentration of CO_2 in the air. The expected equilibrium CO_2 concentration of the water would then be $10^{-5.0}$ M. However, since these reactors were closed to the atmosphere, the dissolved CO_2 concentration can become oversaturated with respect to the atmosphere. CO_2 forms a weak acid, H_2CO_3, in water; thus, as CO_2 concentrations increase in the water, we would expect the pH to decrease. For comparison, the pH of the aerated reactor in Jar Test 5 (Figure 4.7 B, triangle points) is an entire pH unit higher than the reactors closed to the atmosphere. Here, the aeration stripped oversaturated CO_2 from the reactors, resulting in the higher pH.

The results from the ICP analysis for calcium concentrations, seen in Figure 4.8, do not show conclusive evidence of significant dissolution of $CaCO_3$. In fact, there seems to be a general decreasing trend in aqueous calcium in Jar Test 4 (Figure 4.8 A) while the concentrations observed in Jar Test 5 (Figure 4.8 B) remain unchanged. In Figure 4.8 A, the decrease in concentration of all reactors was approximately 4 mg/L over the course of the test. All reactors except the 100 mg/L show a slight increase in Ca^{+2} between 6 and 10 hours. Jar Test 5 was extended to 22 hours, but does not show the continuation of a similar increasing trend after 6 hours. Similar to the pH, the aerated sample (Figure 4.8 B, triangle points) does not match the other reactors that were closed to the atmosphere. The concentration of this reactor steadily increased by approximately 6 mg/L over the 22-hour period. The effect of aeration is discussed in further detail later.

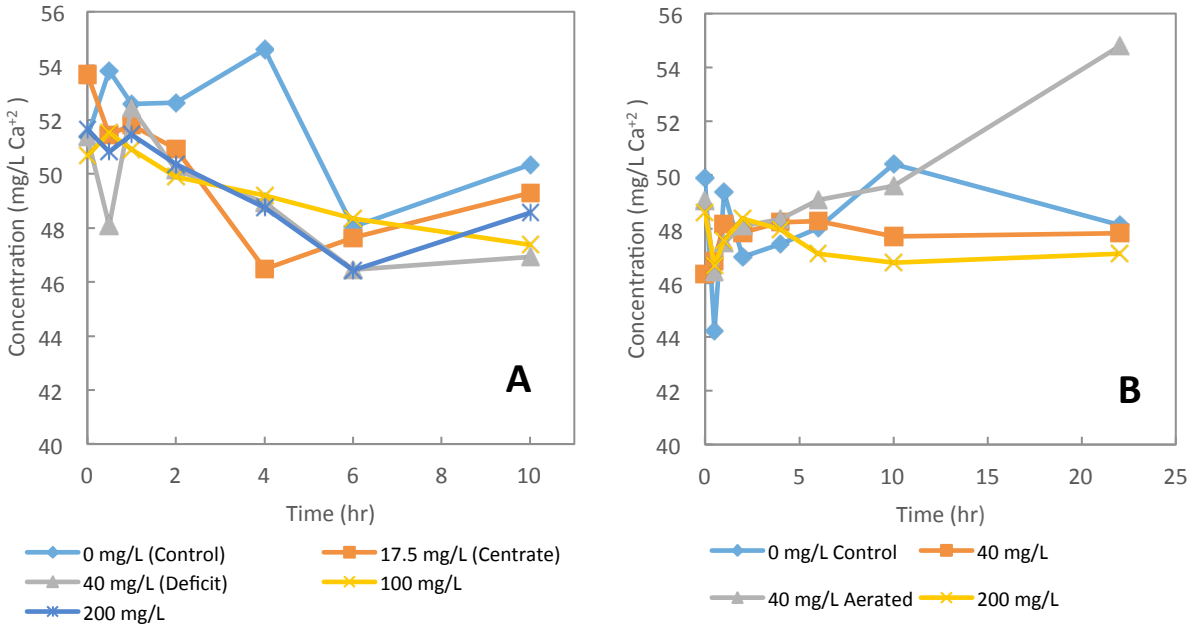

Figure 4.8: Observed Ca^{+2} Concentrations for Jar Test 4 (A) and 5 (B) (WC Wastewater and Davis Solids) for varying initial $CaCO_3$ concentrations.

As seen in both sets of data, the concentrations seem to vary with time in each reactor. In some cases, it is possible to discern minor trends. For example, in Figure 4.8 B, all reactors show initial decreases in Ca^{+2} before rebounding to their initial concentration. It is difficult, however, to draw any concrete conclusions from these minor variations. Most likely these variations should be considered as noise due to procedural error such as not having a completely homogenous sample or errors in measuring the sample volume that get exacerbated by the dilution factor.

In general, the results of these two jar tests make it clear that significant dissolution is not occurring. According to model predictions detailed in Chapter 3, 47 mg/L of solids were expected to dissolve in wastewater to reach equilibrium. That is, all reactors with initial concentrations of solids less than or equal to 47 mg/L were expected to show complete dissolution. Using the 40 mg/L concentration, which

represents the expected deficit, as an example, complete dissolution of this quantity of solids would result in a 16 mg/L increase in Ca^{+2}. Similarly, reactors with higher initial solids concentrations would expect to yield slightly higher final Ca^{+2} concentrations. Unfortunately, the observed concentrations of all reactors in both jar tests do not reflect such a significant increase. This analysis suggests that dissolution does not occur nearly to the extent that was expected, and in reality, only a very small fraction of the solids, if any, dissolve.

As seen above, the results of the aerated reactor from Jar Test 5 showed drastically different pH and Ca^{+2} results compared to the reactors closed to the atmosphere. Jar Test 6 looked to investigate the impacts of an open atmospheric system in more detail. It is important to note that the initial alkalinity of the WC wastewater sample used in Jar Test 6 was measured to be 274 mg/L, which was abnormally high compared to last year's median alkalinity of 245 mg/L. At this concentration, WC would need none or only a little supplemental alkalinity depending on the ammonia concentration. Since the purpose of the experiments was to test the possible dissolution in conditions when alkalinity is needed, i.e., at concentrations at or below 245 mg/L, acid was added to the wastewater to artificially lower the alkalinity to approximately 240 mg/L.

Figure 4.9 A presents pH data collected from Jar Test 6. Similar to the pH results from previous jar tests, the pH of aerated reactors increased to around 8.2 while the pH for the reactor closed to the atmosphere remained unchanged at 7.2. The wastewater was left to aerate for two hours prior to the addition of acid and the start of the test, which explains why the initial pH of the unacidified reactor (triangle points) started above pH 8 compared to the other aerated reactors. The pH values of the reactors containing $CaCO_3$

were expected to be higher than the control due to the dissolution of the solids. However, when comparing the two aerated, acidified samples (square and diamond points), we see that, despite the addition of $CaCO_3$ solids, both reactors increased 0.73 pH units, which suggests that no significant dissolution occurred.

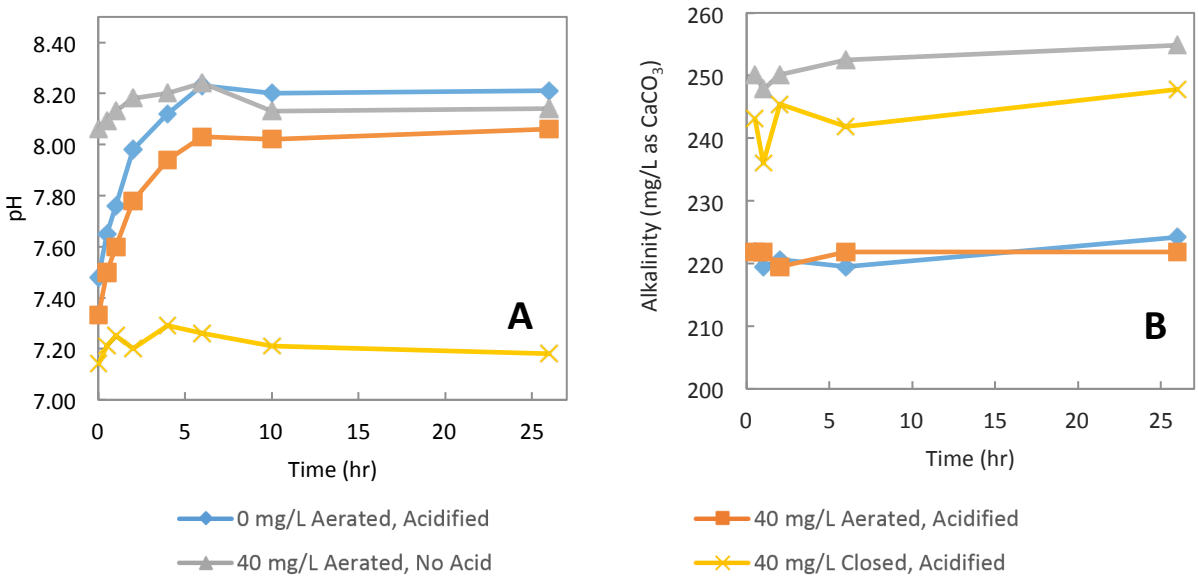

Figure 4.9: A) pH and B) alkalinity data from Jar Test 6.

Since increasing the alkalinity of the wastewater remains the main objective of these experiments, alkalinity measurements were taken for Jar Test 6, and the data are shown in Figure 4.9 B. At first glance the alkalinities of each reactor seem to remain constant over the experiment's duration. Closer inspection shows a slight increase in alkalinity of approximately 5 mg/L as $CaCO_3$ for the reactor closed to the atmosphere (cross points) and the aerated reactor without acid (triangle points). Although it is promising to see a slight increase in alkalinity, it was still much less than the 40 mg/L as $CaCO_3$ increase in alkalinity that was expected if all the solids were to dissolve. In

addition, the increase seen is not consistent for all reactors with added solids. For example, the aerated and acidified reactors with 0 (diamonds) and 40 mg/L $CaCO_3$ solids (squares) have almost identical alkalinity curves, and show virtually no change in alkalinity. The fact that there was no change in alkalinity despite the rise in pH is consistent with the idea that the aeration stripped $CO_{2(g)}$ from the solution. These results are consistent with the earlier observation that the pH change for the same reactors is also equal.

Calcium concentration data for the aerated and unaerated reactors in Jar Test 6 were compared to previous test data. Each test had different initial concentrations of calcium in the wastewater, so to compare these data, they first were normalized using the following equation:

$$\%Change_t = \frac{[Ca^{2+}{}_t] - [Ca^{2+}{}_o]}{[Ca^{2+}{}_o]} \times 100\%$$

where $[Ca^{2+}{}_t]$ = calcium ion concentration at time t

(Equation 4.10)

Only the 40 mg/L samples were compared because this concentration represented the alkalinity deficit and thus is the most important.

The aerated and unaerated concentration data comparisons are shown in Figure 4.10 A and B, respectively. The unaerated trials all exhibit only slight changes in Ca^{+2} from 0%. Two of the trials, Jar Test 5 and 6, ultimately reach approximately 4% change in Ca^{+2} concentration. That is, 4% of the added $CaCO_3$ solids dissolved. Two non-aerated trials show increasing trends (diamonds and squares), ultimately reaching approximately 11% after 24 hours. As stated earlier, acidifying the sample seems to have some negative impact on dissolution since the aerated and acidified sample (triangle points) does not significantly change from 0%. Comparison of aerated versus unaerated trials shows that

overall, the amount of dissolution after 24 hours doubled in aerated samples. These findings suggest that perhaps the initial assumption that dissolution occurs in a system closed to the atmosphere might not be accurate.

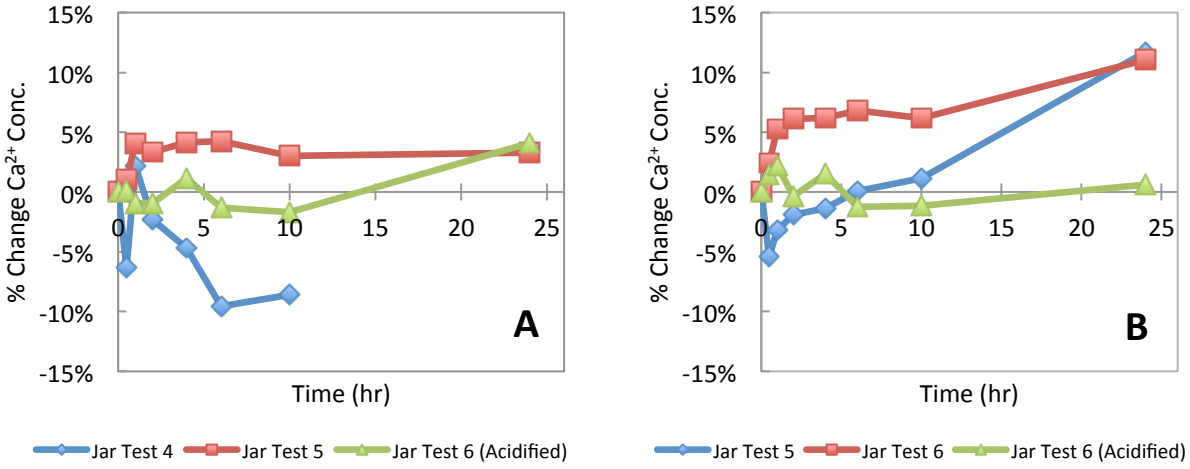

A B

Figure 4.10: Comparison of Ca^{+2} Concentration for multiple trials of unaerated (A) and aerated (B) reactors with 40 mg/L of $CaCO_3$ solids added

Section 4.4.3: Analysis of Solids in Reactor

Further investigation of the solids present before and after the jar test is important for understanding the details of the chemical processes that might have occurred. This detailed focus began because a slight color change of the wastewater was observed over the duration of the jar tests. Figure 4.11 demonstrates this color change after 19.5 hours of experimentation. The color gets darker from left to right as the initial concentration of added $CaCO_3$ solids increases in the reactors from 0 mg/L (far left) to 200 mg/L (far right). We hypothesized that the color change and the lack of noticeable dissolution were related to an independent factor, namely the formation of an unknown precipitate

utilizing Ca^{+2} ions. Since sulfide is known to form precipitates with metals in anaerobic conditions, it was hypothesized that a calcium-sulfide precipitate may explain the results. Therefore, a sulfide analysis was conducted in Jar Test 5. In addition, SEM and EDX were used to quantify the solids before and after the jar test.

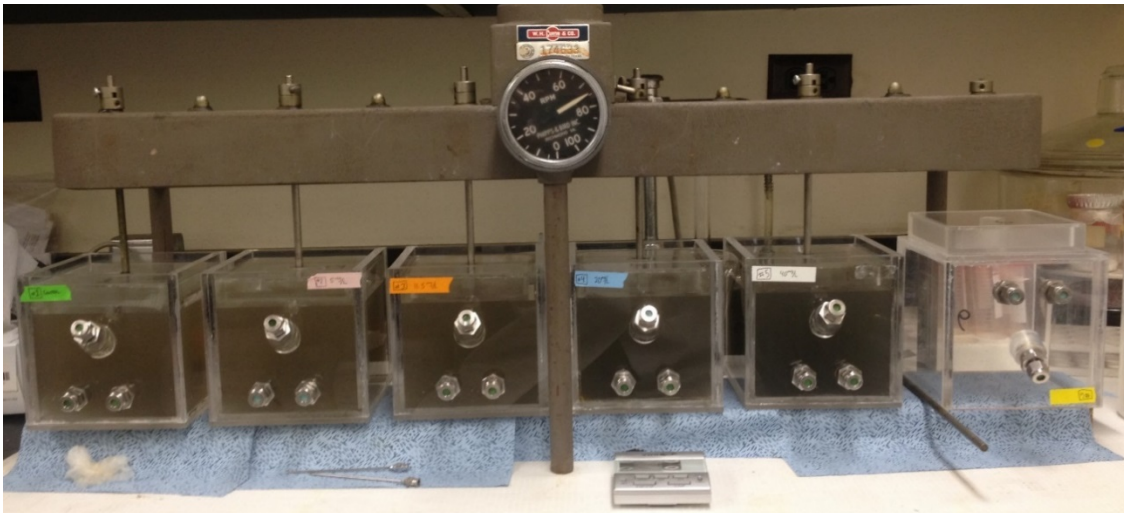

Figure 4.11: Color change observed during Jar Test with Walnut Creek Wastewater and Davis Solids. The concentration of Davis solids that was initially added increases from 0mg/L on the left to 200 mg/L on the right.

Sulfide concentrations were measured during Jar Test 5 and are reported in Figure 4.12. Sulfide concentrations did not follow any trends as the initial $CaCO_3$ solids concentration increased. All reactors except the aerated reactor saw slight increases in S^{-2} concentration with time. It makes sense that the sulfide concentration in the aerated reactor decreased, because when oxygen is present, sulfide is oxidized to sulfate. In addition, the aeration would lead to some stripping of H_2S from the wastewater (Henry's constant value of 10.0 atm per M at 25ºC). The most important conclusion is that the concentrations in general are very low, with the average sulfide concentration around

0.02 mg/L. At such low concentrations, it is unlikely for sulfide precipitates to form and thus unlikely that the color change can be attributed to sulfide.

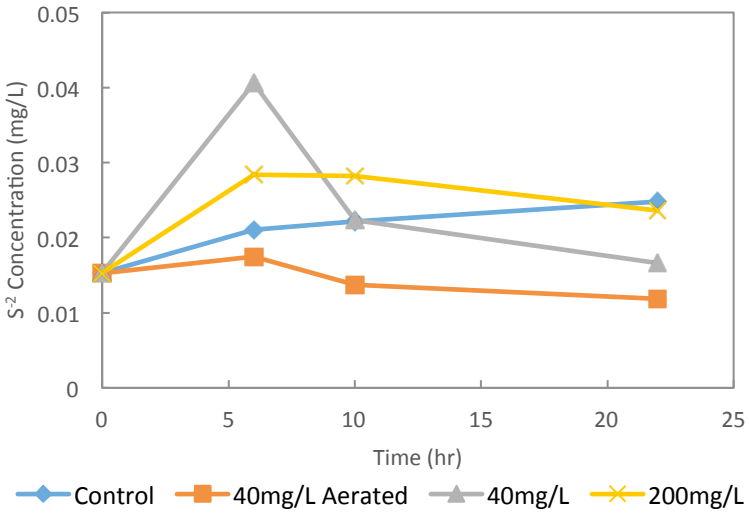

Figure 4.12: Total S^{-2} in mg/L during Jar Test 5 (Walnut Creek Raw Influent Wastewater and Davis Solids) for varying $CaCO_3$ concentrations.

The wastewater samples after a jar test were placed under the SEM. The general characteristics of the samples can be seen in Figure 4.13. Throughout the sample, there were large fibrous structures and large particles, which are both debris from the wastewater itself. Around these large structures, smaller debris formed clumps. The particles that made up the clumps all had similar structure, so it was believed that these particles were solids either directly from Davis WTP or modified solids as a result of the $CaCO_3$ addition. Moreover, the reactors with more solids initially added had a higher concentration of the clumping particulates, while none were seen in the control sample. Figure 4.14 B is a magnified photo of a section of the particulates. Crystal formation was generally amorphous in nature, but the crystals all resembled some hexagonal shape, seemed to grow in layers, and had roughly similar size, approximately 2-7 μm. The structural characteristics match the description of $CaCO_3$ crystals in waters with low

magnesium concentrations as described in Folk (1974) and explained in Section 4.2.2 above, which is one sign that these solids are $CaCO_3$.

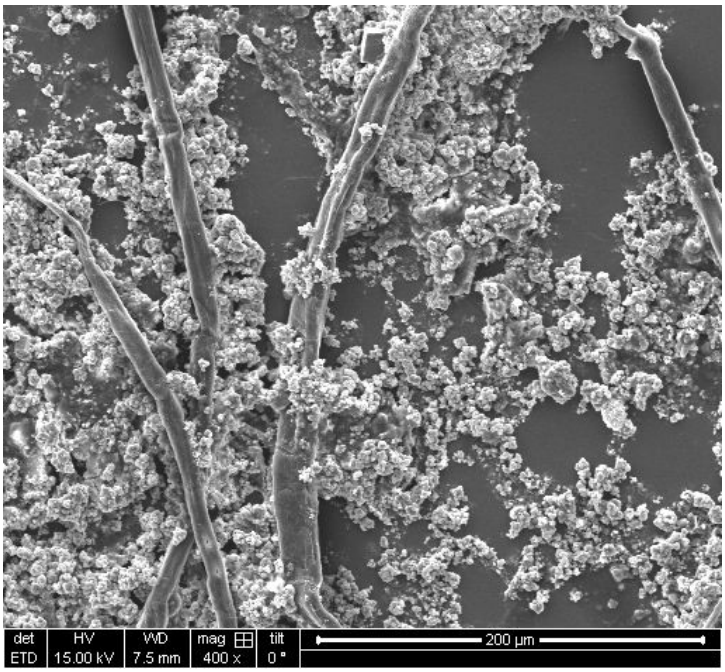

Figure 4.13: SEM image of 200mg/L $CaCO_3$ reactor sample after 22 hours. Clumping of solid participates is clearly seen.

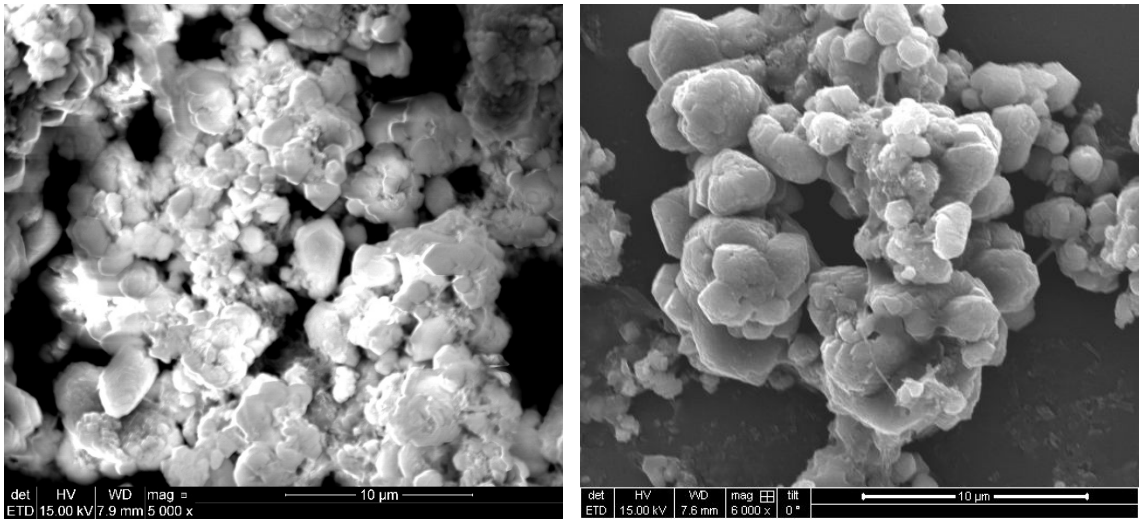

A **B**

Figure 4.14: SEM images comparing crystalline structures of A) Davis solids and B) Jar Test reactor with 200mg/L $CaCO_3$ added after 22 hours.

Raw Davis DWTP $CaCO_3$ solids were analyzed to compare the crystalline properties of the two solids (Figure 4.14 A). The Davis solids show denser clumping and are generally more amorphous when compared to the solids from the Jar Test in Figure 4.14 B. Moreover the particles from Davis are also slightly smaller in size. Despite these slight differences, the crystals are generally similar for both cases and thus were assumed to undergo no significant change during the jar tests. Further, the samples were scanned for other types of crystalline structures in hopes of identifying other precipitate forms such as hydroxyapatite, but none were found.

EDX results, which quantify the elemental composition of the solids, further confirm that the solids at the end of the jar tests were primarily $CaCO_3$ and were similar in composition to the Davis solids. Some caution should be used when analyzing the results of the EDX analysis. Due to the complexity of the wastewater samples and the various matrix effects that create error, the results of the EDX produced for this research were used primarily as a qualitative tool to identify possible major and minor components. It is not possible to compare the percentages of one data set to the other quantitatively. In general, major elements have atomic percentages greater than 10%, minor elements between 1 and 10%, and trace elements are less than 1% (Hafner n.d.).

Table 4.5 summarizes the compositions of both solids in terms of the major compounds. These results show that oxygen and calcium are the two primary elements that comprise the solids before and after the jar tests, which suggests that both the solids seen before and after the jar test were primarily $CaCO_3$. The presence of iron and chlorine

are expected at the WTP because chlorine is used as a disinfectant and iron is used as a coagulant in the form of ferric sulfate ($Fe_2(SO4)_3$). Phosphorus, a known inhibitor of $CaCO_3$ dissolution, was also present as a minor element, so it is possible that a small amount of phosphorus sorbed to the crystal surface and had a minor effect on the dissolution.

Table 4.5: Summary of elemental composition of $CaCO_3$ solids measured with EDX

Element	% Normalized Weight	
	Davis Solids	200 mg/L reactor*
Oxygen	52.68	21.64
Calcium	41.09	15.13
Magnesium	2.31	
Iron	1.17	
Chlorine	0.97	
Phosphorus	0.93	1.06
Aluminum	0.07	

* The sum does not reach 100% because of a high reading of Si, which is a result of the mounting plate the sample was placed on.

4.5 CONCLUSIONS

The use of lime-softening solids from the Davis WTP has been used by the Austin Water Utility to increase the alkalinity of the wastewater at Walnut Creek WWTP. The use of these $CaCO_3$ solids represents a potential cost effective solution to meet the alkalinity deficiency and improve the nitrification efficiency at Walnut Creek. Controlling the flow of $CaCO_3$ solids was shown by theoretical modeling in Chapter 3 to still provide beneficial alkalinity without the cost of problems in the biosolids treatment operations. Experimental jar tests were conducted to test the dissolution of $CaCO_3$ solids in wastewater under varying conditions and verify the predicted results from the model.

ICP analysis was primarily used to measure changes in the soluble calcium concentration over time as a proxy for dissolution. In addition, alkalinity, pH, sulfide, and SEM analyses were conducted on experimental samples to better understand the dissolution process.

The first set of dissolution jar tests were conducted in Millipore water as an initial control. Dissolved Ca^{+2} concentration and pH values were found to be within 90% of the expected values calculated by the model, which indicate that for simple, pure water systems, the model accurately predicts dissolution. Moreover, the expected amount of dissolution was reached with two hours at all initial solids concentrations, which means that the kinetics of the dissolution reaction are rapid enough to reach equilibrium within the detention time of the wastewater collection system.

Jar test results using Walnut Creek were less optimistic. According to the model, a maximum of 47 mg/L of $CaCO_3$ solids was expected to dissolve in the wastewater. However, in trials where the wastewater was closed to the atmosphere, the change in calcium concentration revealed that no significant dissolution was observed. To compare to the model results, less than 5% of the solids actually dissolved. Further, the Ca^{+2} concentration data showed no clear trends in dissolution across various initial solids concentrations. The alkalinity of these reactors remained constant while the pH slightly decreased, confirming the conclusion that dissolution of $CaCO_3$ was minimal.

Jar tests conducted under aerated conditions, showed slightly higher dissolution after 24 hours compared to the unaerated trials. In the aerated trials, pH increased dramatically from approximately 7.5 to 8.2, which was believed to be caused by a decrease in the dissolved CO_2 concentration as a result of the aeration. Despite the pH increase and dissolution results, the alkalinity of these reactors increased only slightly.

Similar to the unaerated trials, these results show that the predicted model values do not match the experimental results.

Further investigation of the solids in the reactor was done to determine if an unknown precipitation reaction was affecting the $CaCO_3$ dissolution. After 24 hours, the color of the wastewater in the reactors grew darker with increasing $CaCO_3$ concentration. Sulfide concentrations were very low suggesting that metal sulfide precipitation was seemingly insignificant for all reactors. In addition, SEM analyses showed that the crystalline structure of the solids after a 24 dissolution test matched the Davis solids. EDX analysis confirmed that both solids were primarily composed of calcium and oxygen. These results confirmed that no significant change in the solids occurred over the course of the dissolution jar tests.

Based on the experimental results, dissolution of $CaCO_3$ in wastewater was not found to dissolve substantially nor to provide additional alkalinity. These results are in disagreement with the observations and data from Walnut Creek, which showed better nitrification performance when solids from Davis WTP were being wasted. The primary explanation to account for the disagreement is that the experimental set-up did not accurately simulate the conditions at Walnut Creek. It is also possible that the model predictions were incorrect and the limited dissolution that was observed in the experiments is indeed all that is theoretically possible. This is to say that the current understanding of the chemical processes occurring in the wastewater are insufficient to properly predict and utilize the dissolution. One possible method to deepen this understanding is develop a more comprehension chemical equilibrium model that incorporates many more constituents in the wastewater. Another possibility is to inhibit

the microbial activity so that the effects of potential chemical changes can be studied separate from biological influences.

Since observed dissolution in the bench-scale tests was insignificant, using $CaCO_3$ solids from Davis to supplement the alkalinity at Walnut Creek is not recommended at this time. The costs associated with detrimental treatment operations at Hornsby Bend would still outweigh the benefit of the limited dissolution. Deeper investigation into the chemical processes might help understand the questions that remain from this work. Such future work could be used to refine the approach and methods used in both the model and experimental tests. It is possible that deeper understanding and a refined approach might prove that the solids could be optimally managed to provide Walnut Creek with free alkalinity and have no negative consequences.

Chapter 5: Impacts of Magnesium on Oxygen Transfer

5.1 INTRODUCTION

As discussed in Chapter 2, the AWU has had difficulties maintaining the effluent pH and nitrification removal efficiency at WC. Since the problem has been identified as an imbalance between the influent ammonia (NH_3) and alkalinity concentrations, the Utility has installed a chemical feed system at the head of the aeration basins where supplemental alkalinity can be added. A study conducted by CH2M Hill investigated the capital and operational costs of various supplemental alkalinity additives specifically to mitigate the situation at Walnut Creek. The Utility decided to use magnesium hydroxide ($Mg(OH)_2$) as the alkalinity source due to the low capital construction cost and relatively low operational cost. A $Mg(OH)_2$ chemical storage and feed system was installed at both treatment plants (WC and SAR) operated by the Utility and became operational in June 2013.

After installation, the utility noticed that the $Mg(OH)_2$ provided benefits in addition to the increased alkalinity. Specifically, operators could maintain the same dissolved oxygen (DO) concentration in the aeration basins despite reducing the volumetric air flow rate. In other words, either the rate of gas transfer increased or the microbial oxygen utilization rate decreased due to the addition of $Mg(OH)_2$. A reduction in the aeration flow rate means reducing the speed of the blowers providing the air. At an average activated sludge WWTP, approximately 50% percent of the total energy use is consumed by the blowers to provide aeration (Metcalf and Eddy 2003). Thus, such a reduction at WC would allow AWU to recover a portion of the cost of the $Mg(OH)_2$ through energy savings.

The goals of this chapter are, first, to identify the change in gas transfer efficiency due to $Mg(OH)_2$, and second, to further understand the mechanisms leading to the increased operational efficiency. The results of this chapter could help AWU quantify its energy savings and possibly recommend operational changes to improve the gas transfer rates. It is important to first understand the basic theories and models that have been used to describe gas transfer, which are provided in Section 5.2. Experiments were conducted to test the gas transfer efficiency using a bubble aeration column under varying $Mg(OH)_2$ concentrations for different water types. The mathematical gas transfer theory was applied to analyze the experimental data. Discussion of the experimental methods is located in Section 5.3, and the results are in Section 5.4.

5.2 LITERATURE REVIEW

Gas transfer is a form of mass transport, which involves the movement of a gas into liquid or vice versa. Every gas-liquid system has a specific equilibrium at which the transfer of gas into and out of the liquid is at steady-state. When the liquid is supersaturated with gas, the net transfer of gas is out of the liquid until the equilibrium is reestablished. Likewise, in undersaturated systems, gas from the atmosphere will dissolve or absorb into the liquid to reach equilibrium. In most engineered systems, the kinetics of gas transfer, that is the rate of change in the concentration of gas dissolved in the liquid, is critical to the proper functioning of the system. The rate is determined by the degree of disequilibrium. That is, gas transfer is faster further from equilibrium compared to the slow rate near equilibrium.

Gas transfer theory assumes that, at the interface between a gas and liquid, two separate interfacial boundary layers develop, one on the gas side and the other on the

liquid side. Transfer of a solute from one phase to another is controlled by transport through the two interfacial layers. It is common to think of the model as two resistors in series, because each layer provides resistance to the overall gas transfer.

A schematic of the two interfacial regions is illustrated in Figure 5.1 for a system in which a solute is transferring from the gas to the liquid phase. The initial bulk concentration of the solute in the bulk gas phase, $c_{G,b}$, decreases as the solute passes through the gaseous interfacial layer. Directly at the interface, the solute changes from the gas phase to the liquid phase. Once the solute is in the liquid phase, it passes through the liquid interfacial layer decreasing in concentration until it reaches the bulk liquid with a concentration of $c_{L,b}$.

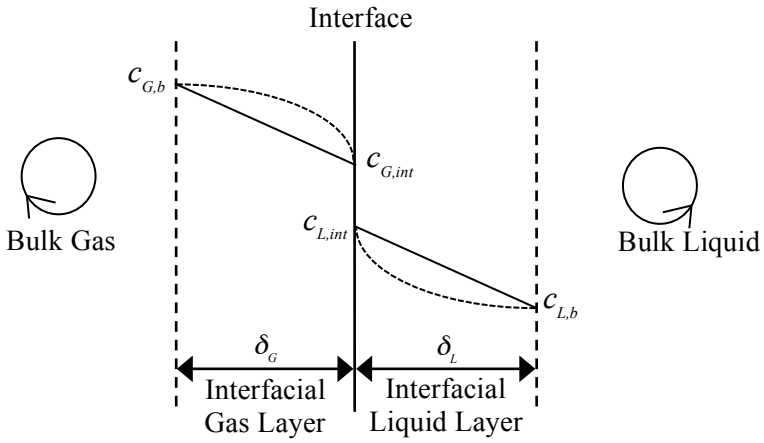

Figure 5.1: Schematic of Gas Transfer Theory (adapted from Benjamin and Lawler 2013)

At the interface, the concentration of solute in the liquid, $c_{L,int}$, and the concentration of the gas at the interface, $c_{G,int}$, are assumed to be in equilibrium. The equilibrium between a solute in the gas and liquid phase in an infinitely dilute solution is described by Henry's Law, where the concentration of a solute in the liquid phase is

proportional to the concentration of the solute in the gas phase by a constant, appropriately named the Henry's constant, H.

$$H = \frac{c_{G,int}}{c_{L,int}}$$

(Equation 5.1)

In the literature, Henry's constant takes on a variety of forms based on the application. For example, the Henry's constant for oxygen can either be written as $31.4\frac{L_L}{LG}$ or $769\frac{atm}{(mol/L)}$ (Benjamin and Lawler 2013).

The first accepted theory to model the kinetics of gas transport, introduced by Lewis and Whitman in 1924, assumed that the two interfacial layers acted as stagnant films and transport across the layers was controlled by diffusion. Diffusion can be explained by Fick's Law (Equation 5.2), which states that the rate of change of mass per unit area, the flux, is dependent on the concentration gradient and a diffusion coefficient that accounts for the physical and chemical properties of the solute (Benjamin and Lawler 2013; Hendricks 2011).

$$J = -D\frac{\partial C}{\partial \mathrm{X}}$$

(Equation 5.2)

where:

J = rate of mass transfer of solute per area per time (M/L^2-T)
D = diffusion coefficient (L^2/T)
$\frac{\partial C}{\partial \mathrm{X}}$ = concentration gradient of the solute in the bulk media in one dimension (M/L^3-L)

In this simplest approach, the concentration profiles of the solute through the interfacial layers are linear, shown in Figure 5.1 as solid lines. However, further investigation into gas transfer has revealed that gas transfer incorporates more active exchange mechanisms between the bulk and the interfacial layer of each phase in

addition to diffusion. Instead of relating flux and the concentration gradient only by the diffusion coefficient, the newer models use complex functions of the diffusion coefficient, which can be simplified to D^n, where n typically ranges from 0.5 - 0.67 depending on the model. These more sophisticated models have non-linear concentration profiles through the interfacial layers; one example is represented in Figure 5.1 as the dashed lines (Benjamin and Lawler 2013).

The flux expressions for the transfer of a solute through the gas (J_G) and liquid (J_L) interfacial films can then be written as shown in Equation 5.3 and 5.4, respectively. In the expressions, the rate constants, k_G and k_L, are used to represent the function of the diffusion coefficient and the interfacial distances (δ_L and δ_G shown in Figure 5.1) that are described by the various kinetic models for gas transfer. It can be seen that the concentration gradient across the interfacial regions are what drive the kinetics of gas transfer. When the gradient is large (further from equilibrium), the rate at which solute is transferred per unit time is also large, and vice versa.

$$J_G = k_G\left(c_{G,int} - c_{G,b}\right) \quad \text{(Equation 5.3)}$$

$$J_L = k_L\left(c_{L,int} - c_{L,b}\right) \quad \text{(Equation 5.4)}$$

In practice, it is not possible to measure the interfacial concentrations. However, the kinetics can be adequately described with the two assumptions that the interfacial concentrations of the gas and liquid are in equilibrium and that there is no accumulation of mass at the interface. The latter assumption means that the rate of transport through the two interfacial layers is equal and thus $J_L = -J_G$. It is also useful to define the term, c^*,

using Henry's Law as shown in Equation 5.5. c^* is the hypothetical concentration that would exist in the bulk liquid phase if it were in equilibrium with the bulk gas phase. (Benjamin and Lawler 2013; Hendricks 2011).

$$c^* = \frac{c_{G,b}}{H}$$

(Equation 5.5)

When the above assumptions are applied, the two flux equations can be combined to form a single overall gas transfer expression through both interfacial layers. Further explanation on how to combine the two flux expressions can be found in Benjamin and Lawler (2013) or most other textbooks on water treatment. This overall gas transfer flux from the gas into the liquid is then written as

$$J_L = K_L(c^* - c)$$

(Equation 5.6)

where K_L is the overall gas transfer coefficient to describe the movement of a solute through both interfacial layers. K_L incorporates the transfer coefficients through both gas and liquid interfacial layers as defined by Equation 5.7.

$$K_L = \frac{k_L k_G H}{k_L + k_G H}$$

(Equation 5.7)

The K_L term can be manipulated to prove that it functions as a system with two resistances. For example, when the liquid layer is rate-limiting, k_L is much smaller than $k_G H$. The denominator of Equation 5.7 will simplify to $k_G H$, and cancel out with the numerator leaving $K_L = k_L$. Likewise, when $k_G H$ is very small, transport through the gas layer is rate-limiting, which is shown by a similar simplification of Equation 5.7 to yield $K_L = k_g H$.

The final step is to convert the overall flux in Equation 5.6 into a rate expression in terms of the solute concentration so that similar units are used on both sides of the equation. First, the flux is multiplied by the interfacial area over which the diffusion occurs, A, to get a rate of mass transfer per unit time. Next, the equation is divided by the volume of the liquid, V_L, to normalize per unit volume. The result is a rate of mass transfer per unit volume per unit time shown as Equation 5.8.

$$r_L = K_L \frac{A}{V_L}(c^* - c)$$

(Equation 5.8)

Since concentration is defined as mass per volume, the rate expression, in terms of mass per volume per time, can be expressed as the rate of change in concentration over time. Also, the term $\frac{A}{V_L}$ is simplified to a_L, and represents the interfacial area for mass transfer per unit volume of liquid. The complete equation for the two-resistance model of gas transfer is shown in Equation 5.10. This equation was used as the primary model for oxygen transfer in this research.

$$\frac{dc}{dt} = K_L a_L (c^* - c)$$

(Equation 5.10)

where:

c = solute concentration in liquid bulk at time, t (M/L^3-T)
c^* = saturation solute concentration in liquid (M/L^3-T)
K_L = overall gas transfer coefficient (L/T)
a_L = interfacial area per unit volume of reactor (1/L)

When combined, $K_L a_L$ is defined as the volumetric gas transfer coefficient, and is a very important term used for gas transfer design applications. In most literature, this term is left lumped together because, in practice, it is difficult to measure the geometric term, a_L, of a system (Benjamin and Lawler 2013). Because it is dependent on the geometry and mixing of the system, it is also unique to a given system. In addition,

temperature, chemical properties of the solute, and chemical properties of liquid and bulk gas all influence $K_L a_L$. To account for temperature impacts, the following relationship is often used to adjust $K_L a_L$ to a standard temperature of 20°C:

$$K_L a_{L_{(T)}} = K_L a_{L_{(20^oC)}} \theta^{T-20}$$

(Equation 5.11)

where θ ranges between 1.015 to 1.040, but 1.024 is typically used for most wastewater aeration systems (ASCE 2007; Metcalf and Eddy 2003) .

5.3 METHODS

The following section contains the experimental methods used to analyze the gas transfer of oxygen in wastewater under varying $Mg(OH)_2$ concentrations. A column reactor was used to conduct bubble aeration tests. Experimental data were collected and analyzed to determine the $K_L a_L$ values for various water samples at increasing $Mg(OH)_2$ concentrations. Section 5.3.1 details the characteristics of the water used for all experimental trials. Section 5.3.2 describes the column aeration reactor and the experimental set-up. In addition, details on how DO measurements were taken are described. Finally, Section 5.3.3 outlines how the experimental data were analyzed to calculate $K_L a_L$ and other gas transfer kinetic information.

5.3.1 Source Water Characteristics

Three water types were tested to compare the changes in gas transfer rates: tap water, activated sludge, and primary effluent. Tap water was used as a control since it contains no microorganisms that would consume DO and it has very little background matrix of dissolved ions compared to the two wastewater samples. That being said, the

average concentration of magnesium in the tap water from 2013 was approximately 8.4 mg/L, which was estimated from hardness and calcium concentrations reported by AWU. According to Metcalf and Eddy (2003), the Mg concentration in wastewater could incrementally increase between 4 and 10 mg/L above the concentration in the domestic drinking water, which means background Mg concentration at WC would range from approximately 12 to 18 mg/L. Although it is important to note the background concentrations, they were never measured analytically because they have little significance to the study. When $Mg(OH)_2$ is added to the wastewater at WC, it is added in addition to the background concentrations, so all additions of $Mg(OH)_2$ for this study were considered incremental Mg concentrations and not total Mg concentrations to remain consistent with the full-scale operation.

Obviously, testing activated sludge was the main thrust of this research, since this suspension is where aeration in full-scale system occurs and where fluctuations in DO at Walnut Creek were observed. At the time of sampling, WC was adding $Mg(OH)_2$ to the aeration basins. The excess $Mg(OH)_2$ concentration above the background levels was undesirable for experimental testing because the goal of this research was to determine the difference between the gas transfer rates with and without the additional $Mg(OH)_2$. Instead of sampling the activated sludge directly from the aeration basins, both return activated sludge (RAS) and primary effluent were sampled and mixed in the laboratory. At WC, primary effluent is fed into the aeration basin and mixed with the RAS, so this method still mimics the conditions of the activated sludge at WC. The benefit is that the primary effluent, sampled prior to $Mg(OH)_2$ addition, diluted the concentration of ($Mg(OH)_2$ from the RAS feed. The RAS and primary effluent were mixed at a ratio of 1:1, which matches the ratio currently used at WC. Primary effluent was used as a third

water type to test the difference in gas transfer in wastewater that was much less biologically active compared to the activated sludge. Wastewater samples were tested on the same day as they were obtained to limit the impact that biological activity would have on changing the sample characteristics.

5.3.2 Column Bubbler Tests

The setup used to conduct bubble aeration tests is shown in Figure 5.2. A column reactor was filled with 8.5 L of sample water. A diffusion stone was placed at the bottom of the column to create bubbles that could transport oxygen into the sample water. Air was blown into the liquid at a rate of 1 standard cubic foot per hour (scfh). This flow rate was set to be as slow as possible to best differentiate changes in the observed $K_L a_L$ values under different chemical conditions. A rotameter was used to monitor the flow rate and ensure it remained consistent between tests. Although it is simple to use, a rotameter is less accurate compared to more sophisticated flow measuring devices.

A model YSI 58 Dissolved Oxygen Meter with a YSI 5905 membrane probe was used to measure the dissolved oxygen content of the water. The probe was positioned at the top of the column reactor, within the top one to two inches of the water surface. The probe was surrounded by a plastic mesh cage to remove error of false readings caused by the air bubbles getting caught under the probe. A stirrer attached to the probe was used to ensure continual mixing of the solution past the probe's membrane.

Figure 5.2: Setup for the bubble aeration tests

Each testing cycle included one complete deaeration and an aeration trial. Each new water sample was aerated for 1 hour prior to testing so it could reach its saturation concentration and the temperature could stabilize. Testing began by deaerating the sample water by bubbling pure nitrogen at the same flow rate of 1 scfh. The densities of air and pure nitrogen are very similar since 77% of the atmosphere is composed of nitrogen, so it was assumed that the mass flow rate of air and nitrogen were equal. DO measurements were recorded every 15 seconds for the first five minutes of the test and every 30 seconds thereafter. Once the DO of the sample water plateaued near zero, the

nitrogen gas was switched to air to begin the aeration cycle. DO measurements were recorded at the same time intervals as in dearation until the concentration of DO plateaued at the steady state concentration. Temperature measurements of the water were taken at the beginning and end of each aeration and deaeration trial. Each testing condition was tested for two complete cycles.

For each water sample, four different concentrations of $Mg(OH)_2$ were tested. The concentrations tested were 0, 3.79, 5.68, and 10 mg/L as Mg. These concentrations were achieved by adding $Mg(OH)_2$ to the desired concentration without consideration for the existing background Mg concentration of the wastewater as explained above. The 0 mg/L concentration was used as a control. The other concentrations were selected to match the operational range of $Mg(OH)_2$ added to the wastewater at WC. According to the operators, between 600 and 900 gallons of $Mg(OH)_2$ slurry are used per day. The slurry is 55% $Mg(OH)_2$ by weight and has a density of 12.5 lb/gal. The median flow at WC was found to be 54 MGD from historic data. Using these parameters, 600 and 900 gallons per day were converted to 3.79 and 5.68 mg/L as Mg, respectively. The final concentration, 10 mg/L, was selected to test the maximum concentration range.

5.3.3 Data Analysis

Using the DO and time data collected from all the experimental trials, the $K_L a_L$ value could be calculated using Equation 5.10. The process to analyze the experimental data for tap water was taken following the ASCE standard (ASCE 2007). Equation 5.12 was solved by first combining like terms and integrating as shown in Equations 5.12 through 5.14. The limits of integration are from initial DO concentration, c_0, to the concentration at time t, c_t.

$$\frac{dc}{K_L a_L (c^* - c)} = dt$$

(Equation 5.12)

$$\frac{1}{K_L a_L} \int_{c_0}^{c_t} \frac{dc}{(c^* - c)} = \int_0^t dt$$

(Equation 5.13)

$$\frac{-1}{K_L a_L} [\ln(c^* - c_t) - \ln(c^* - c_0)] = t$$

(Equation 5.14)

Equation 5.14 was rearranged into a linear form y = mx + b for the known variables c_t and t:

$$\ln(c^* - c_t) = -K_L a_L t + \ln(c^* - c_0)$$

(Equation 5.15)

Plotting $\ln(c^* - c_t)$ vs t from the data for each experimental trial results in a line that has a slope equal to $-K_L a_L$ and a y-intercept equal to $\ln(c^* - c_0)$. The saturation concentration, c^*, was known for all cases in clean water. In deaeration trials, $c^* = 0$ and, in aeration trials, c^* was set to equal the steady-state DO concentration at the beginning of each testing cycle. Linear regression analysis using the least square method was used to determine $K_L a_L$ from the plotted data. In all trials, the last few data points, which represented the DO concentrations already at the saturation concentration, were omitted to improve the accuracy of the linear regression. All trials had R^2 values with 0.99.

The above analysis can only be applied to the tap water trials. In wastewater samples, the original system becomes more involved to account for the consumption of O_2 by the microorganisms found in the wastewater samples, especially in activated sludge. A mass balance on O_2 in the system is described in words in Equation 5.16.

$$[\text{Change in } O_2] = \begin{bmatrix}\text{increase in} \\ O_2 \text{ via} \\ \text{gas transfer}\end{bmatrix} - \begin{bmatrix}\text{consumption} \\ \text{of } O_2 \text{ by} \\ \text{microorganisms}\end{bmatrix}$$

(Equation 5.16)

Mathematically, the mass balance is similar to Equation 5.10 except for the addition of the rate of DO consumption. According to Metcalf and Eddy (2003), the rate of consumption by microorganisms is not dependent on the concentration of oxygen in the system. That is, the rate of consumption is zero order with respect to O_2. Thus, Equation 5.10 is amended as follows:

$$\frac{dc}{dt} = K_L a_L (c^* - c) - r_m$$

(Equation 5.17)

One way to determine $K_L a_L$ and r_m is to estimate $\frac{dc}{dt}$ as $\frac{\Delta c}{\Delta t}$. That is, calculate the change in DO concentration over successive small time intervals. As before, Equation 5.17 was rearranged into the form of a linear equation:

$$\frac{\Delta c}{\Delta t} = -K_L a_L c + (K_L a_L c^* - r_m)$$

(Equation 5.18)

Plotting $\frac{\Delta c}{\Delta t}$ versus c for many time intervals results in a line with a slope equal to $-K_L a_L$, and the y-intercept is a constant that includes r_m, $K_L a_L$, and c^*. In the cases of deaeration, $c^* = 0$, so Equation 5.18 simplifies to Equation 5.19, which has a y-intercept equal to $-r_m$.

$$\frac{\Delta c}{\Delta t} = -K_L a_L c - r_m$$

(Equation 5.19)

However, when aerating, this simplification cannot be used, because c^* is unknown. Therefore, the y-intercept remains equals to $K_L a_L c^* - r_m$ and was not simplified to determine r_m. Trimming of the first and last few data points was done to remove erroneous data caused by changing the aeration stream at the beginning of the test and reaching the saturation concentration at the end. Due to the estimation of $\frac{\Delta c}{\Delta t}$, the linear

regression equations for activated sludge and primary effluent samples had slightly poorer fits compared to the tap water; all trials had R^2 values ≥0.90.

Lastly, all $K_L a_L$ values were standardized to a temperature of 20ºC to make comparison between trials easier. Equation 5.11 was used to convert and θ was set to 1.024. For each testing condition (type of water and concentration of $Mg(OH)_2$ added), the average and standard deviation for the $K_L a_L$ value was calculated and reported.

5.4 RESULTS

One set of data from an oxygen transfer trial is shown in Figure 5.3 to illustrate the interpretation of the results. These particular data were taken during a dearation cycle in activated sludge with a magnesium concentration of 3.79 mg/L. The raw data, measured DO and time, are plotted in Figure 5.3 A. Since this dataset is from a deaeration trial, it makes sense that the DO concentration decreases with time. Moreover, the rate of decrease slows down as the DO concentration approaches 0 mg/L, which is consistent with the theoretical knowledge that the rate of gas transfer is proportional to the degree of disequilibrium. As explained above, to determine the $K_L a_L$ value for these data, it must be plotted in terms of $\frac{\Delta c}{\Delta t}$ versus the DO concentration.

Figure 5.3 B presents the linear plot of the manipulated data from part A. The plot can be interpreted similarly to Figure 5.3 A. For example, at high DO concentrations (further from equilibrium), the rate of change in the concentration is greater than at lower concentrations. The R^2 value of 0.989 indicates that the linear fit matches the experimental data very closely. The slope of the line, -0.0035, is equal to $-K_L a_L$ in units of inverse seconds. The y-intercept is directly equal to the rate of consumption of DO by the microorganisms, r_m, since c^* in dearation trials is 0 mg/L.

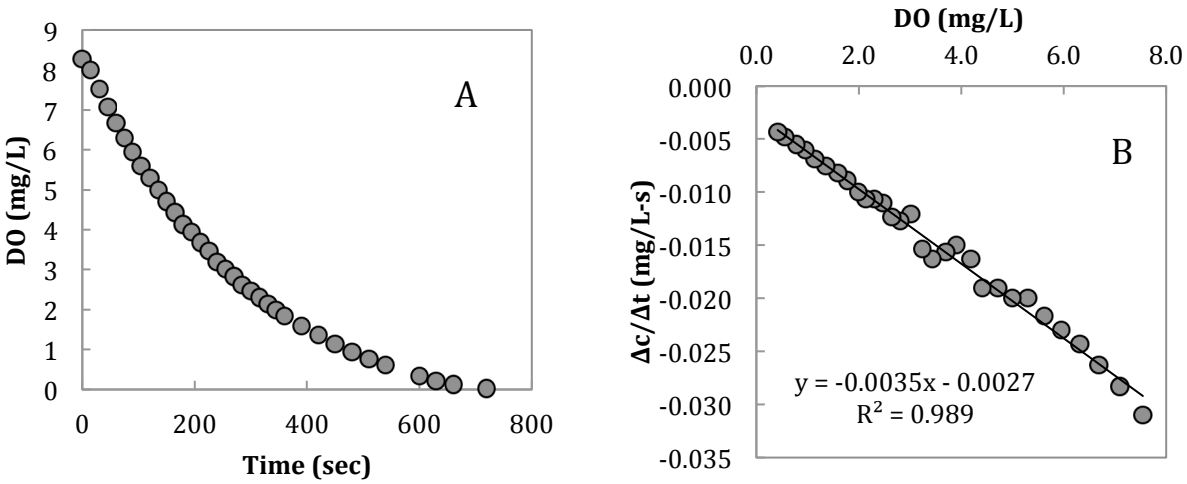

Figure 5.3: Sample raw data from dearation trial in Activated Sludge with 3.79 mg/L Mg added

Figure 5.4 shows the trends in $K_L a_L$ values for all types of water shown at increasing $Mg(OH)_2$ concentrations. The $K_L a_L$ of the activated sludge showed the most drastic change when compared to the other water types. The $K_L a_L$ declined from 18.6 to 13.1 h^{-1} as the added Mg concentration was raised from 0 mg/L to 5.68 mg/L, respectively. The $K_L a_L$ of tap water showed virtually no change between 0 and 5.68 mg/L Mg. Finally, the primary sludge was the only sample that showed a positive trend with increasing Mg concentration; the $K_L a_L$ of these trials showed an increase from 11.1 h^{-1} at 0 mg/L Mg to 13.4 h^{-1} at 10 mg/L Mg.

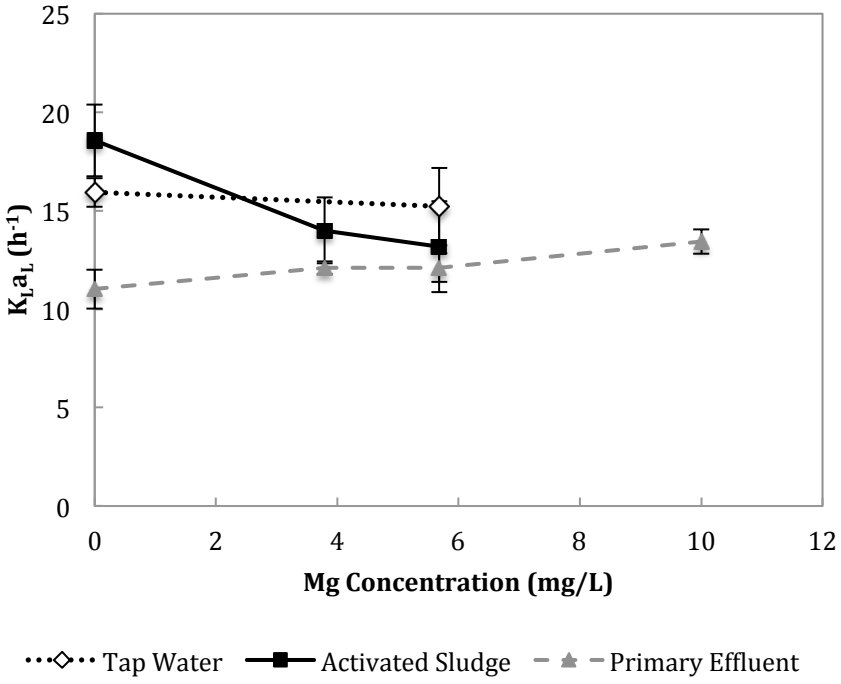

Figure 5.4: Observed $K_L a_L$ values for water types at various added Mg concentrations

The expectation, based on the anecdotal evidence observed by the plant operators at WC, was that the gas transfer coefficients should increase with an increasing concentration of $Mg(OH)_2$. However, the experimental results do not meet this expectation. Instead, these results show the opposite. That is, for activated sludge, the gas transfer coefficient decreased as the $Mg(OH)_2$ concentration increased. The primary effluent was the only water type that showed any positive trend similar to the expectations, but the increase was slight and it was not clear whether the increase is statistically significant compared to the possible error associated with test.

It is not clear why the trends in the experimental $K_L a_L$ values did not match the observed changes in the full-scale aeration basin at Walnut Creek, but possible explanations may exist. The first explanation is that the test did not accurately simulate

the full-scale aeration system. $K_L a_L$ is system specific and can vary based on diffuser characteristics and reactor geometry (Hendricks 2011). When comparing the gas transfer from one system to another, it is important to keep as many parameters similar, such as the diffusion efficiency, water height, or degree of reactor mixing. It was assumed that the experimental setup would be sensitive enough to discern similar trends in $K_L a_L$ regardless of the difference between the bench and full-scale reactors, but perhaps this assumption was incorrect.

The other explanation is that Mg may affect how the microorganisms in the activated sludge consume oxygen. The hypothesis of this study was that Mg impacted the gas transfer via physical and chemical changes in the water and not because of biological changes. That is, the $K_L a_L$ value was expected to change while r_m remained unchanged. To investigate this possibility further, observed r_m were calculated as previously discussed in Section 5.3.3 for the deaeration trials with activated sludge. The average values are presented in Table 5.1. There does not seem to be a clear overall trend between the rate of O_2 consumption by microorganisms and the magnesium concentration, albeit the data set is too small for true interpretation. However, if we look more generally, just comparing trials with Mg to ones without, it may be possible to say that the presence of added Mg lowered r_m.

Table 5.1: Average r_m values Observed in Activated Sludge Deaeration Trials

Mg Conc. (mg/L)	r_m (mg O_2/L-h)
0	35.5
3.79	8.5
5.68	18.1

From these tests, it is not clear if biological processes are in fact affecting the overall rate of oxygen transfer at Walnut Creek. This explanation was hypothesized only because it was the only remain possibility that was not investigated, given the theory of gas transfer presented and the experimental results that did not exhibit the expected trend in $K_L a_L$. Moreover, there is no current literature that provides any insights into the affects Mg may have on the microbial communities with regard to oxygen consumption. Therefore, to better understand the biological changes that may occur when Mg is increased, it is necessary to conduct future experiments where the biological activity is held constant and/or measured using plate counts before and after testing.

5.5 CONCLUSIONS

The use of $Mg(OH)_2$ as a supplemental alkalinity source at Walnut Creek Wastewater Treatment Plant was anecdotally found to indirectly improve the gas transfer efficiency of the aeration basins. Column bubble diffusion tests were conducted under various environmental conditions to calculate $K_L a_L$ values that would help quantify the impact of the magnesium concentration on the wastewater's gas transfer rate. Although data collection from numerous trials yielded high correlation coefficients and deviated very little between similar trials, the resulting $K_L a_L$ values were not consistent with anecdotal expectations. Increasing concentration of Mg in activated sludge resulted in a sharp downward trend in $K_L a_L$, while only a slightly increasing trend was observed for $K_L a_L$ values in primary effluent and no change was observed in tap water.

A few possible reasons that can help explain why the observed results did not match the operational conditions at WC were considered. First, the reactor configuration used in the laboratory might not be sufficiently sensitive to detect the true changes in

$K_L a_L$. The test might not have accurately simulated the physical conditions at WC that could affect the rate of gas transfer. Second, it is possible that Mg impacts the gas transfer rate via biological methods and not physical or chemical methods as originally believed. The rate of oxygen consumption by microorganisms for activated sludge suggested that Mg may reduce the consumption rate, but further study on this topic is recommended to better understand and quantify these impacts.

Chapter 6: Conclusion

6.1 SUMMARY

The Walnut Creek Wastewater Treatment Plant in Austin, Texas, has recently experienced increasing influent ammonia concentrations. Ammonia is treated using nitrification, which consumes alkalinity. As the ammonia concentrations have increased, operators at WC have struggled to manage the nitrification efficiency of the plant. Moreover, the resulting increased consumption of alkalinity makes it difficult to maintain the pH above the required level of pH 6 in accordance with the plant's discharge permit. Complete denitrification at WC is not possible without major infrastructure renovations, so the treatment plant operators have looked to the addition of chemical alkalinity sources to supplement alkalinity.

A creative solution to improve the ammonia to alkalinity balance at WC included using lime-softening solids generated at Davis WTP as the supplemental alkalinity source. The solids are primarily composed of $CaCO_3$ and can dissolve in the wastewater collection system to increase the alkalinity of the wastewater. The benefit of this alkalinity source is that the utility can reuse the solids, which are otherwise wasted at high disposal costs, as an alkalinity source at no additional charge. In 2011, the utility began transferring solids to WC and immediately noticed improvements in both the nitrification efficiency and the effluent pH. However, undissolved solids accumulated at WC and were sent to Hornsby Bend as part of the normal biosolids treatment operation, where they had a detrimental effect on the biosolids treatment efficiency and ultimately forced the utility to examine an alternative alkalinity source.

The goal of this thesis was to better understand the factors influencing the ammonia-alkalinity imbalance at WC and to investigate the possible use of $CaCO_3$ and

$Mg(OH)_2$ as alkalinity sources to develop a long-term solution for WC. Despite the problems of using the $CaCO_3$ solids to supplement alkalinity at WC, the potential benefits that could be gained were deemed too great to simply abandon this idea. Thus, a major thrust of this research attempted to optimize the use of the $CaCO_3$ solids. Theoretical modeling using chemical equilibrium was conducted to determine the maximum amount of dissolution, and therefore the alkalinity benefit, that the solids could provide. This value was used as a threshold concentration and applied to historic operations data at Davis WTP and WC to quantify the expected alkalinity benefit the solids could provide, as well as to estimate the mass of solids that were sent to Hornsby Bend during the time frame that this procedure was used. Experimental dissolution jar tests were conducted to verify the model predictions and estimate the kinetics of dissolution. Analysis of the solids allowed for better understanding of the underlying chemical processes that might influence the dissolution.

6.2 CONCLUSIONS

The following conclusions were made from research conducted in this thesis:

1. The influent ammonia concentration has increased at WC over the past few years. Moreover, the WC wastewater has a weaker overall wastewater strength (lower BOD and lower alkalinity) when compared to SAR. These conditions have made nitrifying all the ammonia while maintaining the pH above the required discharge limit of pH 6 difficult.
2. High concentrations of sulfate and ammonia in the influent at WC were found to be directly attributable to semiconductor manufacturers within the city. This combination of influent characteristics as a result of the semiconductor

manufacturing industries reduces the overall alkalinity, which decreases the ability for the plant to remove standard ammonia concentrations, let alone the increased concentrations from the semiconductor manufacturers.

3. The maximum concentration of solids present in the wastewater that would be expected to dissolve was estimated using the equilibrium model developed for closed systems to be 47 mg/L. This value was applied to operational data from Davis WTP and WC to determine the solids' loading to WC and subsequently, Hornsby Bend.
4. Solids from Davis WTP were transferred to WC either via the centrate or equalization tank overflow waste streams. The overflow stream contributed an average of 395,000 lb/day of $CaCO_3$ solids. However, according to the equilibrium model, only 5% of the solids could dissolve and provide alkalinity to WC, which leaves a substantial volume of undissolved solids that would negatively impact Hornsby Bend. In contrast, the centrate stream contributed 7,250 lb/day of solids, all of which were assumed to dissolve. The overflow provided 17.6% of the total alkalinity at WC, while the centrate provided 7.2%.
5. The alkalinity deficit at WC was conservatively estimated to be 54 mg/L as $CaCO_3$ using an alkalinity balance. The maximum possible amount of $CaCO_3$ solids that could dissolve, 47 mg/L, is slightly less than the conservative deficit, which indicates that the $CaCO_3$ solids from Davis WTP could not meet the total alkalinity needs under the most severe conditions. In these cases, additional alkalinity would still need to be added in addition to the $CaCO_3$ solids.
6. $CaCO_3$ solids were not observed to significantly dissolve during experimental dissolution tests under various initial solids concentrations and aeration condition

in wastewater. After 24 hours, the Ca^{+2} concentration exhibited less than a 5% increase, the alkalinity remained mostly unchanged, and the pH slightly decreased. SEM imagery, along with EDX analysis, further confirmed that no change in the solids' crystalline structure and elemental composition occurred during the dissolution tests.

7. The use of $Mg(OH)_2$ as a supplemental alkalinity source led to an observed increase in the DO transfer efficiency in the aeration basins at WC. Results of laboratory bench-scale experiments, however, showed that the $K_L a_L$ in activated sludge decreased with increasing $Mg(OH)_2$ concentrations, which is opposite of the expected trend. This result might be because the physical parameters of the reactor and diffusion system do no properly match those in the WC aeration basins. It is also possible that Mg does not impact oxygen transfer chemically, but rather impacts how the microorganisms utilize oxygen.

6.3 Recommendations to the City of Austin Water Utility

Three courses of action could be employed by AWU to rebalance the ammonia and alkalinity of the WC wastewater. They are utilizing denitrification, reducing influent ammonia, and supplying additional alkalinity. Complete denitrification would require the construction of designated infrastructure at WC and for this reason was not considered as part of this research. The other two methods were considered in detail as potential solution to be used independently or in tandem. Specific recommendations to AWU are described as follows.

- Institute a local limit or a surcharge on the concentration or mass loadings of ammonia and sulfate discharged by industrial users. A local limit could force

industries to either pretreat their wastewater before discharging to the sewer systems or change their internal processes to lower their discharge amounts. A surcharge could be incorporated into the city's regulations that would charge a user for any concentration or mass loading above a certain value. The surcharge fees could then be used by AWU to offset the costs of the chemical addition at WC that is needed to increase the alkalinity to treat ammonia. It is recommended though, that the local limit or surcharge should not be based solely on an absolute mass loading, but instead on meeting a desired ammonia to alkalinity ratio. This regulation would allow an industrial user flexibility in meeting the limit. For example, if an industry could not reduce ammonia usage in their process, they could instead decide to provide alkalinity themselves. The addition of alkalinity could occur by a direct addition of acceptable chemicals, but also might be achievable in some cases by a decrease in the use of strong acids in their processes.

- The use of $CaCO_3$ solids from Davis WTP beyond the centrate flow currently is not recommended to provide supplemental alkalinity to WC. It is possible that experimental methods did not accurately mimic full-scale conditions, so continued investigation could be considered. However, model results indicated that the maximum amount of alkalinity that could be provided by the solids would not meet the alkalinity deficit even under conservative conditions. Therefore, even if this method was proven experimentally and employed in the future, it is recommended that a supplemental chemical addition, such as $Mg(OH)_2$ be installed anyway, so that in extreme cases, enough alkalinity can be provided to meet the deficit.

Appendix A: Industrial User Data Summary

Table A.1: Walnut Creek Industries Data Summary

Industrial User	Flow (gpd)	pH Std units	NH3-N (mg/L)	NH3-N Loadings (lbs/day)	S04 (mg/L)	SO4 Loadings (lbs/day)	% Flows	% SO4	% NH3
Semiconductor A	2,986,242	8.25	123	4,312.50	842.5	33270.2	5.73%	59.39%	31.53%
Industrial User A	1,273,150	8.55	2	38.30	44.3	348.8	1.71%	0.76%	0.00%
Semiconductor B	682,621	7.87	47	273.71	386.7	1602.1	1.43%	4.17%	2.40%
JJ Pickle Rearch Campus	431,128	8.42	--	--	89.6	291.35	0.81%	0.64%	--
Industrial User B	325,333	8.16	1	3.13	267.8	625.9	0.69%	1.14%	0.03%
Hospital A	115,119	8.05	--	--	55.6	40.77	0.24%	0.10%	0.14%
Hospital B	140,592	7.98	30	43.27	52.0	60.8	0.23%	0.17%	0.00%
Industrial User C	103,133	8.57	39	5.83	43.6	28.80	0.19%	0.06%	0.04%
Hospital C	50,533	8.54	49	18.79	33.4	16.0	0.09%	0.03%	0.12%
Landfill A	26,918	6.88	85	11.55	23.9	0.7	0.05%	0.00%	0.11%
Industrial User D	10,283	8.85	156	1.98	75.1	4.6	0.02%	0.01%	0.02%
Industrial User E	9,189	8.37	35	3.10	31.9	2.4	0.02%	0.01%	0.00%
Industrial User F	5,189	8.70	1.4	0.05	6874.5	0.27	0.01%	0.00%	0.00%
Industrial User G	895	10.17	0	0.00	31.3	0.0	0.00%	0.00%	0.00%
Industrial User H	956	6.85	--	--	177.4	0.2	0.00%	0.00%	--
Industrial User I	689	9.67	--	--	26.6	0.13	0.00%	0.00%	0.00%
Industrial User J	165	8.96	39	0.06	1782.8	3.1	0.00%	0.01%	0.00%
Industrial Sub Total							11.24%	66.50%	34.41%
Other (Res. & Com.)							88.76%	33.50%	65.59%
TOTAL							100.00%	100.00%	100.00%

Table A.2: South Austin Regional Industries Data Summary

Industrial User	Flow (gpd)	pH Std units	NH3-N (mg/L)	NH3-N Loadings (lbs/day)	S04 (mg/L)	SO4 Loadings (lbs/day)	% Flows	% SO4	% NH3
University of Texas	968,391	8.10	38.4	296.71	63.8	511.27	2.34%	3.16%	3.02%
Semiconductor C	926,258	7.51	65.8	576.49	425.0	3118.03	2.11%	17.15%	8.37%
Semiconductor B	469,964	7.24	39.3	155.24	332.8	1310.30	1.15%	7.54%	1.53%
Industrial User K	112,485	7.53	10.3	9.29	202.3	190.15	0.27%	1.20%	0.08%
Hospital D	113,735	8.46	29.7	29.46	38.3	36.47	0.26%	0.22%	0.32%
Industrial User L	97,701	9.58	2.6	2.54	407.0	318.70	0.22%	1.68%	0.02%
Industrial User M	91,955	9.95	1.8	0.84	75.2	77.29	0.21%	0.44%	0.01%
Hospital E	48,187	7.55	6.0	2.40	35.6	14.36	0.11%	0.07%	0.03%
Hospital F	35,247	8.50	24.0	6.37	54.9	16.09	0.08%	0.10%	0.06%
Industrial User N	34,992	9.03	32.3	9.53	249.0	72.70	0.08%	0.39%	0.11%
Industrial User O	30,521	10.09	7.9	2.34	27.2	7.33	0.07%	0.04%	0.02%
Industrial User P	25,775	8.63	1.5	0.21	46.4	11.25	0.06%	0.05%	0.00%
Hospital F2	21,226	8.20	--	--	42.2	7.98	0.05%	0.06%	--
Industrial User Q	19,139	7.93	14.2	2.97	67.2	10.85	0.04%	0.05%	0.03%
Industrial User R	15,537	6.50	--	--	19.4	2.52	0.04%	0.01%	--
Landfill B	15,085	6.45	6.8	0.93	58.7	7.07	0.03%	0.03%	0.01%
Industrial User S	12,499	7.89	44.0	4.41	15.2	1.53	0.03%	0.01%	0.04%
Industrial User T	7,853	8.60	47.5	1.72	73.3	4.02	0.02%	0.03%	0.01%
Industrial User U	7,143	7.39	--	--	12.8	0.61	0.02%	0.00%	--
Industrial User V	4,784	8.09	31.5	1.26	512.7	23.41	0.01%	0.13%	0.01%
Industrial User W	2,137	8.80	180.0	3.00	65.1	1.15	0.01%	0.01%	0.03%
Landfill C	1,523	7.30	20.1	0.26	375.0	4.76	0.00%	0.01%	0.00%
Industrial User X	685	8.05	--	--	1.3	0.01	0.00%	0.00%	--
Industrial Sub Total							7.22%	32.39%	13.72%
Other (Res. & Com.)							92.78%	67.61%	86.28%
TOTAL							100.00%	100.00%	100.00%

Appendix B: Analytical Methods

B.1: Sulfide Analysis

The procedure for measuring sulfide was based on the method developed by Brouwer and Murphy (1994) with slight modifications detailed in the standard operating procedure developed by Johnson et al. (Johnson et al. 2013). This analysis focused solely on measuring Acid Volatile Sulfide (AVS), which is a subset of the total sulfur concentration. When sulfide ions are acidified, they speciate into HS^- and H_2S forms as shown in Equation B.1 and Equation B.2, respectively (Morel and Hering 1993). The pKa values associated with these reactions indicate that, at any acidic pH, sulfur (II) will be primarily in the H_2S form. As shown in Equation B.3, H_2S will partition into the gaseous phase with a Henry's constant of 10.0 atm/M (Benjamin and Lawler 2013). In addition, acidification causes many slightly soluble metal sulfide precipitates to dissolve (APHA et al. 2005). Therefore, the main principle of the AVS method is to capture and measure all sulfide that can be volatilized by the addition of acid to the sample.

$$HS^- \leftrightarrow S^{2-} + H^+ \qquad pKa = 13.9 \qquad \text{(Equation B.11)}$$

$$H_2S_{(aq)} \leftrightarrow HS^- + H^+ \qquad pKa = 7.02 \qquad \text{(Equation B.12)}$$

$$H_2S_{(aq)} \leftrightarrow H_2S_{(g)} \qquad H_{pm} = 10.0\,\frac{\text{atm}}{\text{M}} \qquad \text{(Equation B.13)}$$

Unlike many other AVS procedures that use a purge-and-trap system, the procedure that was used trapped AVS by diffusion. 2.5 mL of sample was placed in a sealed tube. Inside each tube was a smaller vial filled with 2 mL of sulfide antioxidant buffer solution (SAOB). The schematic in Figure B.1 shows the tube setup. All tube

preparation was done in an anoxic glove box to minimize oxidation of S^{-2} into SO_4^- by interaction with O_2. Once capped, 5 mL of 2N HCl was added to the sample using a syringe and needle through the septum in the tube's cap. It is important to keep the SAOB and acidified sample from touching. Samples were then shaken for 24 hours on a shaker table, during which time AVS diffused into the sealed atmosphere of the tube and then diffused into the buffer solution of the inner vial. In the buffer solution, sulfide was quickly stabilized as S^{-2}.

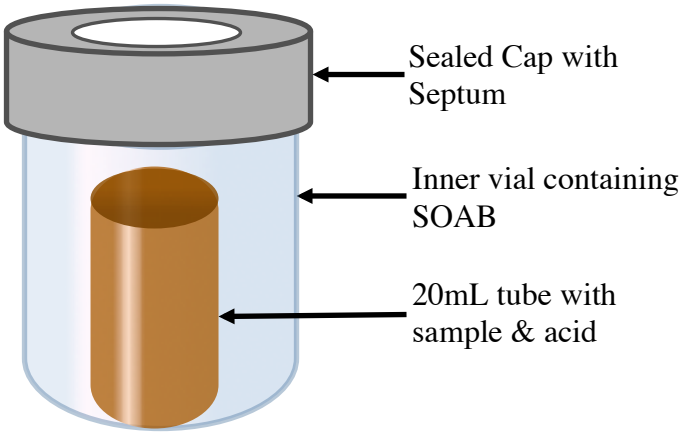

Figure B.1: Schematic of the Sample Tubes Setup for AVS Analysis

After shaking, the SOAB solution was removed and rinsed with an additional 2 mL of SAOB. The electric potential of the SAOB solution was measured using a VWR Combination Silver/Sulfide electrode. Mixing the solution with a stir bar during measurement was important to ensure stable and accurate readings, especially at lower concentrations. The sulfide concentrations were computed by comparing the meV measurements to a standard curve produced from standards of known sulfide concentrations, as shown in Figure B.2. The standards were prepared by directly adding a sulfide stock solution to the SAOB. The R^2 value was 0.99, which indicates that the

accuracy of the method is high. Finally, to account for the dilution caused by the SAOB rinse, the concentration obtained from the standard curve was converted to the actual sample concentration using Equation B.4.

$$C_{sample} = C_{SAOB}\left(\frac{Vol_{SAOB}}{Vol_{sample}}\right) = C_{SAOB}\left(\frac{4\ mL}{2.5\ mL}\right)$$

(Equation B.14)

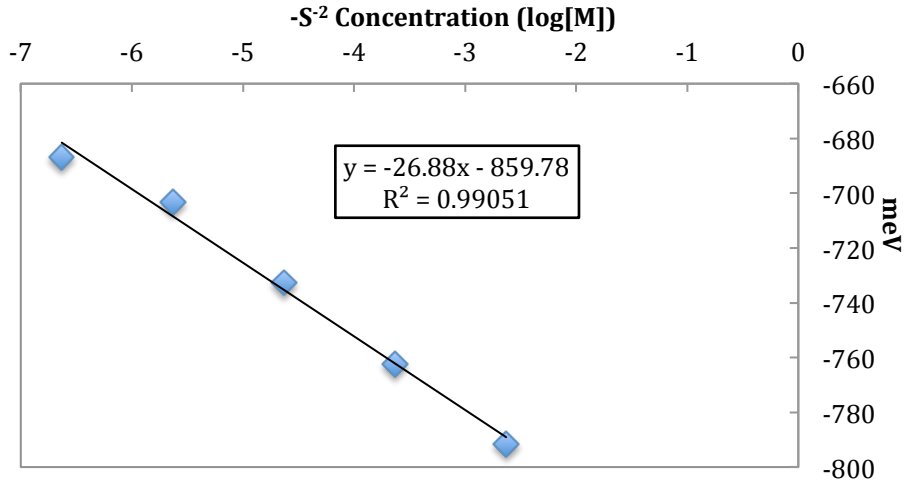

Figure B.2: Standard Curve used for Acid Volatile Sulfide Analysis

Sulfide concentrations were measured in duplicate at 0, 6, 10, and 24 hours for all reactors in Jar Test 5. To measure the percentage of aqueous sulfide versus sulfide bound in precipitate form in the reactors, both total and dissolved sulfide was measured. Total sulfide refers to direct analysis of the reactor solution including any solids that may be present. Dissolved sulfide was measured by first filtering a sample of the reactor solution using a 0.45 μm Nylon syringe filter.

B.2: SEM AND EDX

Scanning Electron Microscopy (SEM) and Energy Dispersive X-Ray Spectrometry (EDX) was used to observe and analyze the solids in the reactor samples from Jar Test 5 at the microscopic level. The goal was to identify any change in crystalline structure of the solids that might have occurred over the course of the jar test and to quantify the atomic composition of the solids. The following section provides additional background on SEM and EDX theory as well as the specific procedures followed to analyze our samples.

SEM uses a high-powered electron beam to visualize samples up to 100,000 times magnification. After the completion of the jar test, the reactors were left to settle. Using a pipette, settled solids from each reactor were plated onto separate silicon wafers. A lab wipe was used to draw away as much water from the sample as possible so that dissolved ions would not precipitate from solution as the water evaporated and therefore interfere with analysis of the settled solids. Samples were coated with a gold-palladium alloy for 2 minutes using vacuum deposition. The purpose of the coating is to increase the conductivity of the samples' surface, which results in an image with lower contrast. A Quanta FEG 650 SEM was used for the analysis.

Energy Dispersive X-Ray Spectrometry (EDX) is a technique used to quantify the elemental composition of a sample. The SEM electron beam causes x-rays of various wavelengths and intensities to emit from the sample as described in further detail below. The instrument detects and records the emitted x-ray spectrum, where intensity of the signal is plotted on the ordinate and the wavelength on the abscissa. A typical spectrum is shown below in Figure B.3. The wavelengths at which peaks occur are matched to the unique wavelengths of each element to identify which elements are present. Peaks are

identified as statistically significant if they are greater than three times the standardized deviation (Hafner n.d.). Some peaks may be the result of overlapping regions where two elements might share a similar wavelength, so prior knowledge of the sample is useful in approaching the analysis. Once the peaks are identified, the software of the EDX system counts the instances of the x-rays and converts it to atomic percentages (Hafner n.d.; Riverside n.d.). Calibration is done by comparing the spectrum to a standard with a known composition, but was not used in this analysis.

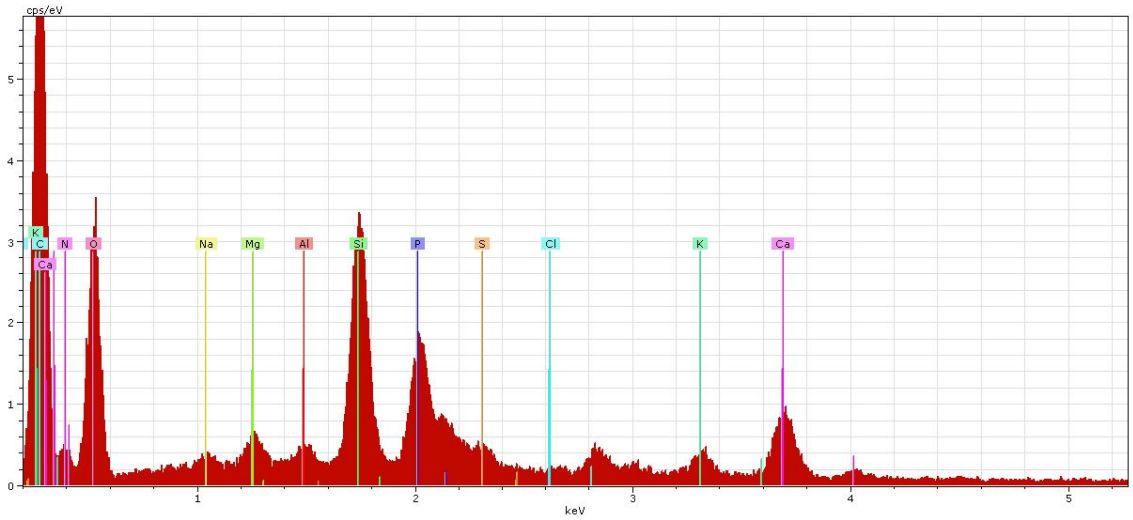

Figure B.3: Typical EDX Spectrum

The basis for EDX analysis is atomic orbital theory and electron quantum energy. Electrons in the atom are organized into shells and subshells, which are collectively known as orbitals, shown in Figure B.4. As the atomic number increases, electrons are added into shells from lowest to highest energy levels. The K shell (quantum number, n=1), is located closest to the nucleus and has the least energy, followed by the L shell (n=2) and M shell (n=3) as the energy is increased and the shells move farther from the

nucleus. Each shell has a specific number of subshells with slightly different energies; the K shell has only one, the L shell has three subshells (L1, L2, and L3), and the M shell has five (M1, M2, M3, M4, and M5).

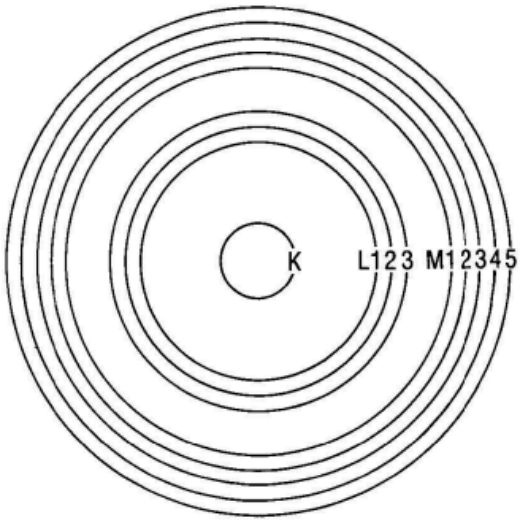

Figure B.4: Schematic of shells and subshells organized within an atom.

The external electron beam causes electrons in the lower shells (K shell for example) to be ejected resulting in a vacancy. To stabilize the atom, an electron from a higher energy shell (let say the L1 shell) drops down into the vacancy. Since the K shell has a lower energy level than the L1 shell, this electron drop results in a release of energy in the form of a specific x-ray wavelength. Electrons from other shells can also drop down to fill the vacancy, resulting in the release of other x-ray wavelengths. Each element has a unique set of characteristic wavelengths associated with all of the element's possible drops. Therefore, EDX compares observed x-ray wavelengths to the known characteristic wavelengths of all the elements to identify the composition of a sample.

Nomenclature has been developed to describe the different types of energy drops. An electron drop spanning one shell level is referred to as α, while a two shell drop is called β. For example, the most common electron drop, from shell L to K, is named Kα, while a drop from M to K is named Kβ. Further, there is additional nomenclature used to identify a drop from a specific shell in a given layer, for instance a drop from L1 to K. The most likely to occur is given the name Kα1 followed by Kα2, etc. However, the energy values released by these drops are similar and typically cannot be differentiated by the EDX system.

References

APHA, AWWA, and WPCF. (2005). Standard Methods for the Examination of Water and Wastewater. American Public Health Association, American Water Works Association, Water Environmental Federation, Washington, DC.

ASCE. (2007). Measurement of Oxygen Transfer in Clean Water. ASCE Standards, Reston, VA.

Benjamin, M. M., and Lawler, D. F. (2013). Water Quality Engineering. John Wiley & Sons, Inc., Hoboken, NJ.

Brouwer, H., and Murphy, T. P. (1994). "Diffusion Method for the Determination of Acid-Volatile Sulfides (AVS) in Sediment." Environ. Toxicology and Chemistry, 13(8), 1273–1275.

Burton, W. K., Cabrera, N., and Frank, F. C. (1951). "The Growth of Crystals and the Equilibrium Structure of their Surfaces." Philosophical Transactions of the Royal Society A: Mathematical, Physical and Engineering Sciences, 243(866), 299–358.

Dytczak, M. A., Londry, K. L., and Oleszkiewicz, J. A. (2008). "Nitrifying Genera in Activated Sludge May Influence Nitrification Rates." Water Environment Research, 80(5), 388–396.

Engineering Toolbox. (2013). "Slurry Density: Calculating Density of Slurries." <http://www.engineeringtoolbox.com/slurry-density-d_1188.html.>.

Folk, R. L. (1974). "The Natural History of Crystalline Calcium Carbonate: Effect of Magnesium Content and Salinity." J. Sedimentary Petrology, 44(1), 40–53.

Hafner, B. (n.d.). Energy Dispersive Spectroscopy on the SEM: A Primer.

Hamza, S. M., and Hamdona, S. K. (1992). "Dissolution of Calcium Carbonate Crystals□: A Constant-composition Kinetic Study." J. Chem, Soc., Faraday Trans., 88(18), 2713–2716.

Hendricks, D. (2011). Fundamentals of Water Treatment Unit Processes. CRC Press, Boca Raton, FL.

Johnson, N., Schierz, A., and Reible, D. (2013). Method for Measuring AVS in Sediment Solid Phase. Austin, TX.

Metcalf and Eddy. (2003). Wastewater Engineering: Treatment and Reuse. McGraw-Hill, New York.

Morel, F. M. M., and Hering, J. G. (1993). Principles and Applications of Aquatic Chemistry. John Wiley & Sons, Inc., New York.

Morse, J. W. (1983). “The Kinetics of Calcium Carbonate Dissolution and Precipitation.” Carbonates: Mineralogy and Chemistry, R. J. Reeder, ed., Chelsea Michigan, 227–264.

Plummer, L. N., Widley, T. M. L., and Parkhurst, D. L. (1978). “The Kinetics of Calcite Dissolution in CO2-Water Systems at 5o to 60oC and 0.0 to 1.0 ATM CO2.” American Journal of Science, 278, 179–216.

Reddy, M. M., and Wang, K. K. (1980). “Crystallization of calcium carbonate in the presence of metal ions: I. Inhibition by magnesium ion at pH 8.8 and 25oC.” J. Crystal Growth, 50(2), 470–480.

Riverside, U. of C. (n.d.). Introduction to Energy Dispersive X-ray Spectrometry (EDS).

Sawyer, C. N., McCarty, P. L., and Parkin, G. F. (2002). Chemistry for Environmental Engineering and Science. McGraw-Hill, New York.

Sjöberg, E. L. (1978). “Kinetics and mechanism of calcite dissolution in aqueous solutions at low temperatures.” Stockholm University.

Stumm, W., and Morgen, J. J. (1996). Aquatic Chemistry: Chemical Equilibria and Rate in Natural Waters. John Wiley & Sons, Inc., New York, 370–387.

Vita

Austin Weidner grew up in Kutztown, Pennsylvania. He graduated from Lafayette College in Easton, Pennsylvania where he studied Civil and Environmental Engineering. During his undergraduate career he developed a passion for sustainable water infrastructure, which he pursued further in graduate school in the Environmental Water Resources Engineering program at the University of Texas at Austin. In May 2014, Austin will receive his Master of Science degree and begin his career as an Environmental Engineer. In addition to water treatment, he enjoys hiking, playing the saxophone, and watching baseball.

Permanent Email Address: austin.weidner@gmail.com

This thesis was typed by the author.